Supplementary Materials

Diastereodivergent Synthesis of Multi-Substituted Cyclohexanes via Alkene Hydroamidation

Zhen Li[a], Yi-Zhou Tong[a], Kai-Ran Duan[a], Bo-Ru Men[a], Qian-Qian Lu[b]*, Xi Lu[a]*, Yao Fu[a]*

E-mails: luqq@njau.edu.cn (Qian-Qian Lu), luxi@mail.ustc.edu.cn (Xi Lu), fuyao@ustc.edu.cn

(Yao Fu)

[a] State Key Laboratory of Precision and Intelligent Chemistry, Anhui Province Key Laboratory of Biomass Chemistry, University of Science and Technology of China, Hefei 230026, China

[b] College of Sciences, Nanjing Agricultural University, Nanjing 210095, China

contents

Supplementary Methods

General Information

Materials

The following chemicals were purchased and used as received: dichloride(1,2-dimethoxyethane)nickel(II) (CAS: 29046-78-4, Leyan.com, 1112958); trimethoxysilane (CAS: 2487-90-3, adamas); potassium fluoride (CAS: 7789-23-3, ACROS); Lithium chloride (CAS: 7447-41-8, 3A); (*S*,*S*)-Ph-Bisbox (CAS: 135532-33-1, Leyan.com, 1168014); [S(R)]-N-[(R)-(2-methylphenyl)[5-(diphenylphosphino)-9,9-dimethyl-9H-xanthen-4-yl]methyl]-2-methyl-2-propanesulfinamide (Leyan.com, 1218264); (2R_S)-1-[(4*S*)-4,5-Dihydro-4-(1-methylethyl)-2-oxazolyl]-2-(diphenylphosphino)ferrocene (CAS: 163169-29-7, Leyan.com, 1022982); *N*,*N*-dimethylacetamide (CAS: 127-19-5); methanol (CAS: 67-56-1); tert-butanol (CAS: 75-65-0);chloroform-d (CAS: 865-49-6);

Analytical methods

All reactions dealing with air- or moisture-sensitive compounds were performed by standard Schlenk techniques in oven-dried reaction vessels under argon atmosphere or in the argon-filled glove box. Most reagents were purchased from commercial sources and used without further purification unless otherwise stated. Reactions were monitored by thin-layer chromatography (TLC) carried out on 0.2 mm commercial silica gel plates, using UV light as the visualizing agent, $KMnO_4$ alkaline solution, ethanol solution of phosphomolybdic acid or heat as a developing agent. ^{1}H NMR, ^{13}C NMR, and ^{19}F NMR spectra were recorded on Bruker 400 MHz spectrometer and Bruker 500 MHz spectrometer at 298 K in $CDCl_3$ unless otherwise noted. Data for ^{1}H NMR were reported as follows: chemical shift (δ ppm), multiplicity, coupling constant (Hz), and integration. Data for ^{13}C NMR were reported as follows: chemical shift (δ ppm), multiplicity, and coupling constant (Hz); Data for ^{19}F NMR were reported as follows:

chemical shift (δ ppm), multiplicity, coupling constant (Hz). Chemical shifts were reported using the residual solvent $CHCl_3$ as the internal reference for ^1H NMR (δ = 7.260 ppm) and $CDCl_3$ peak as the internal reference for ^{13}C NMR (δ = 77.160 ppm). High-resolution mass spectra (HRMS) by electrospray ionization (ESI) method were performed on Water XEVO G2 Q-TOF (Waters Corporation). HRMS by electron impact ion source (EI) were performed on Thermo Fisher GC ULTRA/ ISQ MS (Some compounds could not be analyzed by ESI-HRMS and APPI-HRMS due to their structural characteristics. In the absence of EI-HRMS testing conditions, GC-MS was used to analyze the mass spectrometry data of some compounds). Gas chromatographic (GC) analysis was acquired on a Shimadzu GC-2010 plus Series GC system equipped with a flame-ionization detector. Organic solutions were concentrated under reduced pressure on the Buchi rotary evaporator. Column chromatographic purification of products was accomplished using forced-flow chromatography on Silica Gel (300-400 mesh).

Caution

Eye protections are necessary when handling alkoxysilanes. Alkoxysilanes might be disproportionated to form pyrophoric SiH_4; please take suitable precautions. (For warnings on the potential security risks when handling alkoxysilanes, see: Berk, S. C.; Buchwald, S. L. An air-stable catalyst system for the conversion of esters to alcohols. J. Org. Chem. 1992, 57 (14), 3751− 3753. Berk, S. C.; Buchwald, S. L. An air-stable catalyst system for the conversion of esters to alcohols. [Erratum to document cited in CA117(3):25599z]. J. Org. Chem. 1993, 58 (11), 3221−3221.)

Optimization of Reaction Conditions.

Reaction development

Metal-hydride catalyzed hydrofunctionalization of alkenes has been extensively studied and developed in recent years.[1-4] For instance, copper- and nickel-catalyzed systems are well established for facilitating hydroamidation of alkenes with dioxazolones.[5-8] More recently, iron- and cobalt-catalyzed systems have also been developed to achieve such hydroamination reactions using dioxazolones as the amine source.[9,10] In this work, we evaluated four metal-catalyzed systems for the hydroamidation of 4-*tert*-butylmethylenecyclohexane, aiming to identify a suitable catalytic platform for the subsequent development of diastereodivergent hydroamination of substituted methylenecyclohexanes.

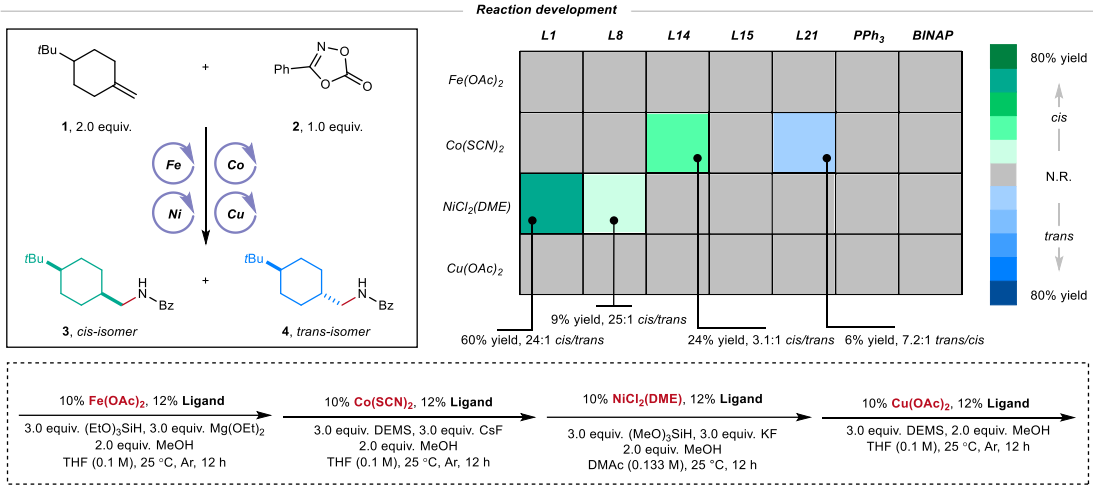

Fig. S1. Reaction development

Optimization of ligand for Ni-catalyzed hydroamination

We screened a series of ligands commonly employed in nickel-catalyzed hydrofunctionalization of alkenes. The selection included bidentate nitrogen-based ligands such as BiOX, PyOX, BOX, and BiM, as well as widely used commercial phosphine ligands (e.g., PPh_3 and BINAP). The reaction proceeded only with BiOX- and PyOX-type ligands, affording the 1,4-*cis* hydroamidation product in high yield and selectivity. In contrast, no desired hydroamidation product was observed with the remaining ligand scaffolds. To achieve the diastereodivergent synthesis envisioned

earlier, we further evaluated ligands based on the PHOX scaffold, which had exhibited remarkable stereoselectivity reversal in our previously developed cobalt-catalyzed system.[11] However, this approach did not yield the desired 1,4-*trans* product.

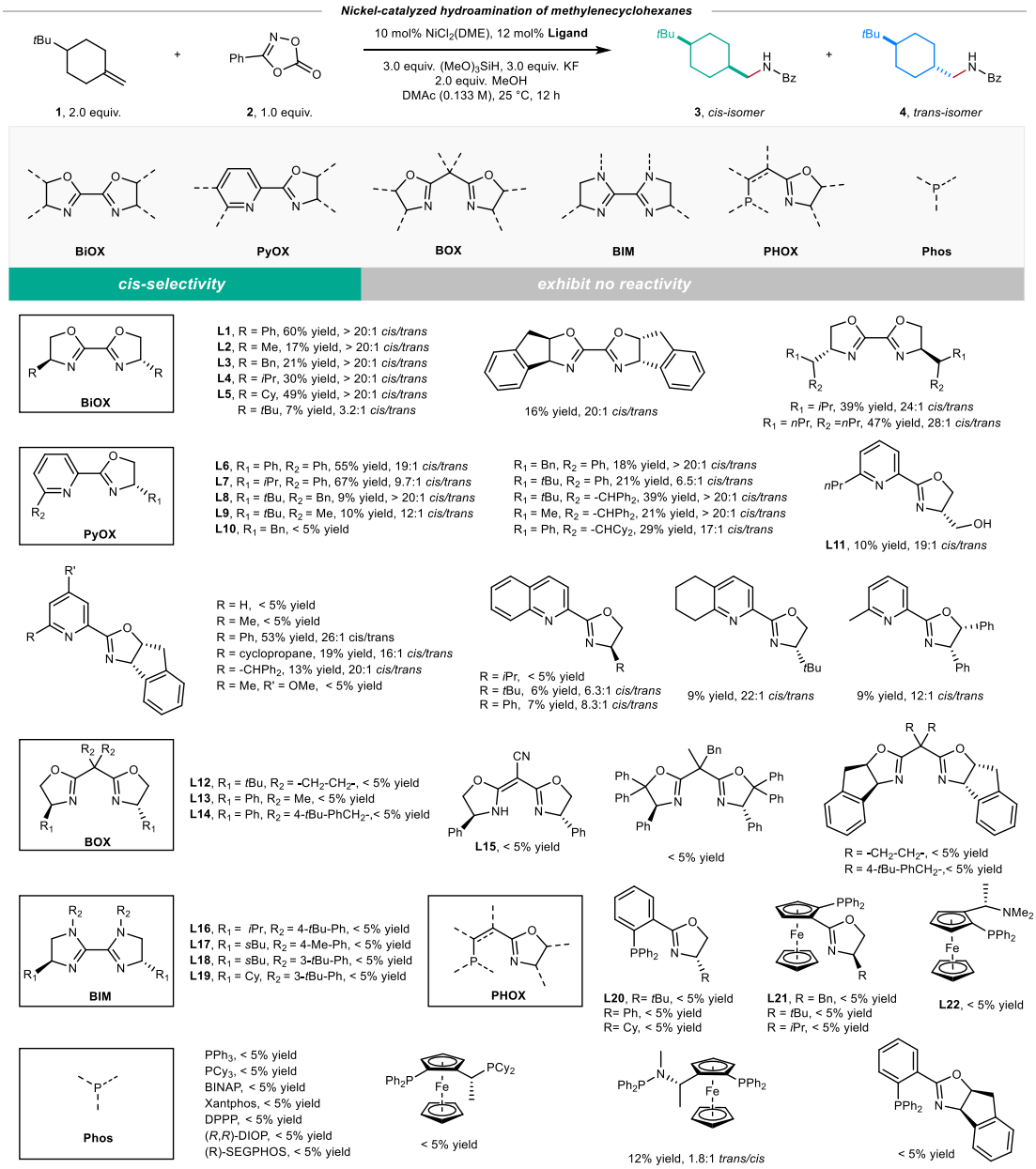

Fig. S2. Optimization of ligand for Ni-catalyzed hydroamination

In our ongoing efforts to develop a diastereodivergent route for constructing substituted cycloalkane frameworks, we continued our ligand screening campaign. We evaluated a range of ligands featuring pyridine, amino alcohol, and ethylenediamine backbones; however, none of these succeeded in reversing the reaction's

stereoselectivity. While pincer-type ligands have found widespread application in recent years, they also failed to deliver satisfactory results in our designed system.

Given the extensive yet unfruitful ligand screening, we recognized the necessity of exploring novel ligand architectures within the nickel-hydride catalytic system. Inspired by the proven efficacy of SadPhos-type ligands in palladium-, gold-, and copper-catalyzed reactions, we applied SadPhos ligand in conjunction with nickel.[12-14] This approach successfully led to the identification of 1,4-*trans* hydroamidation product. Subsequent comprehensive evaluation of the SadPhos-type Ligands (see **Fig. S4**) enabled us to identify the optimal ligand, **L30**.

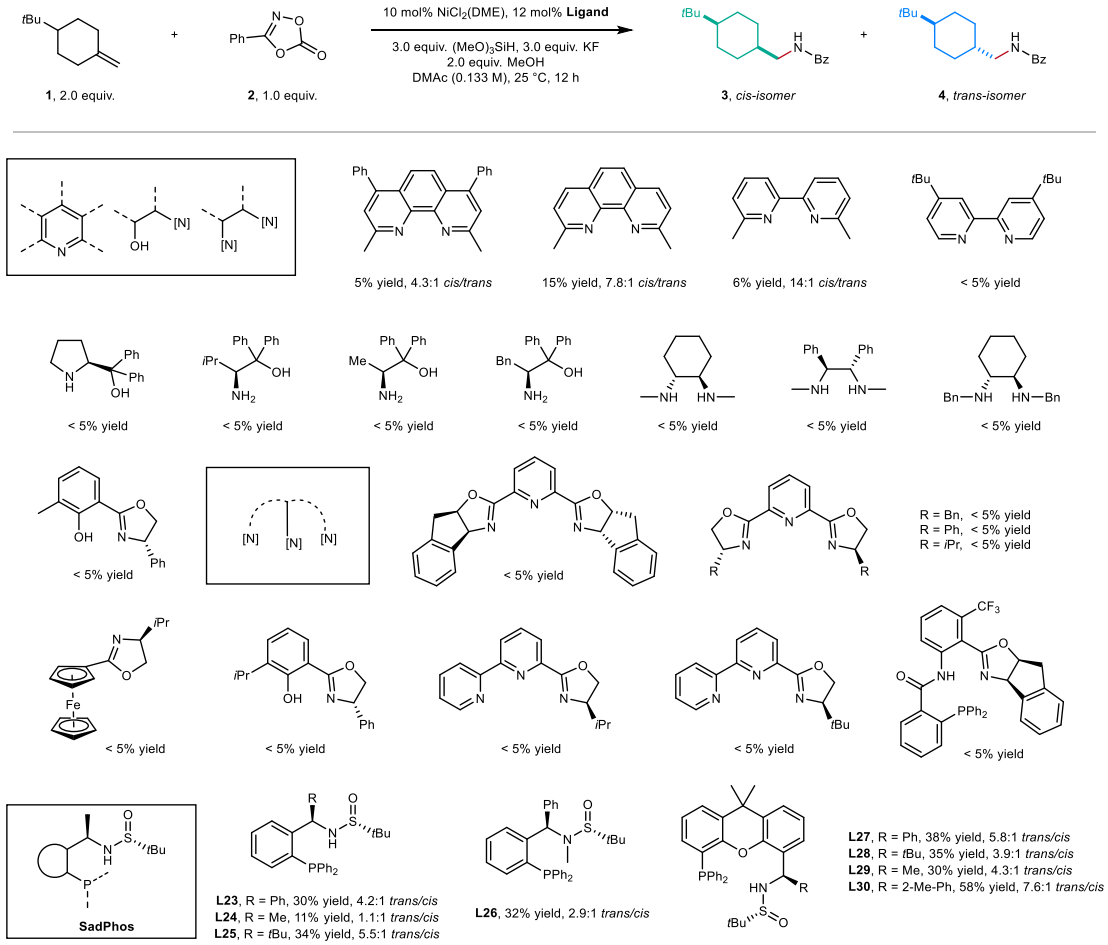

Fig. S3. Ligand screening for stereoselectivity reversal

Further optimization of Reaction Conditions

Table 1. Further optimization for the 1,4-*cis* isomers

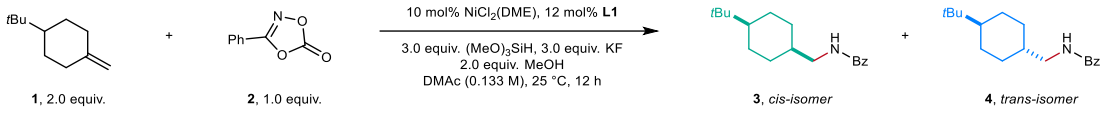

1, 2.0 equiv. **2**, 1.0 equiv. **3**, *cis-isomer* **4**, *trans-isomer*

entry	cobalt source	additive	silane	base	solvent	yield (%) [a]	cis/trans [a]
1	$NiCl_2(DME)$	MeOH	$(MeO)_3SiH$	KF	DMAc	60	>20:1
2	NiI_2	MeOH	$(MeO)_3SiH$	KF	DMAc	< 5	-
3	$Ni(BF_4)_2(6H_2O)$	MeOH	$(MeO)_3SiH$	KF	DMAc	< 5	-
4	$Ni(OTf)_2$	MeOH	$(MeO)_3SiH$	KF	DMAc	< 5	-
5	$Ni(acac)_2$	MeOH	$(MeO)_3SiH$	KF	DMAc	< 5	-
6	$NiCl_2(DME)$	MeOH	$(MeO)_3SiH$	K_2CO_3	DMAc	52	20:1
7	$NiCl_2(DME)$	-	$(MeO)_3SiH$	KF	DMAc/*t*BuOH (4:1)	58	> 20:1
8 [b]	$NiCl_2(DME)$	MeOH	$(MeO)_3SiH$	KF	DMAc	54	>20:1
9 [c]	$NiCl_2(DME)$	MeOH	$(MeO)_3SiH$	KF	DMAc	25	19:1
10 [d]	$NiCl_2(DME)$	MeOH	$(MeO)_3SiH$	KF	DMAc	74	13:1
11 [e]	$NiCl_2(DME)$	MeOH	$(MeO)_3SiH$	KF	DMAc	77(71) [f]	>20:1

Reactions were carried out under an argon atmosphere. Conditions: **1** (2.0 equiv.), **2** (1.0 equiv.), [Ni] catalyst (10 mol%), **L1** (12 mol%), silane (3.0 equiv.), base (3.0 equiv.), solvent (0.133 M), 25 °C, 12 h, 0.10 mmol scales. [a]Yield and facial selectivity (*fs*) were determined by GC (gas chromatography) analysis using triphenylmethane as an internal standard. [b]40 °C. [c]0 °C. [d]LiI (50 mol%) was added. [e]LiCl (50 mol%) was added. [f]Isolated yield are given in parentheses. DME, 1,2-Dimethoxyethane; DMAc, *N*, *N*-dimethylacetamide; OTf, trifluoromethanesulfonate; acac, acetylacetone.

Table 2. Further optimization for the 1,4-*trans* isomers

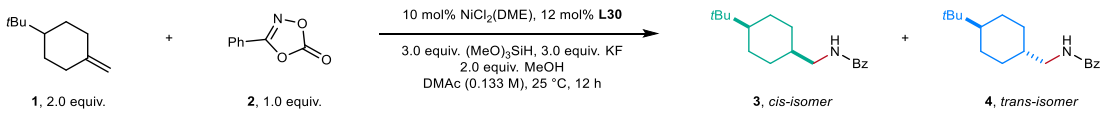

1, 2.0 equiv. **2**, 1.0 equiv. **3**, *cis-isomer* **4**, *trans-isomer*

entry	cobalt source	additive	silane	base	solvent	yield (%) [a]	trans/cis [a]
1	$NiCl_2(DME)$	MeOH	$(MeO)_3SiH$	KF	DMAc	58	7.6:1

2 [b]	$NiCl_2$(DME)	MeOH	$(MeO)_3SiH$	KF	DMAc	78	13:1
3 [b]	$NiBr_2$(DME)	MeOH	$(MeO)_3SiH$	KF	DMAc	61	2.8:1
4 [b]	$Ni(BF_4)_2(6H_2O)$	MeOH	$(MeO)_3SiH$	KF	DMAc	< 5	-
5 [b]	$Ni(acac)_2$	MeOH	$(MeO)_3SiH$	KF	DMAc	< 5	-
6 [b]	$NiCl_2$(DME)	MeOH	$(EtO)_3SiH$	KF	DMAc	34	12:1
7 [b]	$NiCl_2$(DME)	MeOH	DMMS	KF	DMAc	44	9.2:1
8 [b]	$NiCl_2$(DME)	MeOH	DEMS	KF	DMAc	8	13:1
9 [b]	$NiCl_2$(DME)	MeOH	Ph_2SiH_2	KF	DMAc	10	7.0:1
10 [b]	$NiCl_2$(DME)	MeOH	$(MeO)_3SiH$	CsF	DMAc	< 5	-
11 [b]	$NiCl_2$(DME)	MeOH	$(MeO)_3SiH$	K_2CO_3	DMAc	67	10:1
12 [b]	$NiCl_2$(DME)	MeOH	$(MeO)_3SiH$	K_3PO_4	DMAc	< 5	-
13 [b]	$NiCl_2$(DME)	MeOH	$(MeO)_3SiH$	KF	NMP	79	9.8:1
14 [b]	$NiCl_2$(DME)	MeOH	$(MeO)_3SiH$	KF	THF	< 5	-
15 [b]	$NiCl_2$(DME)	MeOH	$(MeO)_3SiH$	KF	MeCN	< 5	-
16 [b]	$NiCl_2$(DME)	MeOH	$(MeO)_3SiH$	KF	DME	12	12:1
17 [b]	$NiCl_2$(DME)	-	$(MeO)_3SiH$	KF	DMAc/*t*BuOH (4:1)	70	15:1
18 [b, c]	$NiCl_2$(DME)	MeOH	$(MeO)_3SiH$	KF	DMAc	82	8.9:1
19 [b, d]	$NiCl_2$(DME)	MeOH	$(MeO)_3SiH$	KF	DMAc	79	4.1:1
20 [c]	$NiCl_2$(DME)	*t*BuOH	$(MeO)_3SiH$	KF	DMAc	86 (78) [e]	13:1

Reactions were carried out under an argon atmosphere. Conditions: **1** (2.0 equiv.), **2** (1.0 equiv.), [Ni] catalyst (10 mol%), **L30** (12 mol%), silane (3.0 equiv.), base (3.0 equiv.), solvent (0.133 M), 25 °C, 12 h, 0.10 mmol scales. [a]Yield and facial selectivity (*fs*) were determined by GC (gas chromatography) analysis using triphenylmethane as an internal standard. [b]0 °C. [c]LiI (50 mol%) was added. [d]LiCl (50 mol%) was added. [e]Isolated yield are given in parentheses. DME, 1,2-Dimethoxyethane; DMAc, *N*, *N*-dimethylacetamide; NMP, *N*-methylpyrrolidone; THF, tetrahydrofuran; acac, acetylacetone; DMMS, methyldimethoxysilane; DEMS, diethoxymethylsilane.

Screening of SadPhos-type Ligands

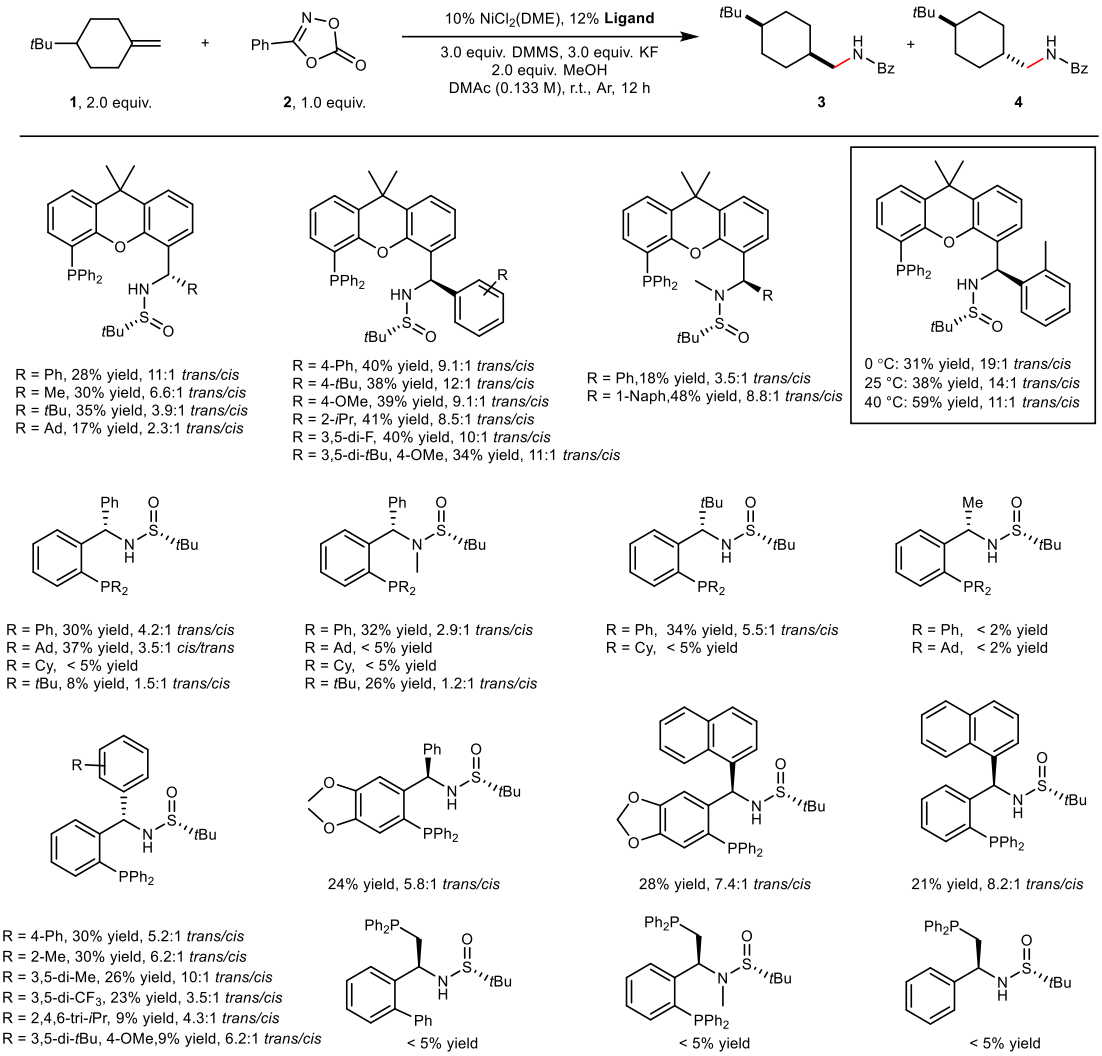

Fig. S4. Screening of SadPhos-type ligands

Additional information for Co-catalyzed hydroamination:

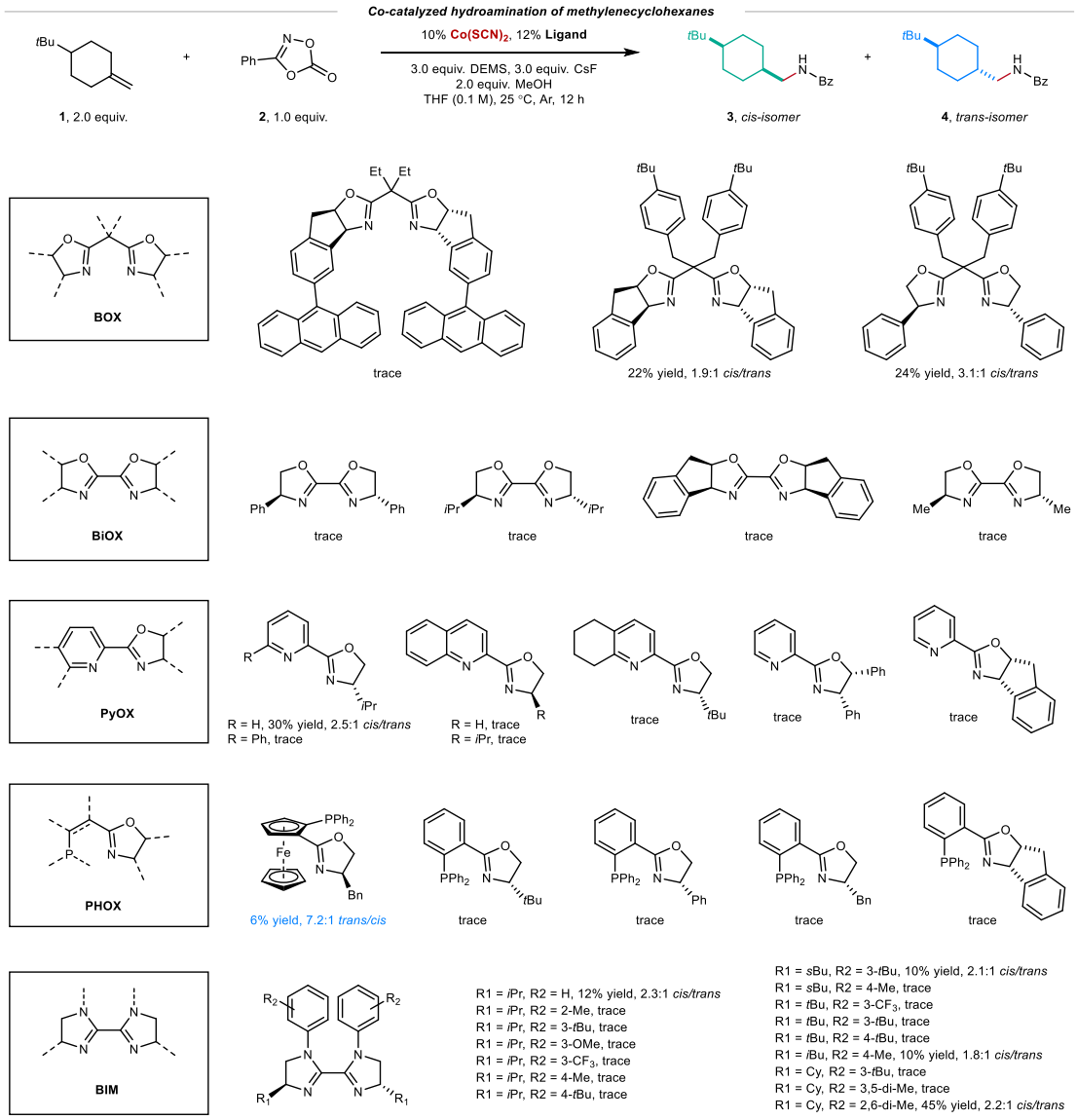

Fig. S5. Optimization of ligand for Co-catalyzed hydroamination

General Procedure for Diastereodivergent Hydroamidation

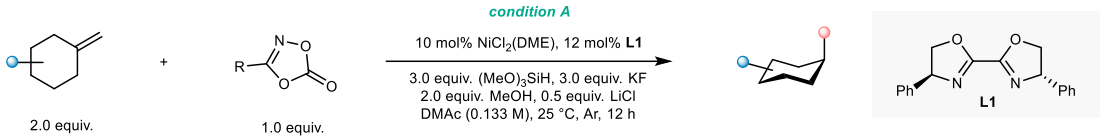

Fig. S6. Condition A

Condition A: In the air, a 10 mL Schlenk flask equipped with a magnetic stirrer was charged with $NiCl_2$(DME) (0.02 mmol, 10 mol%), Ligand (0.024 mmol, 12 mol%), lithium chloride (0.1 mmol, 0.5 equiv.), potassium fluoride (0.6 mmol, 3.0 equiv.) (Note: if the alkene or the dioxazolone were solid, they were also added at this step). The Schlenk flask was evacuated and backfilled with argon for three times, then DMAc (1.5 mL) was added, followed by the alkene (0.4 mmol, 2.0 equiv.), the dioxazolone (0.2 mmol, 1.0 equiv.) and methanol (0.4 mmol, 2.0 equiv.). The resulting solution was stirred for 2 min at 0 °C. Then, $(MeO)_3SiH$ (0.6 mmol, 3.0 equiv.) was added dropwise via syringe. After that, the reaction mixture was stirred at 25 °C for 12 h. The reaction mixture was diluted with H_2O and extracted with EtOAc. The organic layer was dried over anhydrous Na_2SO_4 and concentrated in vacuo. The residue was purified by flash column chromatography on silica gel to give the target product.

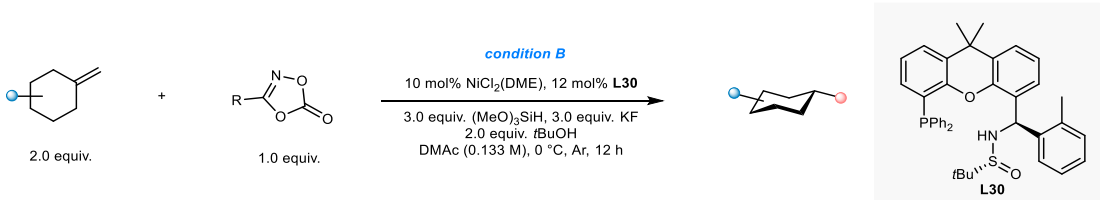

Fig. S7. Condition B

Condition B: In the air, a 10 mL Schlenk flask equipped with a magnetic stirrer was charged with $NiCl_2$(DME) (0.02 mmol, 10 mol%), Ligand (0.024 mmol, 12 mol%), potassium fluoride (0.6 mmol, 3.0 equiv.) (Note: if the alkene or the dioxazolone were solid, they were also added at this step). The Schlenk flask was evacuated and backfilled with argon for three times, then DMAc (1.5 mL) was added, followed by the alkene (0.4 mmol, 2.0 equiv.), the dioxazolone (0.2 mmol, 1.0 equiv.) and tert-butanol (0.4

mmol, 2.0 equiv.). The resulting solution was stirred for 2 min at 0 °C. Then, $(MeO)_3SiH$ (0.6 mmol, 3.0 equiv.) was added dropwise via syringe. After that, the reaction mixture was stirred at 0 °C for 12 h. The reaction mixture was diluted with H_2O and extracted with EtOAc. The organic layer was dried over anhydrous Na_2SO_4 and concentrated in vacuo. The residue was purified by flash column chromatography on silica gel to give the target product.

Analytical Data of Compounds

Note: The cis/trans stereochemistry of the products was determined through single-crystal X-ray diffraction analysis. Additionally, for 1,3-substituted cyclohexane isomers, the cis-trans configuration of the substituents can also be determined through **γ-gauch effect** analysis.[15] For 1,2-substituted cyclohexane isomers, the cis-trans configuration of the substituents can also be determined based on the **vicinal Karplus correlation**.[16]

Part I (with Condition A):

CCDC-2456707

N-((cis-4-(tert-butyl)cyclohexyl)methyl)benzamide (**3**)

Following **Condition A**, **3** was obtained as white solid (38.9 mg, 71% yield, > 20:1 cis/trans).

^{1}H NMR (500 MHz, Chloroform-d) δ 7.84 – 7.69 (m, 2H), 7.56 – 7.46 (m, 1H), 7.45 – 7.37 (m, 2H), 6.13 (brs, 1H), 3.54 – 3.30 (m, 2H), 1.99 – 1.90 (m, 1H), 1.85 – 1.73 (m, 2H), 1.57 – 1.41 (m, 4H), 1.33 – 1.13 (m, 2H), 1.10 – 0.96 (m, 1H), 0.85 (s, 9H).

^{13}C NMR (126 MHz, Chloroform-d) δ 167.74, 135.06, 131.43, 128.68, 126.96, 48.57, 41.34, 33.19, 32.71, 28.77, 27.63, 22.03.

HRMS (ESI) calcd for $C_{18}H_{28}NO^{+}$ [$(M+H)^{+}$] 274.2165, found 274.2178.

Crystal data and structure refinement for **3**

Identification code	**3**
Empirical formula	C18 H27 N O
Formula weight	273.40
Temperature	173.00 K
Wavelength	1.34139 Å
Crystal system	Triclinic
Space group	P-1

Unit cell dimensions	a = 9.6085(9) Å	α= 91.572(4)°.
	b = 9.6455(9) Å	β= 96.350(4)°.
	c = 17.8713(15) Å	γ = 92.976(4)°.
Volume	1643.0(3) $Å^3$	
Z	4	
Density (calculated)	1.105 Mg/m^3	
Absorption coefficient	0.342 mm^{-1}	
F(000)	600	
Crystal size	0.17 x 0.17 x 0.05 mm^3	
Theta range for data collection	3.995 to 55.204°.	
Index ranges	-11<=h<=11, -11<=k<=11, 0<=l<=21	
Reflections collected	6237	
Independent reflections	6237 [R(int) = ?]	
Completeness to theta = 53.594°	99.5 %	
Absorption correction	Semi-empirical from equivalents	
Max. and min. transmission	0.7508 and 0.5745	
Refinement method	Full-matrix least-squares on F^2	
Data / restraints / parameters	6237 / 0 / 368	
Goodness-of-fit on F^2	0.911	
Final R indices [I>2sigma(I)]	R1 = 0.1059, wR2 = 0.2218	
R indices (all data)	R1 = 0.1218, wR2 = 0.2321	
Extinction coefficient	n/a	
Largest diff. peak and hole	0.776 and -0.508 $e.Å^{-3}$	

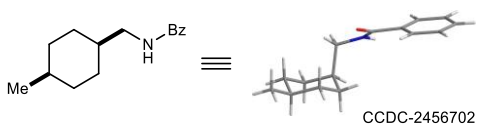

N-((cis-4-methylcyclohexyl)methyl)benzamide (**5**)

Following **Condition A**, 3.0 equivalents of alkene were used, **5** was obtained as white solid (26.9 mg, 58% yield, 14:1 cis/trans).

^{1}H NMR (500 MHz, Chloroform-d) δ 7.89 – 7.71 (m, 2H), 7.56 – 7.45 (m, 1H), 7.43 – 7.36 (m, 2H), 6.27 (brs, 1H), 3.49 – 3.32 (m, 2H), 1.79 – 1.70 (m, 1H), 1.69 – 1.60 (m, 1H), 1.54 – 1.40 (m, 6H), 1.36 – 1.27 (m, 2H), 0.91 (d, J = 6.9 Hz, 3H).

^{13}C NMR (126 MHz, Chloroform-d) δ 167.73, 135.01, 131.40, 128.64, 126.96, 43.80, 35.77, 30.60, 30.09, 26.64, 20.23.

HRMS (ESI) calcd for $C_{15}H_{22}NO^{+}$ [$(M+H)^{+}$] 232.1696, found 232.1700.

Crystal data and structure refinement for **5**

Identification code	**5**	
Empirical formula	C15 H21 N O	
Formula weight	231.33	
Temperature	173.00 K	
Wavelength	1.34139 Å	
Crystal system	Monoclinic	
Space group	Pn	
Unit cell dimensions	a = 7.7547(3) Å	α= 90°.
	b = 10.2279(4) Å	β= 108.534(2)°.
	c = 8.9593(4) Å	γ = 90°.
Volume	673.75(5) Å^3	
Z	2	
Density (calculated)	1.140 Mg/m^3	
Absorption coefficient	0.362 mm^{-1}	
F(000)	252	
Crystal size	0.17 x 0.17 x 0.05 mm^3	
Theta range for data collection	3.760 to 54.932°.	

Index ranges	-9<=h<=9, -11<=k<=12, -10<=l<=9
Reflections collected	8163
Independent reflections	2222 [R(int) = 0.0373]
Completeness to theta = 53.594°	99.5 %
Absorption correction	Semi-empirical from equivalents
Max. and min. transmission	0.7508 and 0.6190
Refinement method	Full-matrix least-squares on F^2
Data / restraints / parameters	2222 / 2 / 159
Goodness-of-fit on F^2	1.081
Final R indices [I>2sigma(I)]	R1 = 0.0266, wR2 = 0.0659
R indices (all data)	R1 = 0.0309, wR2 = 0.0684
Absolute structure parameter	-0.10(16)
Extinction coefficient	n/a
Largest diff. peak and hole	0.141 and -0.117 e.$Å^{-3}$

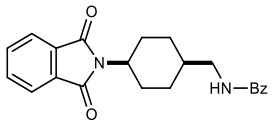

N-((cis-4-(1,3-dioxoisoindolin-2-yl)cyclohexyl)methyl)benzamide (**6**)

Following **Condition A**, **6** was obtained as white solid (37.8 mg, 52% yield, > 20:1 cis/trans).

^{1}H NMR (500 MHz, Chloroform-d) δ 7.86 – 7.76 (m, 4H), 7.74 – 7.66 (m, 2H), 7.55 – 7.46 (m, 1H), 7.46 – 7.38 (m, 2H), 6.31 (brs, 1H), 4.15 (tt, J = 11.5, 3.8 Hz, 1H), 3.73 – 3.56 (m, 2H), 2.60 – 2.34 (m, 2H), 2.16 – 2.06 (m, 1H), 1.92 – 1.83 (m, 2H), 1.70 – 1.63 (m, 1H), 1.62 – 1.57 (m, 2H), 1.38 – 1.12 (m, 1H).

^{13}C NMR (126 MHz, Chloroform-d) δ 168.52, 167.76, 134.94, 133.98, 132.13, 131.50, 128.70, 127.00, 123.21, 50.51, 41.09, 31.88, 27.45, 24.50.

HRMS (ESI) calcd for $C_{22}H_{22}N_2O_3Na^+$ [$(M+Na)^+$] 385.1523, found 385.1524.

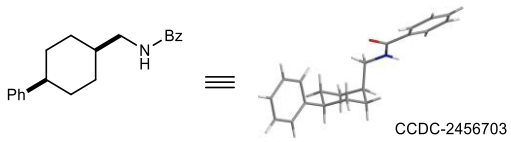

N-((cis-4-phenylcyclohexyl)methyl)benzamide (**7**)

Following **Condition A**, **7** was obtained as white solid (44.7 mg, 76% yield, 16:1 cis/trans).

^{1}H NMR (500 MHz, Chloroform-d) δ 7.83 – 7.72 (m, 2H), 7.55 – 7.47 (m, 1H), 7.46 – 7.40 (m, 2H), 7.35 – 7.27 (m, 2H), 7.27 – 7.23 (m, 2H), 7.22 – 7.14 (m, 1H), 6.17 (brs, 1H), 3.63 – 3.45 (m, 2H), 2.77 – 2.45 (m, 1H), 2.07 – 1.95 (m, 1H), 1.82 – 1.65 (m, 8H).

^{13}C NMR (126 MHz, Chloroform-d) δ 167.77, 147.00, 134.99, 131.51, 128.72, 128.46, 127.08, 126.97, 126.01, 43.42, 42.00, 33.73, 28.99, 28.11.

HRMS (ESI) calcd for $C_{20}H_{24}NO^{+}$ [$(M+H)^{+}$] 294.1852, found 294.1859.

Crystal data and structure refinement for **7**

Identification code	**7**	
Empirical formula	C20 H23 N O	
Formula weight	293.39	
Temperature	173.00 K	
Wavelength	1.34139 Å	
Crystal system	Orthorhombic	
Space group	$Pna2_1$	
Unit cell dimensions	a = 9.8506(2) Å	α= 90°.
	b = 9.6281(2) Å	β= 90°.
	c = 17.2077(3) Å	γ = 90°.
Volume	1632.02(6) $Å^3$	
Z	4	
Density (calculated)	1.194 Mg/m^3	
Absorption coefficient	0.373 mm^{-1}	

F(000)	632
Crystal size	0.17 x 0.17 x 0.05 mm^3
Theta range for data collection	4.471 to 54.888°.
Index ranges	-12<=h<=6, -10<=k<=11, -20<=l<=20
Reflections collected	16386
Independent reflections	3079 [R(int) = 0.0570]
Completeness to theta = 53.594°	99.7 %
Absorption correction	Semi-empirical from equivalents
Max. and min. transmission	0.7508 and 0.5496
Refinement method	Full-matrix least-squares on F^2
Data / restraints / parameters	3079 / 1 / 203
Goodness-of-fit on F^2	1.048
Final R indices [I>2sigma(I)]	R1 = 0.0288, wR2 = 0.0750
R indices (all data)	R1 = 0.0324, wR2 = 0.0763
Absolute structure parameter	-0.01(14)
Extinction coefficient	n/a
Largest diff. peak and hole	0.162 and -0.153 $e.Å^{-3}$

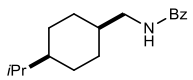

N-((cis-4-isopropylcyclohexyl)methyl)benzamide (**8**)

Following **Condition A**, **8** was obtained as white solid (35.9 mg, 69% yield, 17:1 cis/trans).

^{1}H NMR (500 MHz, Chloroform-d) δ 7.83 – 7.67 (m, 2H), 7.55 – 7.45 (m, 1H), 7.45 – 7.37 (m, 2H), 6.31 (brs, 1H), 3.46 – 3.18 (m, 2H), 1.88 – 1.80 (m, 2H), 1.79 – 1.69 (m, 2H), 1.63 – 1.45 (m, 1H), 1.45 – 1.34 (m, 1H), 1.07 – 0.92 (m, 5H), 0.84 (d, J = 6.9 Hz, 6H).

^{13}C NMR (126 MHz, Chloroform-d) δ 167.72, 135.02, 131.41, 128.65, 126.97, 46.36, 44.10, 38.34, 32.92, 31.16, 29.25, 19.93.

HRMS (ESI) calcd for $C_{17}H_{26}NO^+$ [$(M+H)^+$] 260.2009, found 260.2015.

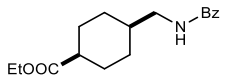

ethyl cis-4-(benzamidomethyl)cyclohexane-1-carboxylate (**9**)

Following **Condition A**, **9** was obtained as light-yellow oil (27.8 mg, 48% yield, 8.9:1 cis/trans).

^{1}H NMR (600 MHz, Chloroform-d) δ 7.80 – 7.69 (m, 2H), 7.56 – 7.44 (m, 1H), 7.44 – 7.37 (m, 2H), 6.30 (brs, 1H), 4.12 (q, J = 7.1 Hz, 2H), 3.33 (t, J = 6.6 Hz, 2H), 2.60 – 2.43 (m, 1H), 2.16 – 1.97 (m, 2H), 1.78 – 1.68 (m, 1H), 1.68 – 1.60 (m, 2H), 1.59 – 1.51 (m, 2H), 1.41 – 1.28 (m, 2H), 1.24 (t, J = 7.1 Hz, 3H).

^{13}C NMR (151 MHz, Chloroform-d) δ 175.29, 167.74, 134.89, 131.48, 128.67, 126.96, 60.32, 44.86, 40.20, 36.37, 27.22, 26.11, 14.38.

HRMS (ESI) calcd for $C_{17}H_{23}NO_3Na^+$ [$(M+Na)^+$] 312.1570, found 312.1572.

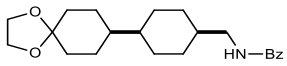

N-((cis-4-(1,4-dioxaspiro[4.5]decan-8-yl)cyclohexyl)methyl)benzamide (**10**)

Following **Condition A**, **10** was obtained as white solid (49.5 mg, 69% yield, 17:1 cis/trans).

^{1}H NMR (500 MHz, Chloroform-d) δ 7.83 – 7.69 (m, 2H), 7.56 – 7.44 (m, 1H), 7.44 – 7.37 (m, 2H), 6.21 (brs, 1H), 3.94 – 3.87 (m, 4H), 3.48 – 3.36 (m, 2H), 1.90 – 1.79 (m, 1H), 1.77 – 1.71 (m, 4H), 1.58 – 1.40 (m, 10H), 1.32 – 1.17 (m, 4H).

^{13}C NMR (126 MHz, Chloroform-d) δ 167.70, 134.97, 131.43, 128.65, 126.94, 109.21, 64.30, 64.27, 43.05, 40.76, 38.96, 35.28, 34.82, 27.60, 27.38, 25.83.

HRMS (ESI) calcd for $C_{22}H_{32}NO_3^+$ [$(M+H)^+$] 358.2377, found 358.2378.

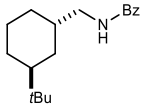

N-((trans-3-(tert-butyl)cyclohexyl)methyl)benzamide (**11**)

Following **Condition A**, 3.0 equivalents of alkene were used, **11** was obtained as white solid (33.5 mg, 61% yield, > 20:1 trans/cis).

^{1}H NMR (500 MHz, Chloroform-d) δ 7.79 – 7.66 (m, 2H), 7.51 – 7.44 (m, 1H), 7.43 – 7.36 (m, 2H), 6.19 (brs, 1H), 3.62 – 3.36 (m, 2H), 2.21 – 2.01 (m, 1H), 1.85 – 1.69 (m, 2H), 1.67 – 1.54 (m, 2H), 1.52 – 1.33 (m, 2H), 1.30 – 1.19 (m, 2H), 0.99 – 0.89 (m, 1H), 0.82 (s, 9H).

^{13}C NMR (126 MHz, Chloroform-d) δ 167.71, 135.12, 131.36, 128.65, 126.93, 41.81, 41.70, 34.13, 32.45, 29.38, 27.83, 27.60, 27.44, 21.71.

HRMS (ESI) calcd for $C_{18}H_{28}NO^+$ [$(M+H)^+$] 274.2165, found 274.2178.

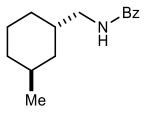

N-((trans-3-methylcyclohexyl)methyl)benzamide (**12**)

Following **Condition A**, 3.0 equivalents of alkene were used, **12** was obtained as white solid (31.6 mg, 68% yield, 7.8:1 trans/cis).

^{1}H NMR (500 MHz, Chloroform-d) δ 7.79 – 7.68 (m, 2H), 7.57 – 7.44 (m, 1H), 7.44 – 7.31 (m, 2H), 6.29 (brs, 1H), 3.50 – 3.17 (m, 2H), 2.08 – 1.86 (m, 1H), 1.82 – 1.70 (m, 1H), 1.63 – 1.52 (m, 2H), 1.51 – 1.45 (m, 2H), 1.42 – 1.33 (m, 1H), 1.32 – 1.23 (m, 2H), 1.20 – 1.10 (m, 1H), 0.90 (d, J = 6.9 Hz, 3H).

^{13}C NMR (126 MHz, Chloroform-d) δ 167.72, 135.02, 131.38, 128.63, 126.96, 44.20, 36.92, 33.60, 33.13, 29.50, 27.22, 20.71.

HRMS (ESI) calcd for $C_{15}H_{22}NO^+$ [$(M+H)^+$] 232.1696, found 232.1700.

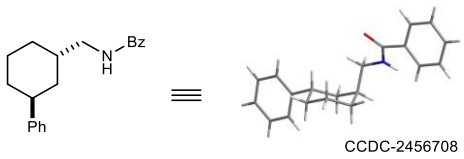

N-((trans-3-phenylcyclohexyl)methyl)benzamide (**13**)

Following **Condition A**, **13** was obtained as white solid (41.2 mg, 70% yield, > 20:1 trans/cis).

^{1}H NMR (500 MHz, Chloroform-d) δ 7.81 – 7.71 (m, 2H), 7.54 – 7.46 (m, 1H), 7.45 – 7.38 (m, 2H), 7.35 – 7.27 (m, 2H), 7.27 – 7.22 (m, 2H), 7.21 – 7.14 (m, 1H), 6.17 (brs, 1H), 3.91 – 3.41 (m, 2H), 2.87 (tt, J = 10.6, 4.1 Hz, 1H), 2.11 (tt, J = 8.0, 4.0 Hz, 1H), 1.95 – 1.86 (m, 1H), 1.85 – 1.74 (m, 2H), 1.71 – 1.52 (m, 5H).

^{13}C NMR (126 MHz, Chloroform-d) δ 167.81, 147.03, 135.00, 131.48, 128.70, 128.48, 127.10, 126.96, 126.02, 42.24, 38.28, 35.96, 34.24, 33.68, 28.11, 21.55.

HRMS (ESI) calcd for $C_{20}H_{24}NO^{+}$ [$(M+H)^{+}$] 294.1852, found 294.1859.

Crystal data and structure refinement for **13**.

Identification code	**13**	
Empirical formula	C20 H23 N O	
Formula weight	293.39	
Temperature	188.00 K	
Wavelength	1.34139 Å	
Crystal system	Monoclinic	
Space group	P 1 21/c 1	
Unit cell dimensions	a = 12.4461(3) Å	α= 90°.
	b = 5.25550(10) Å	β= 95.1120(10)°.
	c = 24.2745(6) Å	γ = 90°.
Volume	1581.49(6) Å^3	
Z	4	
Density (calculated)	1.232 Mg/m^3	
Absorption coefficient	0.384 mm^{-1}	
F(000)	632	
Crystal size	0.17 x 0.17 x 0.05 mm^3	
Theta range for data collection	3.101 to 55.080°.	
Index ranges	-15<=h<=15, -6<=k<=4, -29<=l<=29	
Reflections collected	20277	

Independent reflections	3014 [R(int) = 0.0530]
Completeness to theta = 53.594°	99.5 %
Absorption correction	Semi-empirical from equivalents
Max. and min. transmission	0.7508 and 0.6720
Refinement method	Full-matrix least-squares on F^2
Data / restraints / parameters	3014 / 0 / 199
Goodness-of-fit on F^2	1.026
Final R indices [I>2sigma(I)]	R1 = 0.0444, wR2 = 0.1045
R indices (all data)	R1 = 0.0598, wR2 = 0.1138
Extinction coefficient	n/a
Largest diff. peak and hole	0.222 and -0.216 e.$Å^{-3}$

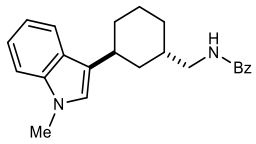

N-((trans-3-(1-methyl-1H-indol-3-yl)cyclohexyl)methyl)benzamide (**14**)

Following **Condition A**, **14** was obtained as light-yellow oil (43.8 mg, 63% yield, 13:1 trans/cis).

^{1}H NMR (500 MHz, Chloroform-d) δ 7.85 – 7.72 (m, 2H), 7.70 – 7.62 (m, 1H), 7.55 – 7.46 (m, 1H), 7.45 – 7.38 (m, 2H), 7.34 – 7.25 (m, 1H), 7.24 – 7.18 (m, 1H), 7.14 – 7.02 (m, 1H), 6.86 (s, 1H), 6.24 (brs, 1H), 3.74 (s, 3H), 3.60 – 3.52 (m, 2H), 3.32 – 3.23 (m, 1H), 2.13 – 2.06 (m, 1H), 2.05 – 1.99 (m, 1H), 1.98 – 1.87 (m, 2H), 1.80 – 1.64 (m, 4H), 1.60 – 1.49 (m, 1H).

^{13}C NMR (126 MHz, Chloroform-d) δ 167.79, 137.05, 134.99, 131.42, 128.65, 127.28, 126.97, 125.26, 121.52, 120.05, 119.51, 118.56, 109.28, 43.35, 35.60, 34.00, 32.81, 32.72, 29.90, 29.06, 21.72.

HRMS (ESI) calcd for $C_{23}H_{27}N_2O^+$ [$(M+H)^+$] 347.2118, found 347.2119.

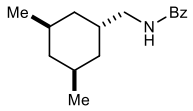

cis,trans-N-((3,5-dimethylcyclohexyl)methyl)benzamide (**25**)

Following **Condition A**, 3.0 equivalents of alkene were used, **25** was obtained as white solid (26.1 mg, 53% yield, 12:1 fs).

^{1}H NMR (400 MHz, Chloroform-d) δ 7.96 – 7.67 (m, 2H), 7.54 – 7.44 (m, 1H), 7.44 – 7.35 (m, 2H), 6.29 (brs, 1H), 3.60 – 3.32 (m, 2H), 2.21 – 1.99 (m, 1H), 1.70 – 1.52 (m, 5H), 1.14 – 0.97 (m, 2H), 0.84 (d, J = 6.1 Hz, 6H), 0.62 – 0.42 (m, 1H).

^{13}C NMR (101 MHz, Chloroform-d) δ 167.74, 134.99, 131.39, 128.63, 126.96, 44.42, 42.37, 36.63, 34.54, 27.10, 23.06.

HRMS (ESI) calcd for $C_{16}H_{24}NO^{+}$ [(M+H)$^{+}$] 246.1852, found 246.1853.

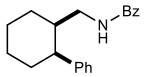

N-((cis-2-phenylcyclohexyl)methyl)benzamide (**27**)

Following **Condition A**, 3.0 equivalents of alkene were used, **27** was obtained as white solid (28.3 mg, 48% yield, > 20:1 cis/trans).

^{1}H NMR (500 MHz, Chloroform-d) δ 7.46 – 7.15 (m, 10H), 5.43 (brs, 1H), 4.00 – 3.61 (m, 1H), 3.25 – 3.07 (m, 1H), 3.00 (dt, J = 12.5, 3.9 Hz, 1H), 2.37 – 2.19 (m, 1H), 1.99 – 1.88 (m, 3H), 1.85 – 1.78 (m, 1H), 1.77 – 1.65 (m, 1H), 1.62 – 1.51 (m, 2H), 1.50 – 1.38 (m, 1H).

^{13}C NMR (126 MHz, Chloroform-d) δ 167.02, 145.46, 134.55, 131.23, 128.81, 128.36, 127.62, 126.77, 126.37, 45.13, 41.48, 38.75, 30.69, 26.50, 25.40, 21.14.

HRMS (ESI) calcd for $C_{20}H_{24}NO^{+}$ [(M+H)$^{+}$] 294.1852, found 294.1859.

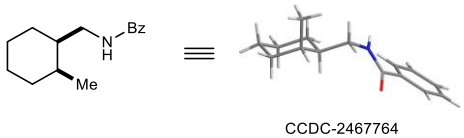

N-((cis-2-methylcyclohexyl)methyl)benzamide (**28**)

Following **Condition A**, 3.0 equivalents of alkene were used, **28** was obtained as white solid (30.2 mg, 65% yield, 14:1 cis/trans).

^{1}H NMR (600 MHz, Chloroform-d) δ 7.77 – 7.63 (m, 2H), 7.55 – 7.44 (m, 1H), 7.44 – 7.34 (m, 2H), 6.25 (brs, 1H), 3.42 – 3.18 (m, 2H), 1.94 – 1.86 (m, 1H), 1.82 – 1.74 (m, 1H), 1.70 – 1.60 (m, 1H), 1.52 – 1.42 (m, 4H), 1.41 – 1.31 (m, 2H), 1.31 – 1.18 (m, 1H), 0.92 (d, J = 7.2 Hz, 3H).

^{13}C NMR (151 MHz, Chloroform-d) δ 167.73, 135.02, 131.38, 128.62, 126.95, 42.44, 40.26, 32.51, 30.98, 25.75, 24.97, 21.87, 14.05.

HRMS (ESI) calcd for $C_{15}H_{22}NO^{+}$ [$(M+H)^{+}$] 232.1696, found 232.1700.

Crystal data and structure refinement for **28**

Identification code	**28**	
Empirical formula	C15 H21 N O	
Formula weight	231.33	
Temperature	173.00 K	
Wavelength	1.34139 Å	
Crystal system	Monoclinic	
Space group	Pn	
Unit cell dimensions	a = 5.17050(10) Å	α= 90°.
	b = 10.7104(3) Å	β= 92.5400(10)°.
	c = 11.9033(3) Å	γ = 90°.
Volume	658.53(3) Å^3	
Z	2	
Density (calculated)	1.167 Mg/m^3	
Absorption coefficient	0.371 mm^{-1}	
F(000)	252	
Crystal size	0.17 x 0.17 x 0.05 mm^3	
Theta range for data collection	3.590 to 63.560°.	

Index ranges	-6<=h<=6, -14<=k<=14, -15<=l<=15
Reflections collected	10244
Independent reflections	2853 [R(int) = 0.0547]
Completeness to theta = 53.594°	99.2 %
Absorption correction	None
Max. and min. transmission	0.7523 and 0.6421
Refinement method	Full-matrix least-squares on F^2
Data / restraints / parameters	2853 / 2 / 155
Goodness-of-fit on F^2	1.071
Final R indices [I>2sigma(I)]	R1 = 0.0629, wR2 = 0.1706
R indices (all data)	R1 = 0.0705, wR2 = 0.1786
Absolute structure parameter	0.4(2)
Extinction coefficient	n/a
Largest diff. peak and hole	0.562 and -0.246 e.$Å^{-3}$

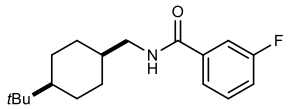

N-((cis-4-(tert-butyl)cyclohexyl)methyl)-3-fluorobenzamide (**29**)

Following **Condition A**, 3.0 equivalents of alkene were used, **29** was obtained as white solid (36.2 mg, 62% yield, > 20:1 cis/trans).

^{1}H NMR (600 MHz, Chloroform-d) δ 7.54 – 7.46 (m, 2H), 7.44 – 7.34 (m, 1H), 7.20 – 7.11 (m, 1H), 6.21 (brs, 1H), 3.59 – 3.39 (m, 2H), 2.03 – 1.89 (m, 1H), 1.83 – 1.66 (m, 2H), 1.58 – 1.53 (m, 2H), 1.53 – 1.46 (m, 2H), 1.22 – 1.11 (m, 2H), 1.08 – 0.95 (m, 1H), 0.84 (s, 9H).

^{13}C NMR (151 MHz, Chloroform-d) δ 166.47, 162.87 (d, J = 247.7 Hz), 137.28 (d, J = 6.6 Hz), 130.32 (d, J = 7.7 Hz), 122.42 (d, J = 3.1 Hz), 118.43 (d, J = 21.3 Hz), 114.44 (d, J = 22.6 Hz), 48.51, 41.43, 33.08, 32.69, 28.70, 27.60, 21.98.

^{19}F NMR (376 MHz, Chloroform-d) δ -111.90.

HRMS (ESI) calcd for $C_{18}H_{27}FNO^+$ [$(M+H)^+$] 292.2071, found 292.2081.

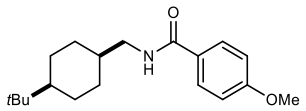

N-((cis-4-(tert-butyl)cyclohexyl)methyl)-4-methoxybenzamide (**30**)

Following **Condition A**, 3.0 equivalents of alkene were used, **30** was obtained as white solid (43.2 mg, 71% yield, > 20:1 cis/trans).

^{1}H NMR (600 MHz, Chloroform-d) δ 7.73 (d, J = 8.5 Hz, 2H), 6.89 (d, J = 8.5 Hz, 2H), 6.15 (brs, 1H), 3.83 (s, 3H), 3.56 – 3.34 (m, 2H), 2.02 – 1.87 (m, 1H), 1.79 – 1.67 (m, 2H), 1.60 – 1.52 (m, 2H), 1.50 – 1.43 (m, 2H), 1.22 – 1.11 (m, 2H), 1.03 – 0.92 (m, 1H), 0.83 (s, 9H).

^{13}C NMR (151 MHz, Chloroform-d) δ 167.24, 162.10, 128.74, 127.25, 113.78, 55.49, 48.53, 41.22, 33.14, 32.67, 28.73, 27.59, 21.99.

HRMS (ESI) calcd for $C_{19}H_{30}NO_2^+$ [$(M+H)^+$] 304.2271, found 304.2278.

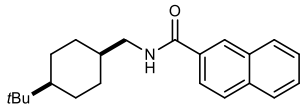

N-((cis-4-(tert-butyl)cyclohexyl)methyl)-2-naphthamide (**31**)

Following **Condition A**, 3.0 equivalents of alkene were used, **31** was obtained as white solid (42.1 mg, 65% yield, > 20:1 cis/trans).

^{1}H NMR (600 MHz, Chloroform-d) δ 8.28 (s, 1H), 7.92 – 7.78 (m, 4H), 7.60 – 7.44 (m, 2H), 6.36 (brs, 1H), 3.59 – 3.29 (m, 2H), 2.05 – 1.93 (m, 1H), 1.89 – 1.74 (m, 2H), 1.68 – 1.46 (m, 4H), 1.30 – 1.15 (m, 2H), 1.05 – 0.97 (m, 1H), 0.86 (s, 9H).

^{13}C NMR (151 MHz, Chloroform-d) δ 167.80, 134.76, 132.75, 132.20, 128.99, 128.53, 127.85, 127.66, 127.35, 126.83, 123.72, 48.55, 41.44, 33.18, 32.70, 28.77, 27.62, 22.02.

HRMS (ESI) calcd for $C_{22}H_{30}NO^+$ [$(M+H)^+$] 324.2322, found 324.2335.

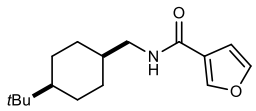

N-((cis-4-(tert-butyl)cyclohexyl)methyl)furan-3-carboxamide (**32**)

Following **Condition A**, 3.0 equivalents of alkene were used, **32** was obtained as white solid (27.4 mg, 52% yield, 18:1 cis/trans).

^{1}H NMR (600 MHz, Chloroform-d) δ 7.93 – 7.76 (m, 1H), 7.49 – 7.35 (m, 1H), 7.35 – 7.30 (m, 1H), 5.98 (brs, 1H), 3.58 – 3.28 (m, 2H), 1.95 – 1.86 (m, 1H), 1.80 – 1.65 (m, 3H), 1.58 – 1.53 (m, 2H), 1.53 – 1.43 (m, 2H), 1.22 – 1.11 (m, 2H), 1.02 – 0.93 (m, 1H), 0.84 (s, 9H).

^{13}C NMR (151 MHz, Chloroform-d) δ 163.33, 137.90, 128.03, 126.60, 126.07, 48.54, 41.05, 33.19, 32.70, 28.71, 27.62, 22.00.

HRMS (ESI) calcd for $C_{16}H_{25}NO_2Na^+$ [$(M+Na)^+$] 296.1778, found 296.1786.

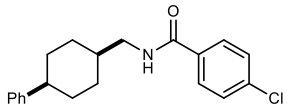

4-chloro-N-((cis-4-phenylcyclohexyl)methyl)benzamide (**33**)

Following **Condition A**, 3.0 equivalents of alkene were used, **33** was obtained as white solid (26.2 mg, 40% yield, > 20:1 cis/trans).

^{1}H NMR (400 MHz, Chloroform-d) δ 7.76 – 7.62 (m, 2H), 7.41 – 7.34 (m, 2H), 7.34 – 7.27 (m, 2H), 7.27 – 7.22 (m, 2H), 7.22 – 7.14 (m, 1H), 6.32 (brs, 1H), 3.70 – 3.31 (m, 2H), 2.66 – 2.53 (m, 1H), 2.08 – 1.96 (m, 1H), 1.84 – 1.57 (m, 8H).

^{13}C NMR (101 MHz, Chloroform-d) δ 166.77, 146.90, 137.67, 133.21, 128.90, 128.44, 127.02, 126.00, 43.32, 42.03, 33.57, 28.90, 28.02.

HRMS (ESI) calcd for $C_{20}H_{23}ClNO^+$ [$(M+H)^+$] 328.1463, found 328.1468.

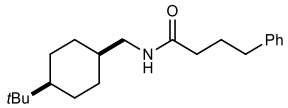

N-((cis-4-(tert-butyl)cyclohexyl)methyl)-4-phenylbutanamide (**34**)

Following **Condition A**, 3.0 equivalents of alkene were used, **34** was obtained as white

solid (40.1 mg, 63% yield, > 20:1 cis/trans).

^{1}H NMR (600 MHz, Chloroform-d) δ 7.30 – 7.26 (m, 2H), 7.22 – 7.15 (m, 3H), 5.37 (brs, 1H), 3.50 – 3.05 (m, 2H), 2.65 (t, J = 7.5 Hz, 2H), 2.17 (t, J = 7.5 Hz, 2H), 2.02 – 1.92 (m, 2H), 1.81 – 1.73 (m, 1H), 1.69 – 1.60 (m, 2H), 1.55 – 1.49 (m, 2H), 1.49 – 1.40 (m, 2H), 1.17 – 1.06 (m, 2H), 1.05 – 0.92 (m, 1H), 0.83 (s, 9H).

^{13}C NMR (151 MHz, Chloroform-d) δ 172.80, 141.68, 128.64, 128.51, 126.08, 48.52, 40.74, 36.14, 35.33, 33.05, 32.68, 28.66, 27.60, 27.33, 21.93.

HRMS (ESI) calcd for $C_{21}H_{34}NO^+$ [$(M+H)^+$] 316.2635, found 316.2643.

Part I (with Condition B):

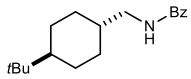

N-((trans-4-(tert-butyl)cyclohexyl)methyl)benzamide (**4**)

Following **Condition B**, **4** was obtained as white solid (42.8 mg, 78% yield, 13:1 trans/cis).

^{1}H NMR (500 MHz, Chloroform-d) δ 7.84 – 7.67 (m, 2H), 7.56 – 7.47 (m, 1H), 7.45 – 7.38 (m, 2H), 6.27 (brs, 1H), 3.32 – 3.18 (m, 2H), 2.12 – 1.70 (m, 4H), 1.64 – 1.43 (m, 1H), 1.07 – 0.92 (m, 5H), 0.83 (s, 9H).

^{13}C NMR (126 MHz, Chloroform-d) δ 167.73, 135.09, 131.40, 128.66, 126.97, 48.19, 46.36, 38.28, 32.54, 31.47, 27.67, 26.91.

HRMS (ESI) calcd for $C_{18}H_{28}NO^+$ [$(M+H)^+$] 274.2165, found 274.2178.

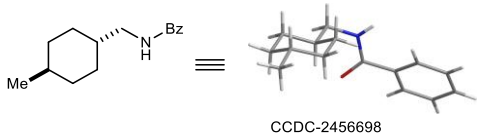

N-((trans-4-methylcyclohexyl)methyl)benzamide (**15**)

Following **Condition B**, 3.0 equivalents of alkene were used, **15** was obtained as white solid (33.4 mg, 72% yield, 7.9:1 trans/cis).

^{1}H NMR (500 MHz, Chloroform-d) δ 7.78 – 7.67 (m, 2H), 7.57 – 7.45 (m, 1H), 7.44 – 7.32 (m, 2H), 6.34 (brs, 1H), 3.34 – 3.22 (m, 2H), 1.86 – 1.74 (m, 2H), 1.74 – 1.64 (m, 2H), 1.60 – 1.44 (m, 1H), 1.34 – 1.26 (m, 1H), 1.05 – 0.88 (m, 4H), 0.87 (d, J = 6.6 Hz, 3H).

^{13}C NMR (126 MHz, Chloroform-d) δ 167.73, 135.01, 131.40, 128.63, 126.97, 46.33, 37.94, 34.75, 32.78, 30.98, 22.69.

HRMS (ESI) calcd for $C_{15}H_{22}NO^{+}$ [$(M+H)^{+}$] 232.1696, found 232.1700.

Crystal data and structure refinement for **15**

Identification code	**15**	
Empirical formula	C15 H21 N O	
Formula weight	231.33	
Temperature	173.00 K	
Wavelength	1.34139 Å	
Crystal system	Orthorhombic	
Space group	$Pna2_1$	
Unit cell dimensions	a = 9.27820(10) Å	α= 90°.
	b = 12.5154(2) Å	β= 90°.
	c = 11.8770(2) Å	γ = 90°.
Volume	1379.16(4) $Å^3$	
Z	4	
Density (calculated)	1.114 Mg/m^3	
Absorption coefficient	0.354 mm^{-1}	
F(000)	504	
Crystal size	0.17 x 0.17 x 0.05 mm^3	
Theta range for data collection	5.163 to 54.855°.	
Index ranges	-11<=h<=10, -15<=k<=15, -14<=l<=11	
Reflections collected	11115	
Independent reflections	2401 [R(int) = 0.0352]	

Completeness to theta = 53.594°	99.3 %
Absorption correction	Semi-empirical from equivalents
Max. and min. transmission	0.7508 and 0.6627
Refinement method	Full-matrix least-squares on F^2
Data / restraints / parameters	2401 / 1 / 159
Goodness-of-fit on F^2	1.041
Final R indices [I>2sigma(I)]	R1 = 0.0284, wR2 = 0.0709
R indices (all data)	R1 = 0.0334, wR2 = 0.0734
Absolute structure parameter	0.35(13)
Extinction coefficient	n/a
Largest diff. peak and hole	0.126 and -0.108 e.$Å^{-3}$

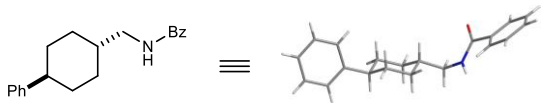

CCDC-2456699

N-((trans-4-phenylcyclohexyl)methyl)benzamide (**16**)

Following **Condition B**, **16** was obtained as white solid (45.2 mg, 77% yield, 10:1 trans/cis).

^{1}H NMR (500 MHz, Chloroform-d) δ 7.85 – 7.70 (m, 2H), 7.55 – 7.47 (m, 1H), 7.44 (dd, J = 8.2, 6.6 Hz, 2H), 7.36 – 7.27 (m, 2H), 7.23 – 7.13 (m, 3H), 6.25 (brs, 1H), 3.47 – 3.27 (m, 2H), 2.50 (tt, J = 12.3, 3.2 Hz, 1H), 2.05 – 1.87 (m, 4H), 1.78 – 1.62 (m, 1H), 1.56 – 1.41 (m, 2H), 1.34 – 1.12 (m, 2H).

^{13}C NMR (126 MHz, Chloroform-d) δ 167.76, 147.36, 134.99, 131.52, 128.73, 128.48, 126.98, 126.93, 126.12, 46.30, 44.46, 37.91, 33.78, 31.27.

HRMS (ESI) calcd for $C_{20}H_{24}NO^+$ [$(M+H)^+$] 294.1852, found 294.1859.

Crystal data and structure refinement for **16**

Identification code	**16**
Empirical formula	C20 H23 N O

Formula weight	293.39	
Temperature	173.00 K	
Wavelength	1.34139 Å	
Crystal system	Orthorhombic	
Space group	Fdd2	
Unit cell dimensions	a = 19.9053(4) Å	α= 90°.
	b = 61.9989(12) Å	β= 90°.
	c = 5.18930(10) Å	γ = 90°.
Volume	6404.1(2) $Å^3$	
Z	16	
Density (calculated)	1.217 Mg/m^3	
Absorption coefficient	0.380 mm^{-1}	
F(000)	2528	
Crystal size	0.17 x 0.17 x 0.05 mm^3	
Theta range for data collection	4.059 to 54.860°.	
Index ranges	-23<=h<=24, -74<=k<=74, -6<=l<=5	
Reflections collected	14385	
Independent reflections	2914 [R(int) = 0.0493]	
Completeness to theta = 53.594°	99.0 %	
Absorption correction	Semi-empirical from equivalents	
Max. and min. transmission	0.7508 and 0.5743	
Refinement method	Full-matrix least-squares on F^2	
Data / restraints / parameters	2914 / 1 / 199	
Goodness-of-fit on F^2	1.048	
Final R indices [I>2sigma(I)]	R1 = 0.0350, wR2 = 0.0865	
R indices (all data)	R1 = 0.0376, wR2 = 0.0885	
Absolute structure parameter	-0.25(19)	

Extinction coefficient	n/a
Largest diff. peak and hole	0.183 and -0.160 e.Å^{-3}

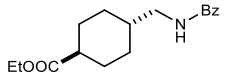

ethyl trans-4-(benzamidomethyl)cyclohexane-1-carboxylate (**17**)

Following **Condition B**, **17** was obtained as light-yellow oil (35.9 mg, 62% yield, 4.1:1 trans/cis).

^{1}H NMR (600 MHz, Chloroform-d) δ 7.76 – 7.62 (m, 2H), 7.53 – 7.46 (m, 1H), 7.45 – 7.37 (m, 2H), 6.28 (brs, 1H), 4.10 (q, J = 7.1 Hz, 2H), 3.31 (t, J = 6.5 Hz, 2H), 2.23 (tt, J = 12.2, 3.5 Hz, 1H), 2.11 – 1.97 (m, 2H), 1.93 – 1.81 (m, 2H), 1.69 – 1.53 (m, 1H), 1.42 (qd, J = 13.1, 3.5 Hz, 2H), 1.24 (t, J = 7.1 Hz, 3H), 1.04 (qd, J = 13.1, 3.5 Hz, 2H).

^{13}C NMR (151 MHz, Chloroform-d) δ 176.04, 167.77, 134.83, 131.54, 128.70, 126.97, 60.35, 45.98, 43.38, 37.59, 30.00, 28.53, 14.34.

HRMS (ESI) calcd for $C_{17}H_{23}NO_3Na^+$ [$(M+Na)^+$] 312.1570, found 312.1572.

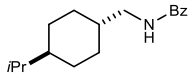

N-((trans-4-isopropylcyclohexyl)methyl)benzamide (**18**)

Following **Condition B**, **18** was obtained as white solid (41.1 mg, 79% yield, 11:1 trans/cis).

^{1}H NMR (500 MHz, Chloroform-d) δ 7.87 – 7.64 (m, 2H), 7.55 – 7.44 (m, 1H), 7.44 – 7.38 (m, 2H), 6.25 (brs, 1H), 3.56 – 3.26 (m, 2H), 1.90 – 1.70 (m, 1H), 1.66 – 1.31 (m, 9H), 1.14 – 1.03 (m, 1H), 0.86 (d, J = 6.7 Hz, 6H).

^{13}C NMR (126 MHz, Chloroform-d) δ 167.73, 135.01, 131.40, 128.64, 126.96, 43.03, 42.98, 35.10, 30.54, 27.46, 25.59, 20.40.

HRMS (ESI) calcd for $C_{17}H_{26}NO^+$ [$(M+H)^+$] 260.2009, found 260.2015.

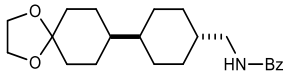

N-((trans-4-(1,4-dioxaspiro[4.5]decan-8-yl)cyclohexyl)methyl)benzamide (**19**)

Following **Condition B**, **19** was obtained as white solid (48.7 mg, 68% yield, 8.0:1 trans/cis).

^{1}H NMR (400 MHz, Chloroform-d) δ 7.90 – 7.60 (m, 2H), 7.57 – 7.46 (m, 1H), 7.45 – 7.36 (m, 2H), 6.23 (brs, 1H), 3.93 (s, 4H), 3.29 (t, J = 6.4 Hz, 2H), 1.88 – 1.62 (m, 8H), 1.56 – 1.40 (m, 4H), 1.35 – 1.17 (m, 2H), 1.11 (p, J = 5.2, 4.3 Hz, 2H), 1.06 – 0.91 (m, 3H).

^{13}C NMR (151 MHz, Chloroform-d) δ 167.72, 134.99, 131.46, 128.69, 126.96, 109.26, 64.34, 64.29, 46.33, 42.45, 42.00, 38.29, 34.98, 31.17, 29.66, 27.27.

HRMS (ESI) calcd for $C_{22}H_{32}NO_3^+$ [$(M+H)^+$] 358.2377, found 358.2378.

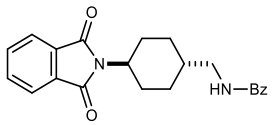

N-((trans-4-(1,3-dioxoisoindolin-2-yl)cyclohexyl)methyl)benzamide (**20**)

Following **Condition B**, **20** was obtained as white solid (42.9 mg, 59% yield, 6.4:1 trans/cis).

^{1}H NMR (500 MHz, Chloroform-d) δ 7.85 – 7.76 (m, 4H), 7.73 – 7.65 (m, 2H), 7.50 (t, J = 7.4 Hz, 1H), 7.47 – 7.39 (m, 2H), 6.25 (brs, 1H), 4.12 (tt, J = 12.4, 4.0 Hz, 1H), 3.37 (t, J = 6.4 Hz, 2H), 2.52 – 2.19 (m, 2H), 2.06 – 1.87 (m, 2H), 1.85 – 1.71 (m, 3H), 1.24 – 1.14 (m, 2H).

^{13}C NMR (126 MHz, Chloroform-d) δ 168.54, 167.77, 134.85, 133.97, 132.12, 131.57, 128.74, 126.98, 123.20, 50.64, 45.79, 37.13, 30.24, 29.04.

HRMS (ESI) calcd for $C_{22}H_{22}N_2O_3Na^+$ [$(M+Na)^+$] 385.1523, found 385.1524.

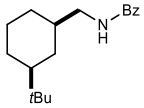

N-((cis-3-(tert-butyl)cyclohexyl)methyl)benzamide (**21**)

Following **Condition B**, **21** was obtained as white solid (30.7 mg, 56% yield, 11:1 cis/trans).

^{1}H NMR (500 MHz, Chloroform-d) δ 7.83 – 7.64 (m, 2H), 7.51 – 7.46 (m, 1H), 7.46 – 7.38 (m, 2H), 6.27 (brs, 1H), 3.42 – 3.10 (m, 2H), 2.08 – 1.70 (m, 4H), 1.64 – 1.51 (m, 1H), 1.31 – 1.14 (m, 2H), 1.11 – 0.98 (m, 1H), 0.97 – 0.86 (m, 1H), 0.84 (s, 9H), 0.75 – 0.65 (m, 1H).

^{13}C NMR (126 MHz, Chloroform-d) δ 167.74, 135.10, 131.42, 128.68, 126.97, 47.71, 46.73, 38.72, 32.63, 32.06, 31.05, 27.65, 27.33, 26.31.

HRMS (ESI) calcd for $C_{18}H_{28}NO^+$ [$(M+H)^+$] 274.2165, found 274.2178.

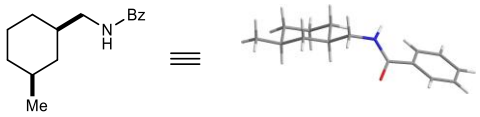

CCDC-2456700

N-((cis-3-methylcyclohexyl)methyl)benzamide (**22**)

Following **Condition B**, 3.0 equivalents of alkene were used, **22** was obtained as white solid (30.6 mg, 66% yield, 9.1:1 cis/trans).

^{1}H NMR (500 MHz, Chloroform-d) δ 7.91 – 7.65 (m, 2H), 7.55 – 7.44 (m, 1H), 7.44 – 7.37 (m, 2H), 6.36 (brs, 1H), 3.42 – 3.17 (m, 2H), 1.83 – 1.70 (m, 3H), 1.69 – 1.63 (m, 1H), 1.63 – 1.54 (m, 1H), 1.41 – 1.32 (m, 1H), 1.30 – 1.19 (m, 1H), 0.97 – 0.75 (m, 5H), 0.63 (q, J = 12.1 Hz, 1H).

^{13}C NMR (126 MHz, Chloroform-d) δ 167.71, 134.99, 131.40, 128.63, 126.98, 46.43, 39.75, 38.22, 35.19, 32.42, 30.64, 25.89, 22.95.

HRMS (ESI) calcd for $C_{15}H_{22}NO^+$ [$(M+H)^+$] 232.1696, found 232.1700.

Crystal data and structure refinement for **22**

Identification code	**22**
Empirical formula	C15 H21 N O
Formula weight	231.33
Temperature	173.00 K
Wavelength	1.34139 Å

Crystal system	Monoclinic
Space group	P 1 21/n 1
Unit cell dimensions	a = 5.15980(10) Å α= 90°.
	b = 24.1702(5) Å β= 101.1060(10)°.
	c = 10.6833(2) Å γ = 90°.
Volume	1307.40(4) $Å^3$
Z	4
Density (calculated)	1.175 Mg/m^3
Absorption coefficient	0.374 mm^{-1}
F(000)	504
Crystal size	0.17 x 0.17 x 0.05 mm^3
Theta range for data collection	3.181 to 54.895°.
Index ranges	-6<=h<=4, -29<=k<=29, -13<=l<=12
Reflections collected	15431
Independent reflections	2413 [R(int) = 0.0403]
Completeness to theta = 53.594°	96.9 %
Absorption correction	Semi-empirical from equivalents
Max. and min. transmission	0.7508 and 0.6575
Refinement method	Full-matrix least-squares on F^2
Data / restraints / parameters	2413 / 0 / 155
Goodness-of-fit on F^2	1.036
Final R indices [I>2sigma(I)]	R1 = 0.0608, wR2 = 0.1612
R indices (all data)	R1 = 0.0699, wR2 = 0.1702
Extinction coefficient	n/a
Largest diff. peak and hole	0.763 and -0.306 $e.Å^{-3}$

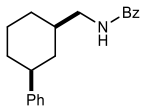

N-((cis-3-phenylcyclohexyl)methyl)benzamide (**23**)

Following **Condition B**, **23** was obtained as white solid (44.2 mg, 75% yield, 10:1 cis/trans).

^{1}H NMR (500 MHz, Chloroform-d) δ 7.83 – 7.64 (m, 2H), 7.51 – 7.45 (m, 1H), 7.44 – 7.37 (m, 2H), 7.33 – 7.26 (m, 2H), 7.22 – 7.13 (m, 3H), 6.26 (brs, 1H), 3.46 – 3.27 (m, 2H), 2.55 (tt, J = 12.0, 3.4 Hz, 1H), 2.01 – 1.94 (m, 1H), 1.94 – 1.85 (m, 3H), 1.85 – 1.75 (m, 1H), 1.55 – 1.35 (m, 2H), 1.24 – 1.11 (m, 1H), 1.11 – 0.96 (m, 1H).

^{13}C NMR (126 MHz, Chloroform-d) δ 167.70, 147.31, 134.93, 131.48, 128.68, 128.52, 126.97, 126.93, 126.18, 46.37, 44.08, 38.82, 38.58, 34.21, 30.59, 26.19.

HRMS (ESI) calcd for $C_{20}H_{24}NO^+$ [$(M+H)^+$] 294.1852, found 294.1859.

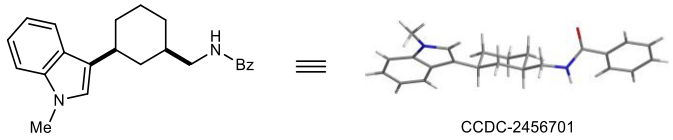

N-((cis-3-(1-methyl-1H-indol-3-yl)cyclohexyl)methyl)benzamide (**24**)

Following **Condition B**, **24** was obtained as light-yellow oil (50.7 mg, 73% yield, 8.1:1 cis/trans).

^{1}H NMR (500 MHz, Chloroform-d) δ 7.77 (d, J = 7.6 Hz, 2H), 7.64 (d, J = 7.9 Hz, 1H), 7.51 – 7.45 (m, 1H), 7.45 – 7.38 (m, 2H), 7.29 (d, J = 8.2 Hz, 1H), 7.25 – 7.19 (m, 1H), 7.14 – 7.05 (m, 1H), 6.82 (s, 1H), 6.36 (brs, 1H), 3.73 (s, 3H), 3.46 – 3.26 (m, 2H), 3.02 – 2.82 (m, 1H), 2.30 – 2.09 (m, 2H), 1.98 – 1.81 (m, 3H), 1.57 – 1.38 (m, 2H), 1.34 – 1.19 (m, 1H), 1.16 – 1.03 (m, 1H).

^{13}C NMR (126 MHz, Chloroform-d) δ 167.75, 137.08, 134.93, 131.41, 128.63, 126.99, 126.96, 124.53, 121.53, 120.97, 119.33, 118.54, 109.35, 46.34, 38.58, 38.47, 34.92, 34.11, 32.67, 30.83, 26.23.

HRMS (ESI) calcd for $C_{23}H_{27}N_2O^+$ [$(M+H)^+$] 347.2118, found 347.2119.

Crystal data and structure refinement for **24**

Identification code	**24**	
Empirical formula	C23 H26 N2 O	
Formula weight	346.46	
Temperature	173.00 K	
Wavelength	1.34139 Å	
Crystal system	Monoclinic	
Space group	P 1 21/c 1	
Unit cell dimensions	a = 13.0639(15) Å	α= 90°.
	b = 5.0429(6) Å	β= 98.463(4)°.
	c = 28.831(3) Å	γ = 90°.
Volume	1878.7(4) $Å^3$	
Z	4	
Density (calculated)	1.225 Mg/m^3	
Absorption coefficient	0.386 mm^{-1}	
F(000)	744	
Crystal size	0.17 x 0.17 x 0.05 mm^3	
Theta range for data collection	2.975 to 55.256°.	
Index ranges	-15<=h<=15, -6<=k<=5, -35<=l<=35	
Reflections collected	16481	
Independent reflections	3575 [R(int) = 0.0652]	
Completeness to theta = 53.594°	99.5 %	
Absorption correction	Semi-empirical from equivalents	
Max. and min. transmission	0.7508 and 0.5447	
Refinement method	Full-matrix least-squares on F^2	
Data / restraints / parameters	3575 / 0 / 236	
Goodness-of-fit on F^2	1.119	
Final R indices [I>2sigma(I)]	R1 = 0.0759, wR2 = 0.1952	

R indices (all data)	R1 = 0.0995, wR2 = 0.2081
Extinction coefficient	n/a
Largest diff. peak and hole	0.306 and -0.273 e.Å^{-3}

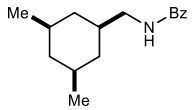

cis,cis-N-((3,5-dimethylcyclohexyl)methyl)benzamide (**26**)

Following **Condition B**, 3.0 equivalents of alkene were used, **26** was obtained as white solid (24.7 mg, 50% yield, 11:1 fs).

^{1}H NMR (400 MHz, Chloroform-d) δ 7.75 – 7.57 (m, 2H), 7.44 – 7.38 (m, 1H), 7.38 – 7.29 (m, 2H), 6.30 (brs, 1H), 3.25 – 3.11 (m, 2H), 1.76 – 1.52 (m, 4H), 1.44 – 1.27 (m, 2H), 0.81 (d, J = 6.5 Hz, 6H), 0.57 – 0.36 (m, 3H).

^{13}C NMR (101 MHz, Chloroform-d) δ 167.69, 134.94, 131.43, 128.65, 126.98, 46.29, 44.08, 39.27, 38.02, 32.15, 22.76.

HRMS (ESI) calcd for $C_{16}H_{24}NO^{+}$ [$(M+H)^{+}$] 246.1852, found 246.1853.

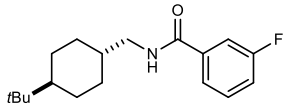

N-((trans-4-(tert-butyl)cyclohexyl)methyl)-3-fluorobenzamide (**35**)

Following **Condition B**, 3.0 equivalents of alkene were used, **35** was obtained as white solid (44.3 mg, 76% yield, 16:1 trans/cis).

^{1}H NMR (600 MHz, Chloroform-d) δ 7.57 – 7.46 (m, 2H), 7.41 – 7.32 (m, 1H), 7.19 – 7.09 (m, 1H), 6.39 (brs, 1H), 3.34 – 3.08 (m, 2H), 1.95 – 1.70 (m, 4H), 1.58 – 1.40 (m, 1H), 1.04 – 0.92 (m, 5H), 0.82 (s, 9H).

^{13}C NMR (151 MHz, Chloroform-d) δ 166.49 (d, J = 2.7 Hz), 162.85 (d, J = 247.7 Hz), 137.30 (d, J = 6.6 Hz), 130.29 (d, J = 7.9 Hz), 122.45 (d, J = 3.2 Hz), 118.39 (d, J = 21.2 Hz), 114.44 (d, J = 22.9 Hz), 48.13, 46.45, 38.18, 32.52, 31.43, 27.65, 26.85.

^{19}F NMR (376 MHz, Chloroform-d) δ -111.91.

HRMS (ESI) calcd for $C_{18}H_{27}FNO^{+}$ [$(M+H)^{+}$] 292.2071, found 292.2081.

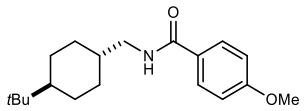

N-((trans-4-(tert-butyl)cyclohexyl)methyl)-4-methoxybenzamide (**36**)

Following **Condition B**, 3.0 equivalents of alkene were used, **36** was obtained as white solid (49.3 mg, 81% yield, 16:1 trans/cis).

^{1}H NMR (600 MHz, Chloroform-d) δ 7.73 (d, J = 8.8 Hz, 2H), 6.90 (d, J = 8.8 Hz, 2H), 6.26 (brs, 1H), 3.83 (s, 3H), 3.34 – 3.18 (m, 2H), 1.88 – 1.71 (m, 4H), 1.52 – 1.40 (m, 1H), 1.01 – 0.92 (m, 5H), 0.82 (s, 9H).

^{13}C NMR (151 MHz, Chloroform-d) δ 167.23, 162.10, 128.75, 127.29, 113.78, 55.49, 48.15, 46.28, 38.26, 32.51, 31.44, 27.65, 26.87.

HRMS (ESI) calcd for $C_{19}H_{30}NO_2^+$ [$(M+H)^+$] 304.2271, found 304.2278.

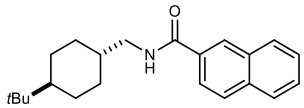

N-((trans-4-(tert-butyl)cyclohexyl)methyl)-2-naphthamide (**37**)

Following **Condition B**, 3.0 equivalents of alkene were used, **37** was obtained as white solid (50.6 mg, 78% yield, 15:1 trans/cis).

^{1}H NMR (600 MHz, Chloroform-d) δ 8.27 (s, 1H), 7.92 – 7.75 (m, 4H), 7.67 – 7.46 (m, 2H), 6.49 (brs, 0H), 3.62 – 2.85 (m, 2H), 1.92 – 1.85 (m, 2H), 1.85 – 1.76 (m, 2H), 1.57 – 1.51 (m, 1H), 1.04 – 0.94 (m, 5H), 0.84 (s, 9H).

^{13}C NMR (151 MHz, Chloroform-d) δ 167.80, 134.75, 132.74, 132.25, 128.99, 128.52, 127.85, 127.64, 127.34, 126.81, 123.75, 48.14, 46.48, 38.27, 32.53, 31.48, 27.66, 26.88.

HRMS (ESI) calcd for $C_{22}H_{30}NO^+$ [$(M+H)^+$] 324.2322, found 324.2335.

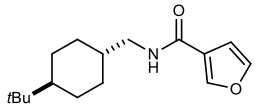

N-((trans-4-(tert-butyl)cyclohexyl)methyl)furan-3-carboxamide (**38**)

Following **Condition B**, 3.0 equivalents of alkene were used, **38** was obtained as white solid (33.8 mg, 64% yield, 13:1 trans/cis).

^{1}H NMR (600 MHz, Chloroform-d) δ 8.01 – 7.78 (m, 1H), 7.48 – 7.34 (m, 1H), 7.34 – 7.28 (m, 1H), 6.24 (brs, 1H), 3.36 – 3.07 (m, 2H), 2.12 – 1.71 (m, 4H), 1.58 – 1.41 (m, 1H), 1.07 – 0.91 (m, 5H), 0.82 (s, 9H).

^{13}C NMR (151 MHz, Chloroform-d) δ 163.35, 137.91, 128.03, 126.51, 126.15, 48.14, 46.08, 38.25, 32.52, 31.43, 27.66, 26.87.

HRMS (ESI) calcd for $C_{16}H_{25}NO_2Na^+$ [$(M+Na)^+$] 296.1778, found 296.1786.

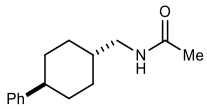

N-((trans-4-phenylcyclohexyl)methyl)acetamide (**39**)

Following **Condition B**, 3.0 equivalents of alkene were used, **39** was obtained as white solid (36.2 mg, 78% yield, 14:1 trans/cis).

^{1}H NMR (500 MHz, Chloroform-d) δ 7.35 – 7.26 (m, 2H), 7.24 – 7.15 (m, 3H), 5.73 (brs, 1H), 3.20 – 3.11 (m, 2H), 2.47 (tt, J = 12.3, 3.4 Hz, 1H), 2.00 (s, 3H), 1.97 – 1.84 (m, 4H), 1.61 – 1.52 (m, 1H), 1.52 – 1.40 (m, 2H), 1.21 – 1.05 (m, 2H).

^{13}C NMR (126 MHz, Chloroform-d) δ 170.36, 147.33, 128.44, 126.88, 126.08, 45.90, 44.39, 37.69, 33.72, 31.13, 23.50.

HRMS (ESI) calcd for $C_{15}H_{22}NO^+$ [$(M+H)^+$] 232.1696, found 232.1700.

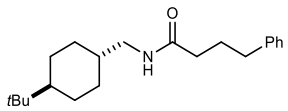

N-((trans-4-(tert-butyl)cyclohexyl)methyl)-4-phenylbutanamide (**40**)

Following **Condition B**, 3.0 equivalents of alkene were used, **40** was obtained as white solid (50.5 mg, 80% yield, 16:1 trans/cis).

^{1}H NMR (600 MHz, Chloroform-d) δ 7.31 – 7.24 (m, 2H), 7.21 – 7.11 (m, 3H), 5.46 (brs, 1H), 3.15 – 2.97 (m, 2H), 2.63 (t, J = 7.6 Hz, 2H), 2.15 (t, J = 7.6 Hz, 2H), 2.04 – 1.88 (m, 2H), 1.78 – 1.63 (m, 4H), 1.38 – 1.29 (m, 1H), 1.05 – 0.85 (m, 5H), 0.81 (s,

9H).

^{13}C NMR (151 MHz, Chloroform-d) δ 172.78, 141.68, 128.63, 128.51, 126.08, 48.15, 45.80, 38.15, 36.15, 35.34, 32.53, 31.37, 27.66, 27.36, 26.86.

HRMS (ESI) calcd for $C_{21}H_{34}NO^+$ [$(M+H)^+$] 316.2635, found 316.2643.

Additional Experiments

Capture of metal-nitrenoid intermediate

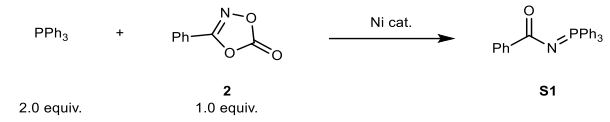

condition A	72% yield of **S1**
w/o Ni catalyst	*Not found*
condition B	78% yield of **S1**
w/o Ni catalyst	*Not found*

Under Conditions A/B: In the air, a 10 mL Schlenk flask equipped with a magnetic stirrer was charged with $NiCl_2$(DME) (0.02 mmol, 10 mol%), Ligand (0.024 mmol, 12 mol%), potassium fluoride (0.6 mmol, 3.0 equiv.), **2** (0.2 mmol, 1.0 equiv.) and PPh_3 (0.4 mmol, 2.0 equiv.). The Schlenk flask was evacuated and backfilled with argon three times, then DMAc (1.5 mL) was added, the solution was stirred for 2 min at 0 °C. Then, $(MeO)_3SiH$ (0.6 mmol, 3.0 equiv.) was added dropwise via syringe. After that, the reaction mixture was stirred at 25 °C for 12 h. The reaction mixture was diluted with H_2O and extracted with EtOAc. The organic layer was dried over anhydrous Na_2SO_4 and concentrated in vacuo. The residue was purified by flash column chromatography on silica gel to give the target product **S1** as a white solid.

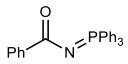

N-(triphenyl-λ^5-phosphaneylidene)benzamide (**S1**)

^{1}H NMR (500 MHz, Chloroform-d) δ 8.51 – 8.20 (m, 2H), 8.10 – 7.79 (m, 6H), 7.70 – 7.54 (m, 3H), 7.54 – 7.36 (m, 9H).

^{13}C NMR (126 MHz, Chloroform-d) δ 176.37, 133.29 (d, J = 10.0 Hz), 132.38, 132.36, 130.85, 129.64, 129.62, 128.80 (d, J = 12.2 Hz), 127.78.

^{31}P NMR (202 MHz, Chloroform-d) δ 20.73.

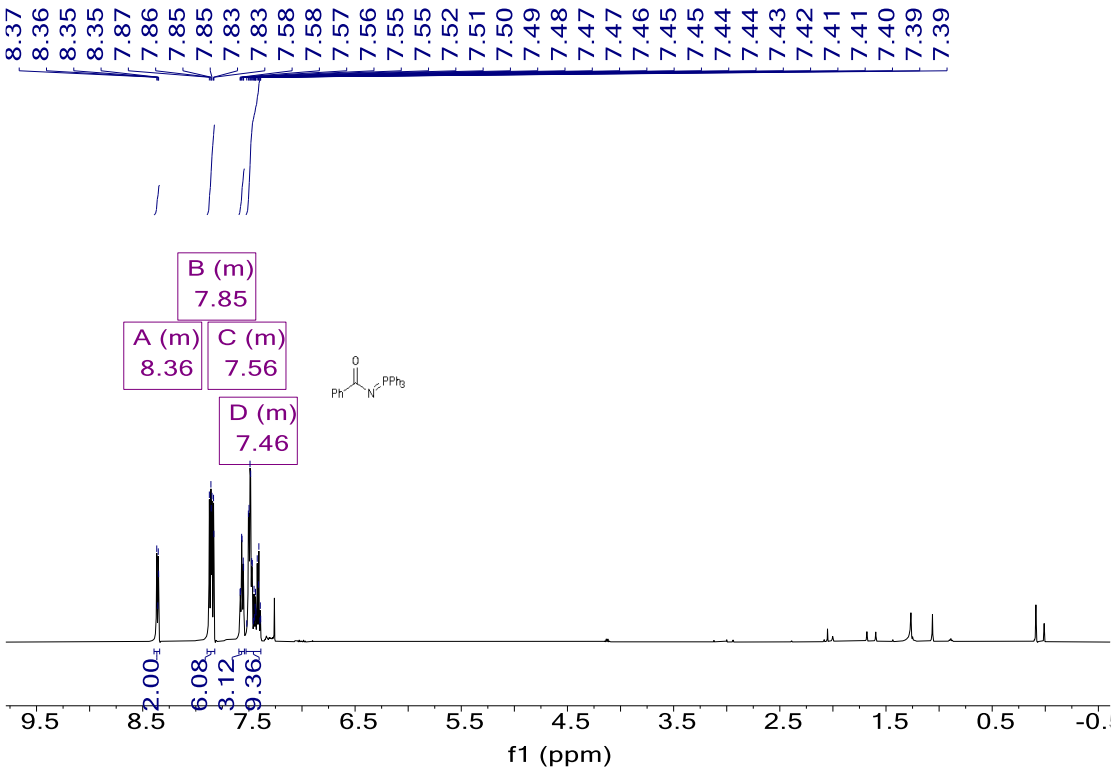

^{1}H-NMR of **S1**

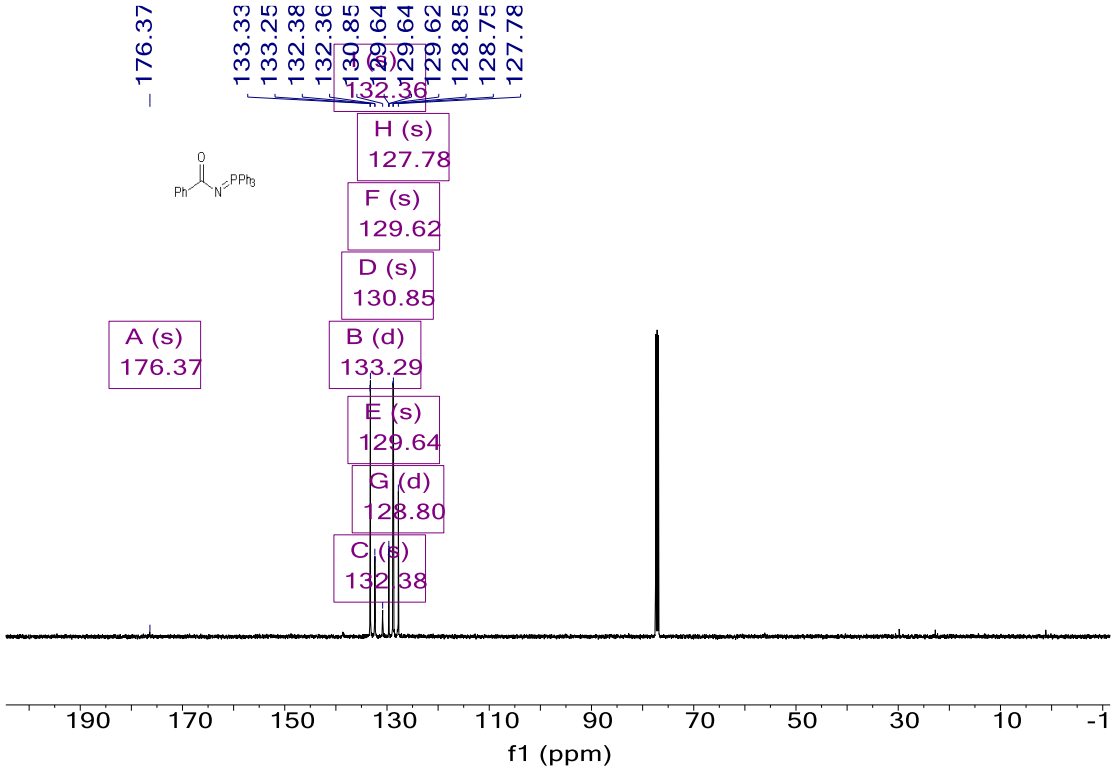

^{13}C-NMR of **S1**

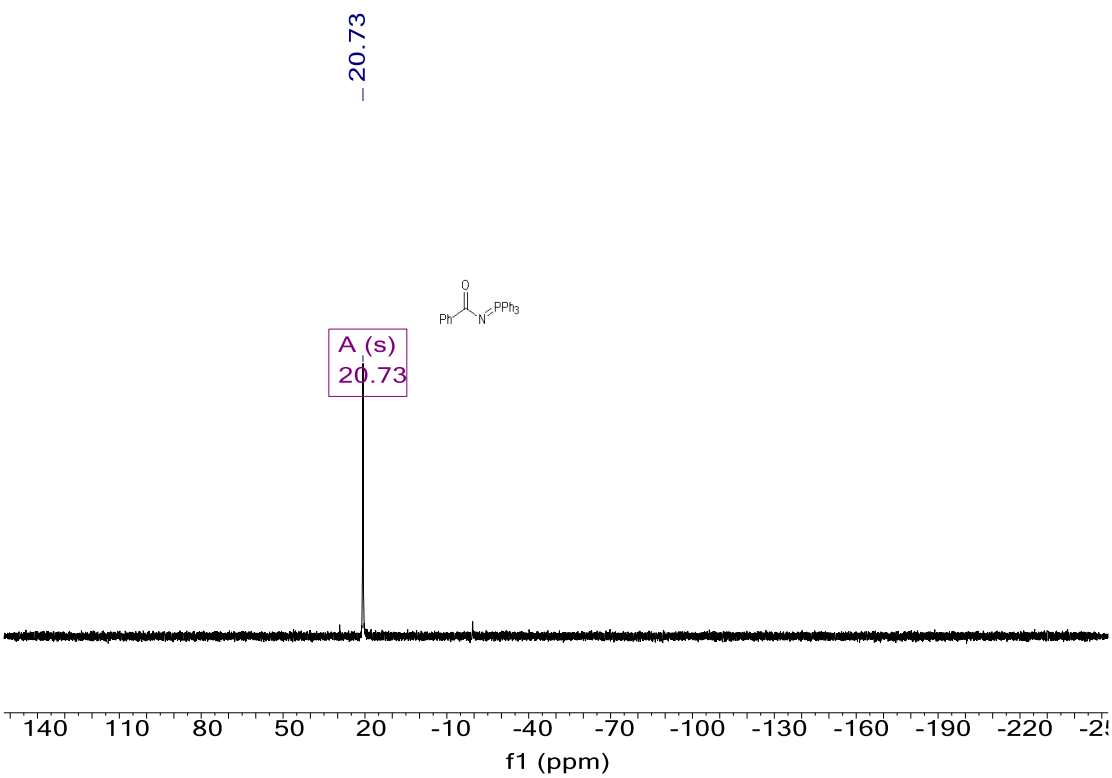
20.73
A (s)
20.73
Ph
O
N
PPh3
140
110
80
50
20
-10
-40
-70
-100
-130
-160
-190
-220
f1 (ppm)

^{31}P-NMR of **S1**

Hydrogenation of methylenecyclohexanes

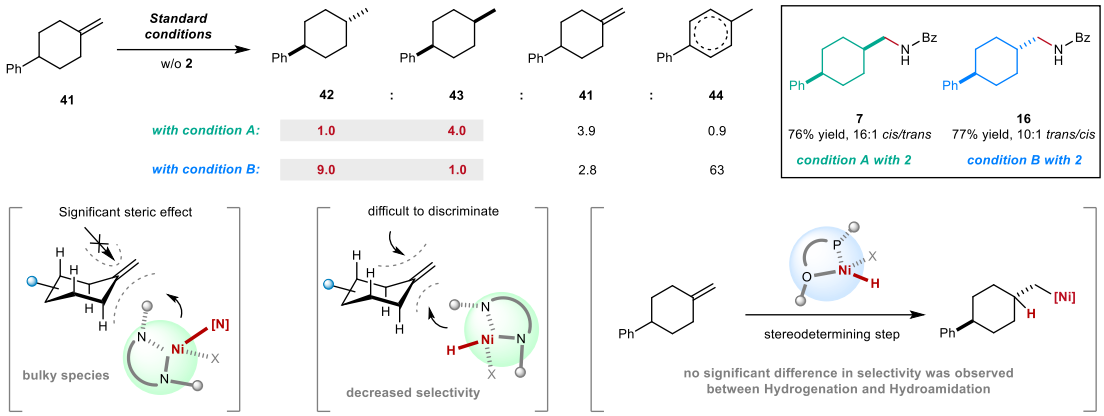

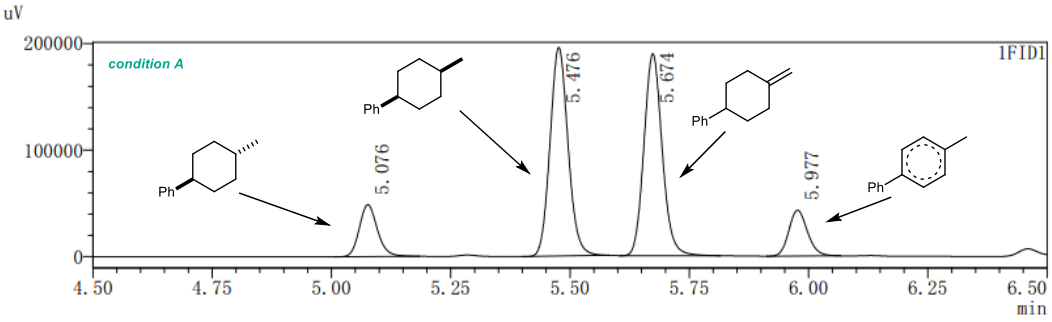

FID1

1	5.076	128729	48634	10.166	M
2	5.476	515224	195316	40.687	M
3	5.674	505114	188795	39.888	M
4	5.977	117258	42838	9.260	M
总计		1266324	475583		

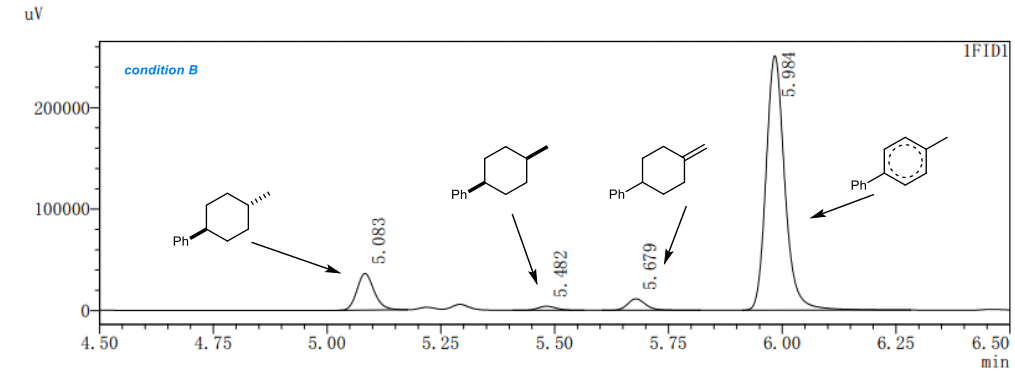

FID1

1	5.083	94845	35778	11.100	M
2	5.482	10789	3965	1.263	M
3	5.679	31282	11272	3.661	M
4	5.984	717526	248785	83.976	M
总计		854442	299801		

GC analysis

To gain deeper insights into the stereodivergent hydroamidation reaction, hydrogenation experiments were conducted using alkene **41** as the substrate in the absence of dioxazolones under both condition A and condition B. Under both reaction

conditions, the alkene hydrogenation product was observed along with partial residual starting material, while a substantial amount of alkene isomerization product was detected under condition B. Notably, under condition A, the *cis/trans* selectivity of the hydrogenation product (4.0:1) was significantly reduced compared to that of hydroamidation product (**7**), whereas no substantial difference in *cis/trans* selectivity was observed between the two products under condition B. These results suggest that distinct catalytically active species may be involved in the two hydroamidation catalytic systems.

Stereodivergent hydroamination to access 1,2-isomers via cobalt catalysis

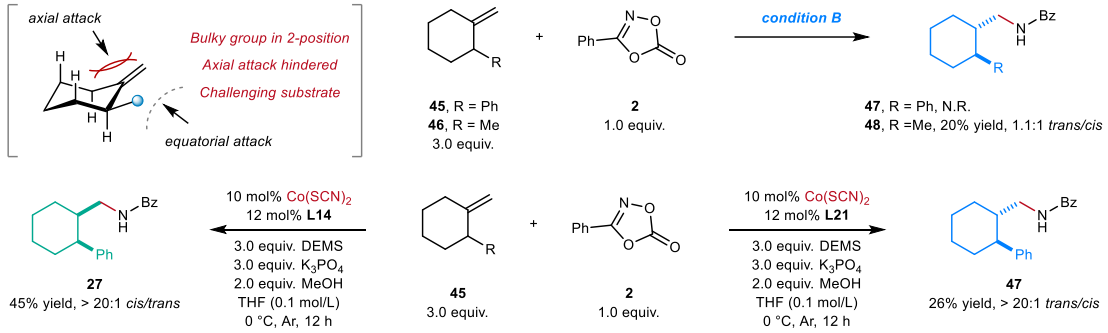

We analyzed the differences between the nickel catalytic system developed in this work and the previously established cobalt catalytic system through the hydroamidation of 2-substituted methylenecyclohexanes. In the context of stereodivergent hydrogenation of exocyclic unsaturations, substrates with bulky substituents at the 2-position including not only methylenecyclohexanes but also 2-substituted cyclohexanones pose significant challenges. The underlying reason is that axial attack is hindered by the bulky group at the 2-position.[17] As expected, our nickel catalytic system exclusively afforded 1,2-cis isomers via equatorial attack. Moreover, the combination of sterically hindered SadPhos ligand and the mechanism involving alkene insertion into Ni-N active species resulted in a complete inability to obtain 1,2-*trans* selective products. In contrast, cobalt-catalyzed systems exhibit remarkable stereocontrol and achieve stereodivergent hydroamination, which may involve alkene insertion into Co-H active species.

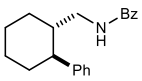

N-((*trans*-2-phenylcyclohexyl)methyl)benzamide (**47**)

1H NMR (400 MHz, Chloroform-d) δ 7.64 – 6.70 (m, 10H), 5.65 (brs, 1H), 3.44 – 3.23 (m, 1H), 3.15 – 2.85 (m, 1H), 2.45 – 2.17 (m, 1H), 2.06 – 1.90 (m, 1H), 1.90 – 1.71 (m, 3H), 1.63 – 1.44 (m, 1H), 1.42 – 1.00 (m, 4H).

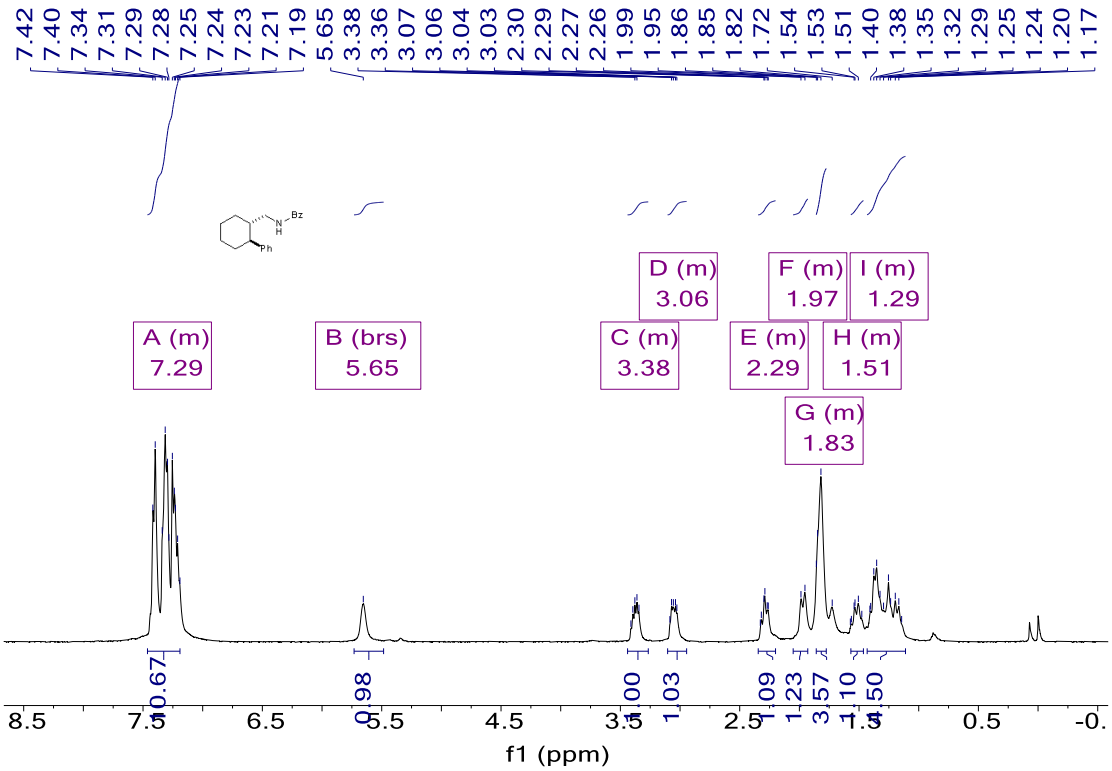
7.42 7.40 7.34 7.31 7.29 7.28 7.25 7.24 7.23 7.21 7.19 5.65 3.38 3.36 3.07 3.06 3.04 3.03 2.30 2.29 2.27 2.26 1.99 1.95 1.86 1.85 1.82 1.72 1.54 1.53 1.51 1.40 1.38 1.35 1.32 1.29 1.25 1.24 1.20 1.17
A (m) 7.29
B (brs) 5.65
C (m) 3.38
D (m) 3.06
E (m) 2.29
F (m) 1.97
G (m) 1.83
H (m) 1.51
I (m) 1.29
10.67 0.98 1.00 1.03 1.09 1.23 3.57 1.10 4.50
8.5 7.5 6.5 5.5 4.5 3.5 2.5 1.5 0.5 -0.
f1 (ppm)

^{1}H-NMR of **47**

DFT Calculations

Computational Methods

All calculations were performed with Gaussian 16 suite of programs[18]. The B3LYP functional[19-21] including Grimme empirical dispersion correction (D3BJ)[22,23] was used for the geometry optimization of all species. The SDD basis set[24,25] was used for nickel and the 6-31G(d) basis set was used for the other atoms. Frequency calculations were conducted at the same level of theory to confirm the stationary point as energy minimum (no imaginary frequency) or transition state (one imaginary frequency), and to obtain thermal corrections. The single-point calculations of the optimized geometries were computed by using M06 functional[26] with the SDD basis set for Ni atom and the 6-311+G(d,p) for the other atoms. The solvent effects were evaluated with the SMD[27] model using DMAc as the solvent. The non-covalent interactions of transition states were analyzed by the independent gradient model based on Hirshfeld partition (IGMH) method[28] through Multiwfn[29] software. Fragment distortion and interaction energies were computed at the M06/6-311+G(d,p)-SDD level of theory.

N-activation by L1-Ni^{I}-H species

The activation of dioxazolone starts from the active catalyst **L1-Ni^{I}-H**, from which the dioxazolone **2** coordinates with the Ni center to generate intermediate **L1-CP1**. The activation occurs through transition state **L1-TS1** and then produce the Ni-nitrenoid intermediate **L1-CP2**. Therefore, the N-activation from **L1-Ni^{I}-H** only has an energy barrier of 7.8 kcal/mol, and is highly exergonic by 37.6 kcal/mol.

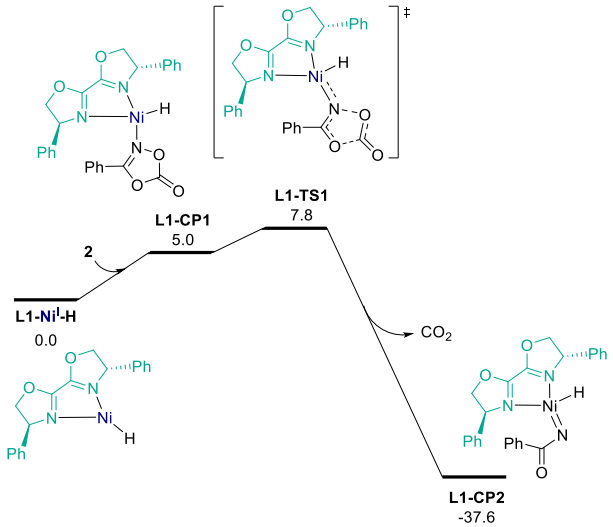

Fig. S8. The Gibbs free energy profiles of N-activation from **L1-Ni^{I}-H** species.

Hydronickelation of olefin from L1-Ni^{I}-H species

As shown in **Fig. S9**, coordination of methylenecyclohexane **1** to the Ni center of active catalyst **L1-Ni^{I}-H** would form two possible intermediates **L1-CP3-*cis*** and **L1-CP3-*trans***, which then undergo hydronickelation to generate alkyl-Ni^{I} intermediates **L1-CP4-*cis*** and **L1-CP4-*trans***. The hydronickelation of methylenecyclohexane **1** by **L1-Ni^{I}-H** requires about 20 kcal/mol energy barrier, and the energies of two competing transition states are comparable.

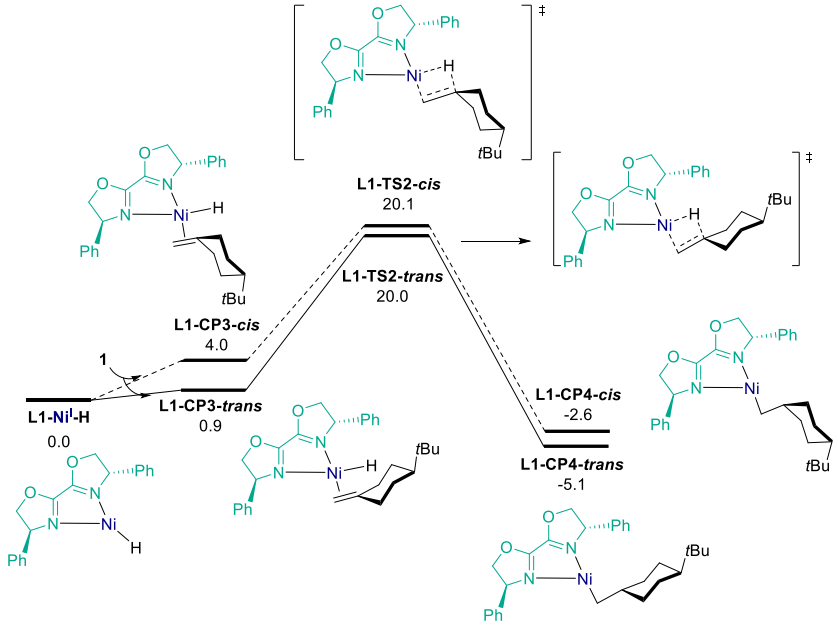

Fig. S9. The Gibbs free energy profiles of hydronickelation of olefin by **L1-Ni^{I}-H** species.

Hydronickelation of olefin from neutral L1-Ni^{II}-H species

Starting from the neutral **L1-Ni^{II}-H** active catalyst, hydronickelation of methylenecyclohexane **1** through transition state **L1-TS3-*cis*** and **L1-TS3-*trans*** would deliver the 1,4-*cis*/*trans* intermediates **L1-CP5-*cis*** and **L1-CP5-*trans***. The energy of **L1-TS3-*trans*** is 1.5 kcal/mol lower than that of **L1-TS3-*cis***.

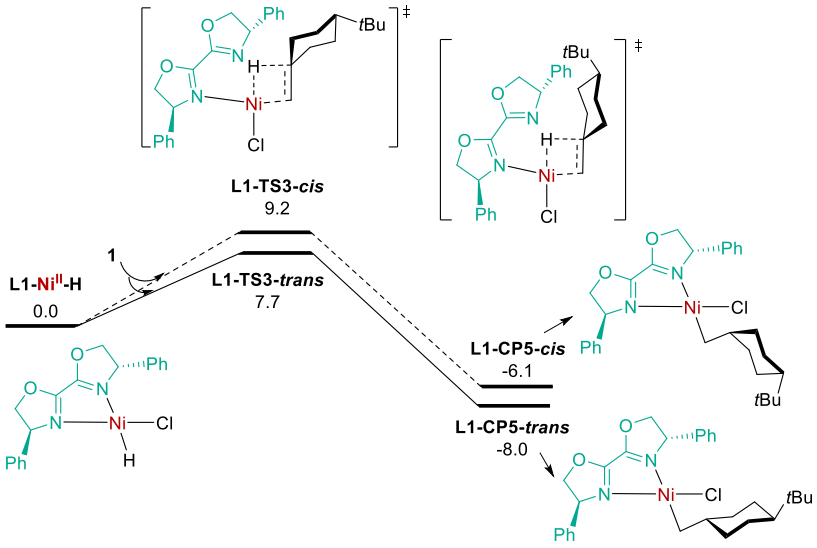

Fig. S10. The Gibbs free energy profiles of hydronickelation of olefin by neutral **L1-Ni^{II}-H** species.

Summary on the calculated results of L1-Ni catalytic system

The above computational explorations of hydronickelation suggest that hydronickelation of olefin by Ni^{II} is more favorable than that by Ni^{I} (**Fig. S9** and **S10**). Moreover, activation of dioxazolone is thermodynamically more favored than the olefin hydronickelation by Ni^{II} (**Fig. S8** and **S10**). Therefore, we proposed that Cl-Ni^{II}-NHCOPh is the active species in **L1-Ni** catalytic system, in accordance with researches of Yin and Chang[8,30].

N-activation by L30-Ni^{I}-H species

The dioxazolone activation starts from active catalyst **L30-Ni^{I}-H**, from which dioxazolone **2** coordinates with the Ni center to generate intermediate **L30-CP1**. The activation proceeds via transition state **L30-TS1** and forms the Ni-nitrenoid intermediate **L30-CP2**. Therefore, the N-activation by **L30-Ni^{I}-H** requires an energy barrier of 8.3 kcal/mol, and is highly exergonic by 35.0 kcal/mol.

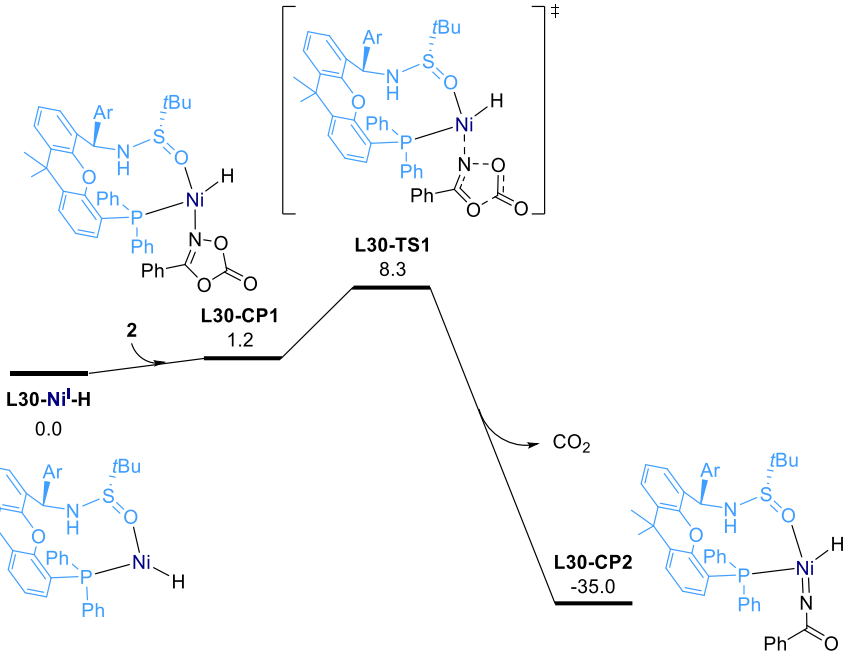

Fig. S11. The Gibbs free energy profiles of N-activation from **L30-Ni^{I}-H** species.

Hydronickelation of olefin from L30-Ni^{I}-H species

As shown in **Fig. S12**, coordination of methylenecyclohexane **1** to the Ni center of active catalyst **L30-Ni^{I}-H** would form two possible intermediates **L30-CP3-*cis*** and **L30-CP3-t*rans***, which then undergo hydronickelation to generate alkyl-Ni^{I} intermediates **L30-CP4-*cis*** and **L30-CP4-*trans***. The hydronickelation via **L30-TS2-*trans*** giving 1,4-*trans* intermediate is more preferred than that via **L30-TS2-*cis*** giving 1,4-*cis* intermediate.

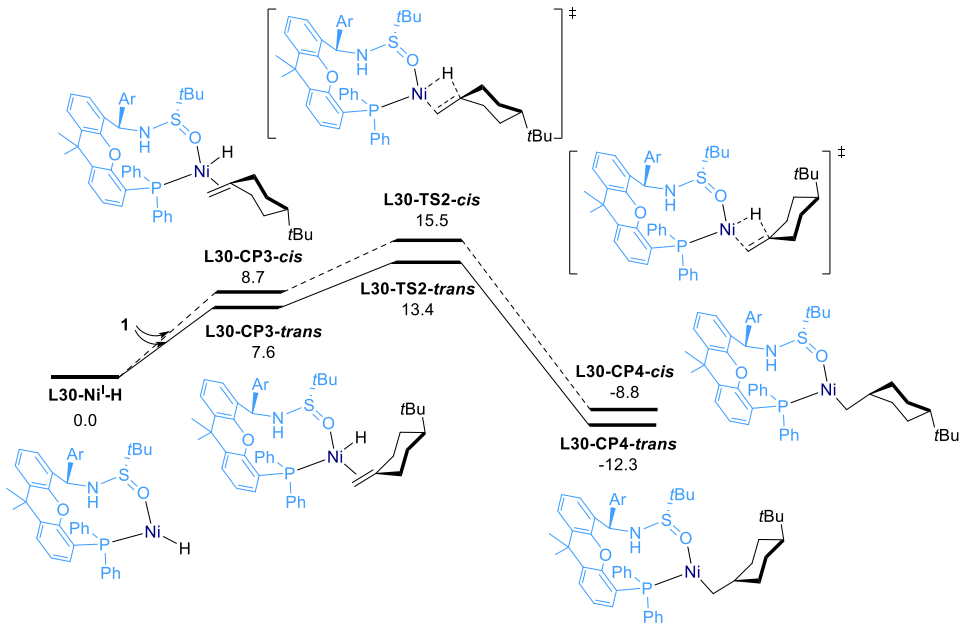

Fig. S12. The Gibbs free energy profiles of hydronickelation of olefin by **L30-Ni^{I}-H** species.

Hydronickelation of olefin from neutral L30-Ni^{II}-H species

Starting from the neutral **L30-Ni^{II}-H** active catalyst, hydronickelation of methylenecyclohexane **1** through transition state **L30-TS3-*cis*** and **L30-TS3-*trans*** would deliver the 1,4-*cis*/*trans* intermediates. The energy of **L30-TS3-*trans*** is 1.7 kcal/mol lower than that of **L30-TS3-*cis***.

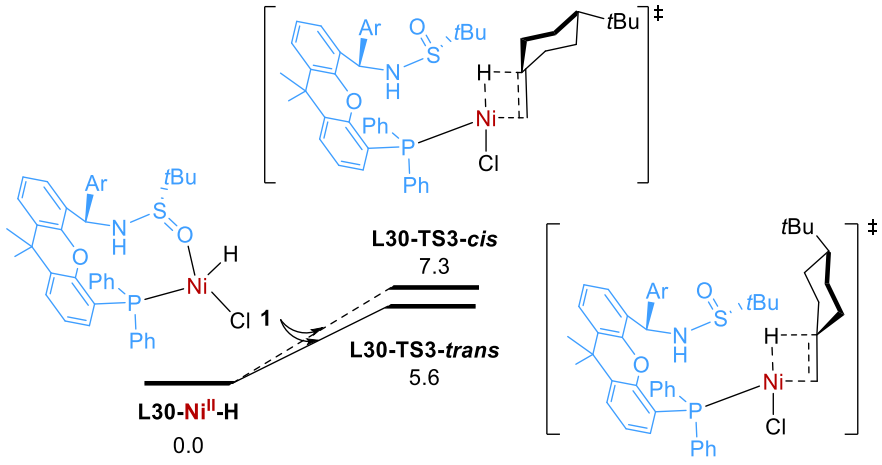

Fig. S13. The Gibbs free energy profiles of hydronickelation of olefin by neutral **L30-Ni^{II}-H** species.

Summary on the calculated results of L30-Ni catalytic system

In accordance with the calculated results of **L1-Ni** catalytic system, hydronickelation of olefin by Ni^{II} is more favorable than that by Ni^{I} (**Fig. S12** and **S13**). However, hydronickelation by Ni^{II} is more facile than dioxazolone activation (**Fig. S11** and **S13**). Therefore, Cl-Ni^{II}-H is proposed the active species in L30-Ni catalytic system.

Table 3. Thermal corrections of Gibbs free energies (TCG, hartree) and total electronic energies (E, hartree) in DMAc solvent for optimized species calculated at the M06/6-311+G(d,p)-SDD/ SMD//B3LYP/D3(BJ)/6-31G(d)-SDD level of theory.

Compounds	TCG	E
1	0.252005	-430.979196829
2	0.085123	-588.050676374
CO2	-0.008204	-188.561258488
L1-Ni^{I}-H	0.259396	-1126.62620045
L1-Ni^{II}-H	0.265345	-1586.89687852
L1-Ni^{II}-NHCOPh	0.366820	-1986.52214347
L1-CP1	0.369840	-1714.69428451
L1-TS1	0.366991	-1714.68695170
L1-CP2	0.356197	-1526.17908619
L1-CP3-*cis*	0.534288	-1557.62196807
L1-CP3-*trans*	0.536987	-1557.62953694
L1-TS2-*cis*	0.539261	-1557.60114783
L1-TS2-*trans*	0.541614	-1557.60364839
L1-CP4-*cis*	0.542010	-1557.64023439
L1-CP4-*trans*	0.541204	-1557.64326526
L1-TS3-*cis*	0.540692	-2017.88469226
L1-TS3-*trans*	0.542867	-2017.88928104
L1-CP5-*cis*	0.546319	-2017.91471487
L1-CP5-*trans*	0.544372	-2017.91583516
L1-TS4-*cis*	0.642342	-2417.47415561

L1-TS4-*trans*	0.644167	-2417.46210152
L30-Ni^{I}-H	0.626109	-2625.70769332
L30-Ni^{II}-H	0.633043	-3085.97866495
L30-CP1	0.737202	-3213.78238328
L30-TS1	0.734918	-3213.76888380
L30-CP2	0.727700	-3025.26113155
L30-CP3-cis	0.906203	-3056.70103818
L30-CP3-*trans*	0.911029	-3056.70769353
L30-TS2-*cis*	0.906977	-3056.69103783
L30-TS2-*trans*	0.909019	-3056.69638930
L30-CP4-*cis*	0.910262	-3056.73309328
L30-CP4-*trans*	0.908384	-3056.73671157
L30-TS3-*cis*	0.909789	-3516.97089370
L30-TS3-*trans*	0.911169	-3516.97503952

Supplementary Figures

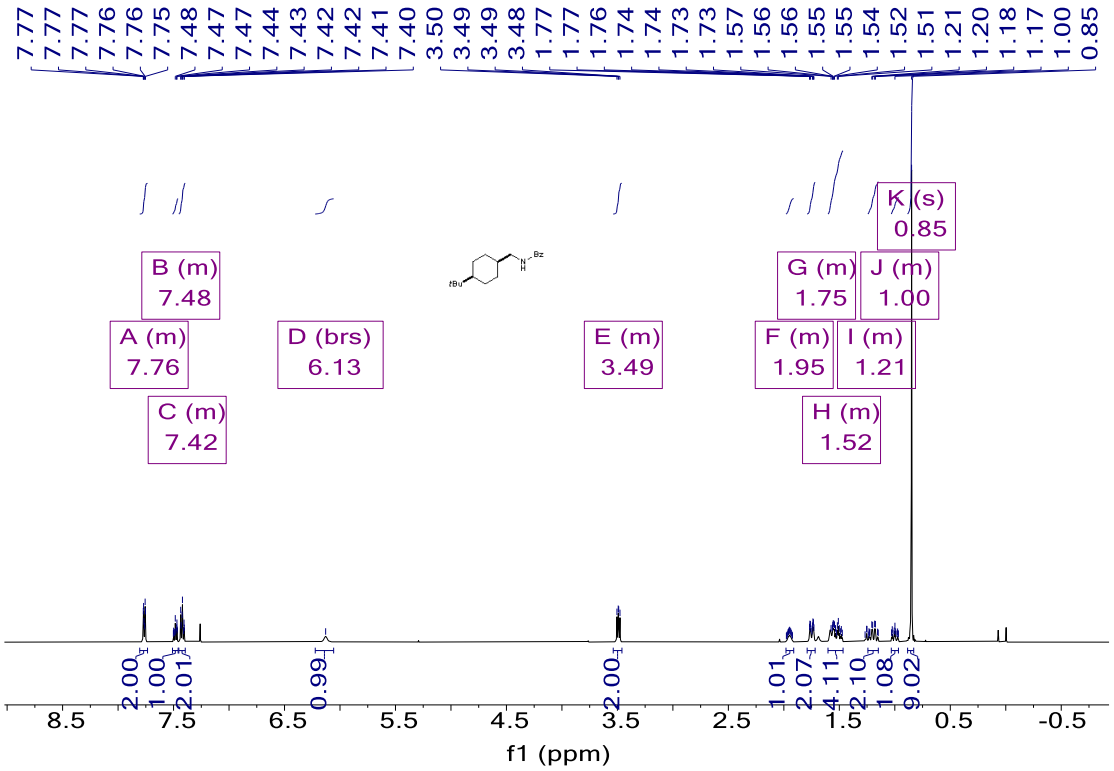

^{1}H-NMR of **3**

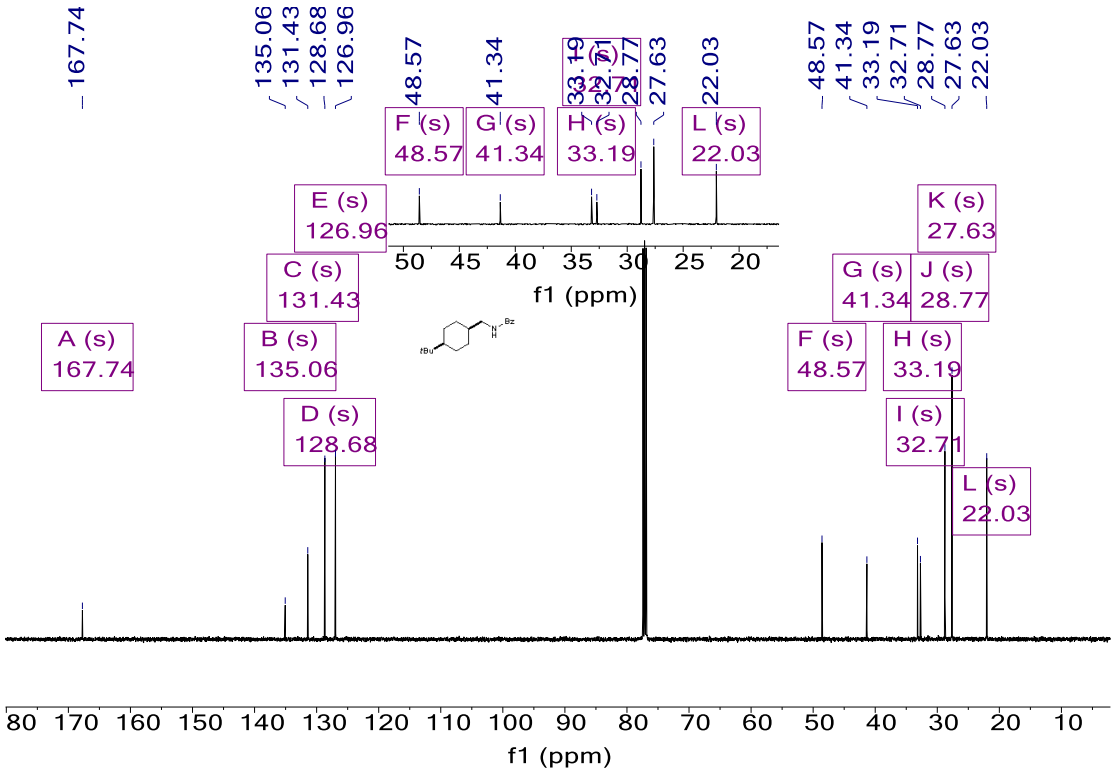

^{13}C-NMR of **3**

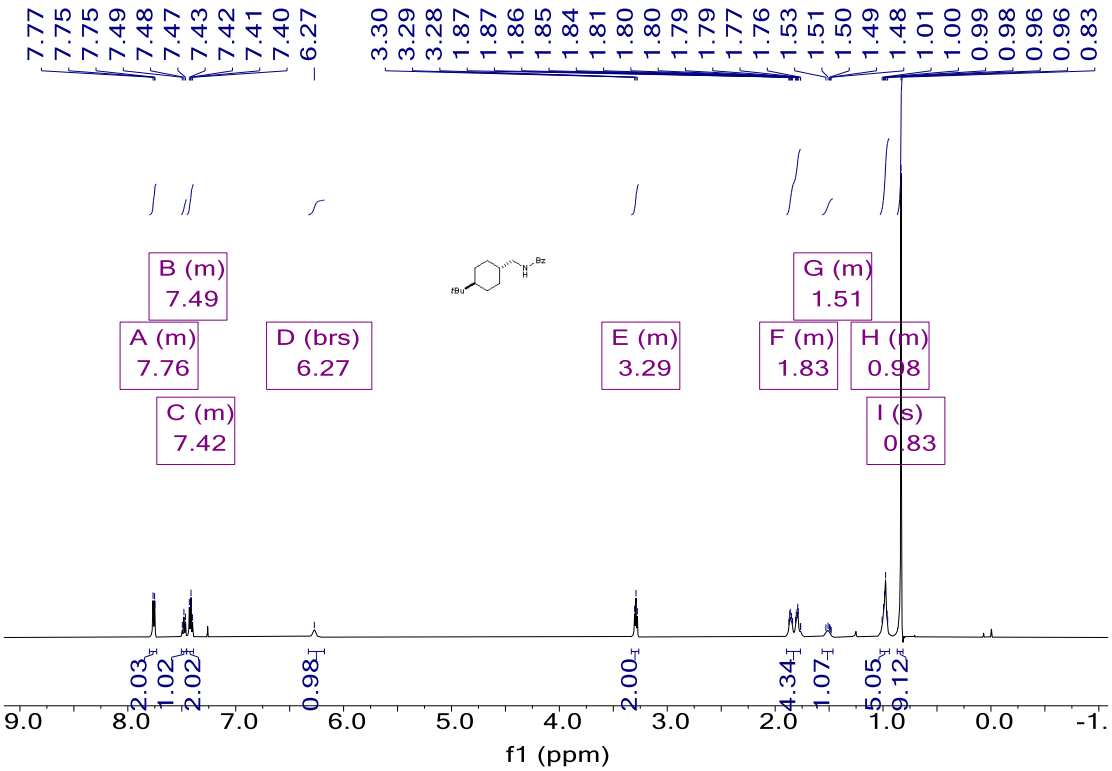

^{1}H-NMR of **4**

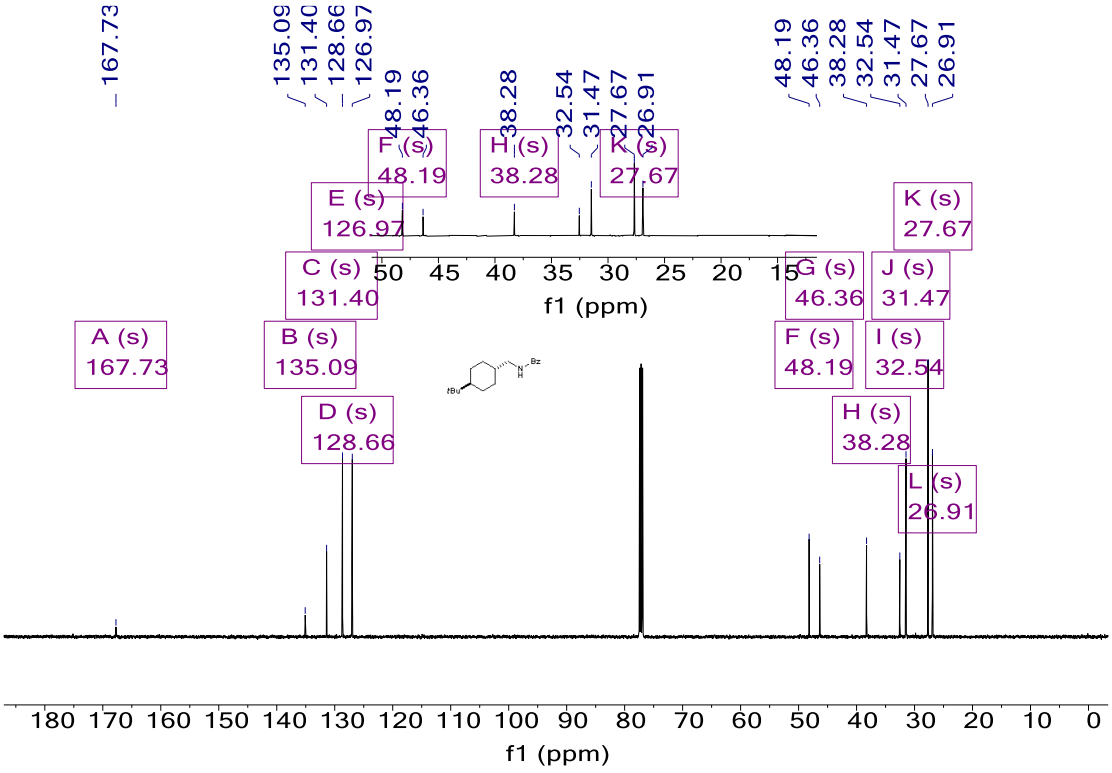

^{13}C-NMR of **4**

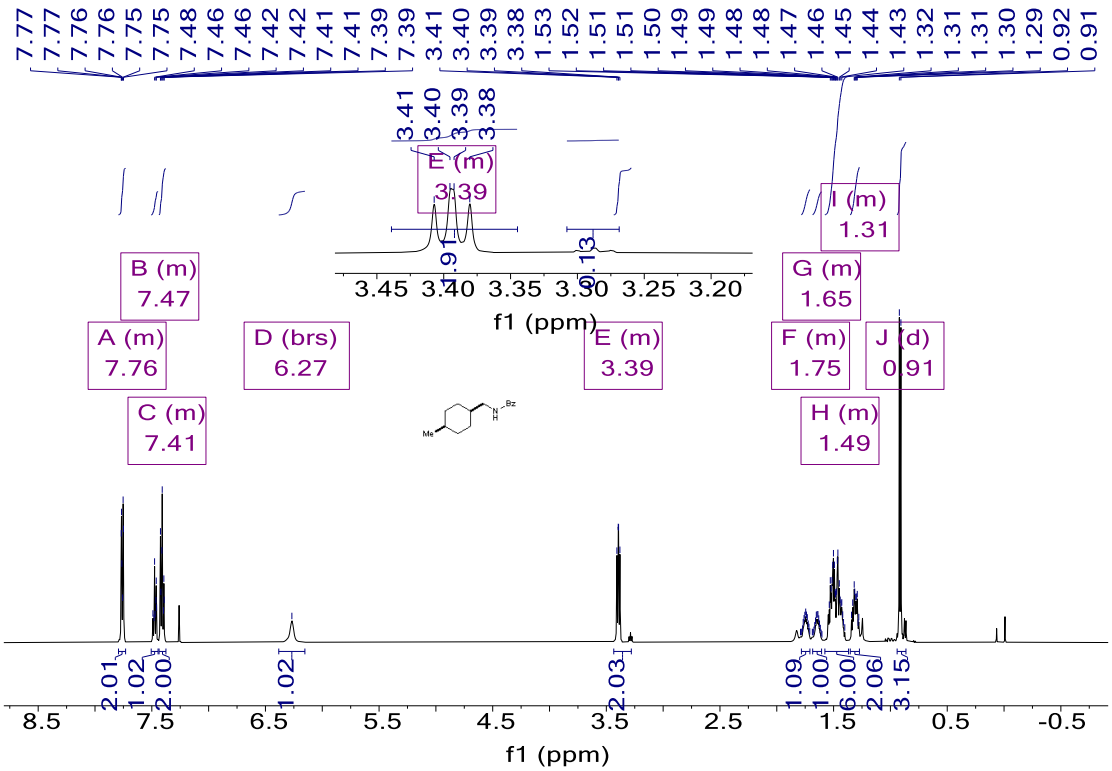

^{1}H-NMR of **5**

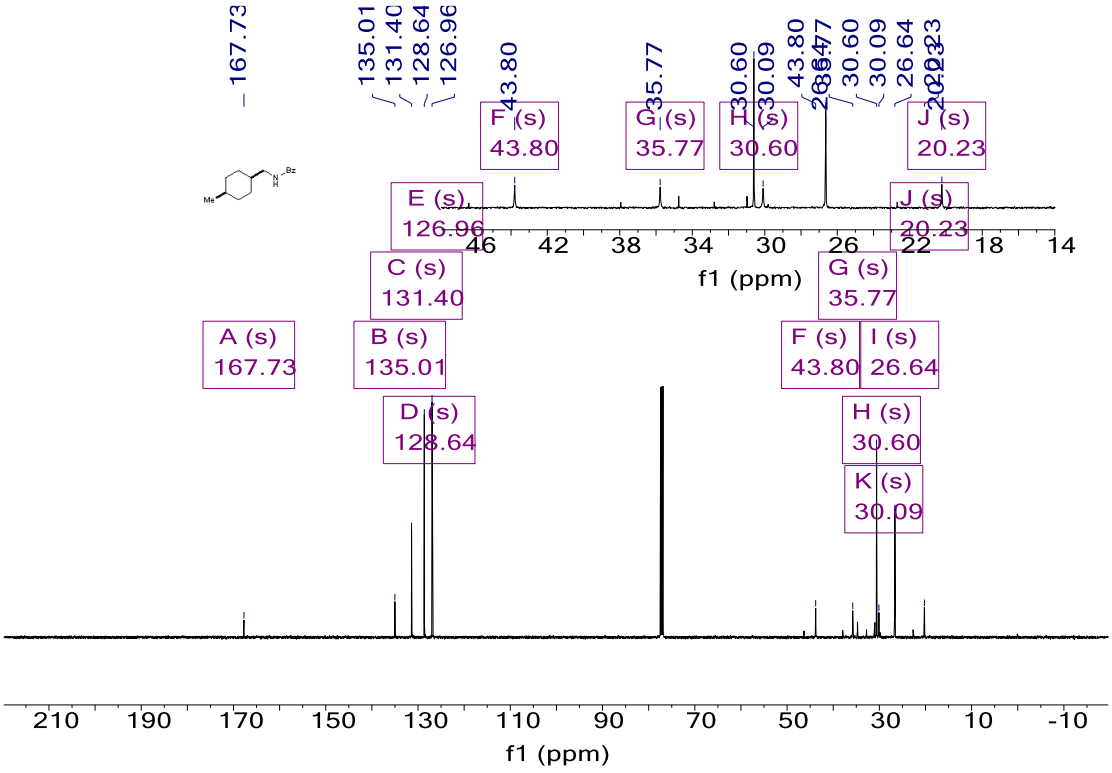

^{13}C-NMR of **5**

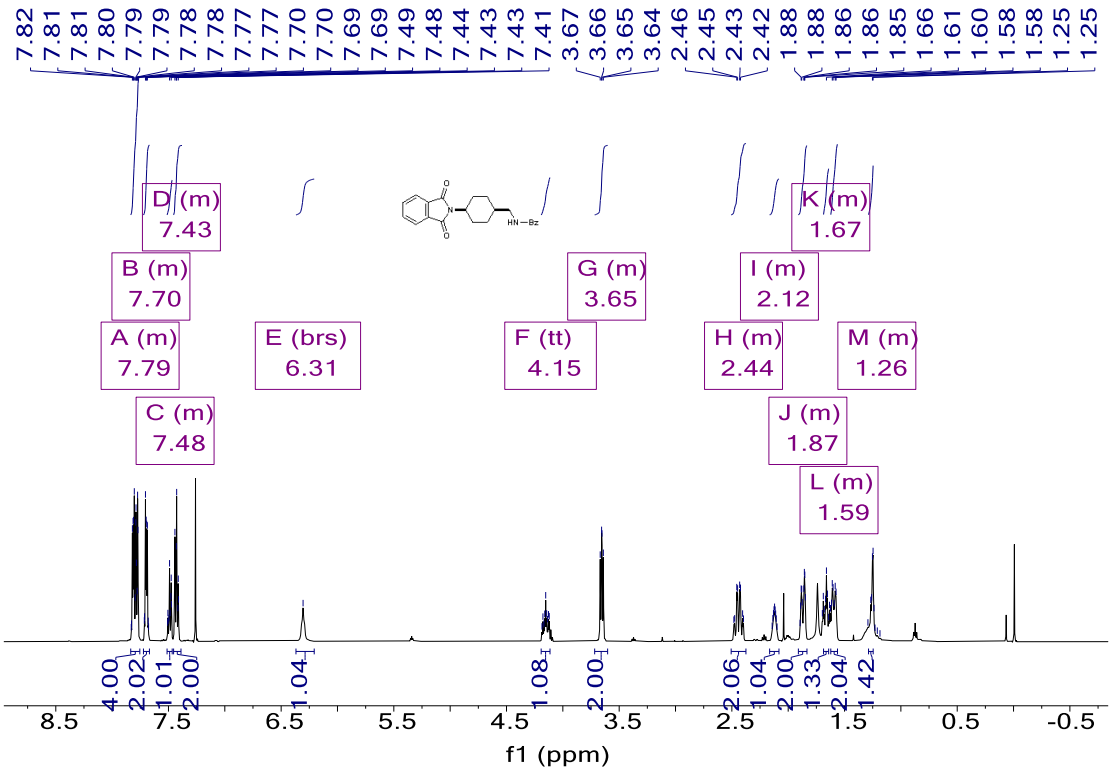

^{1}H-NMR of **6**

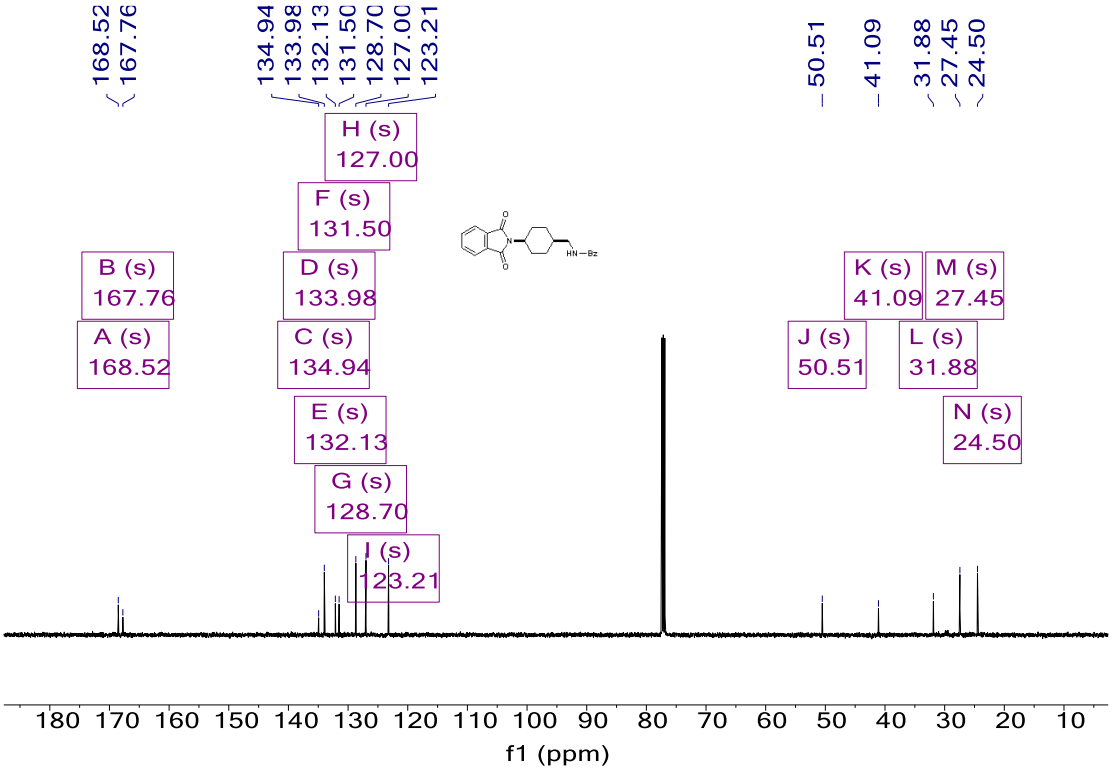

^{13}C-NMR of **6**

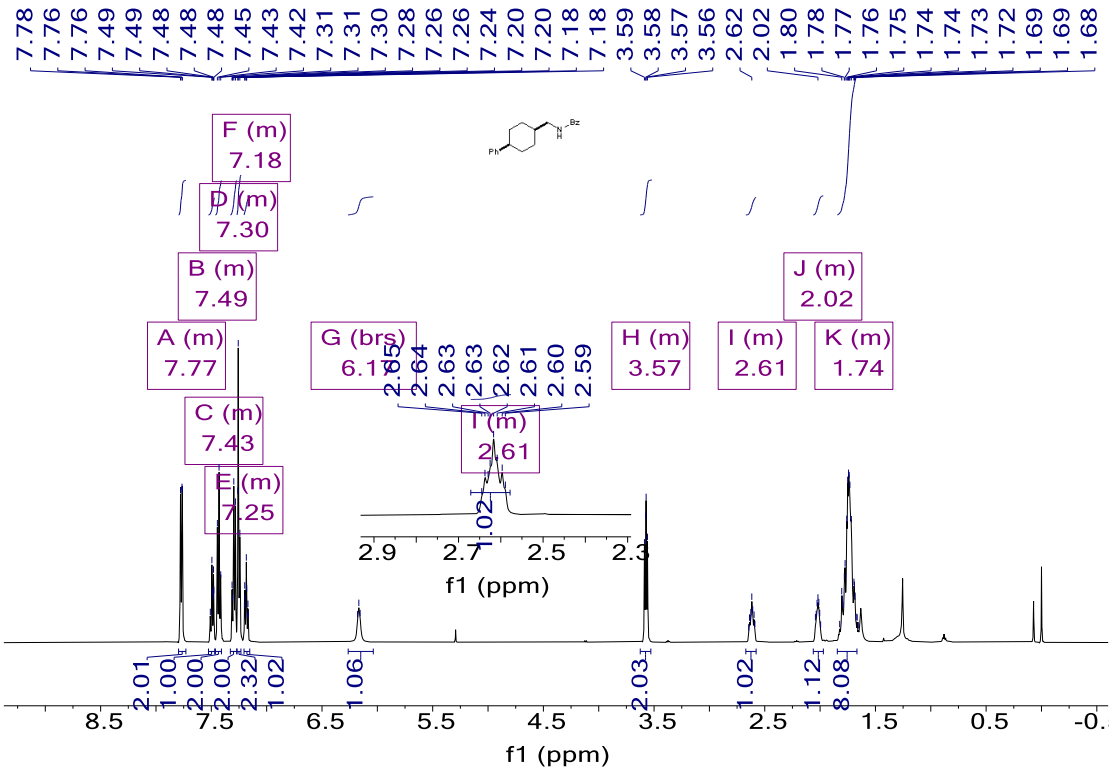

^{1}H-NMR of **7**

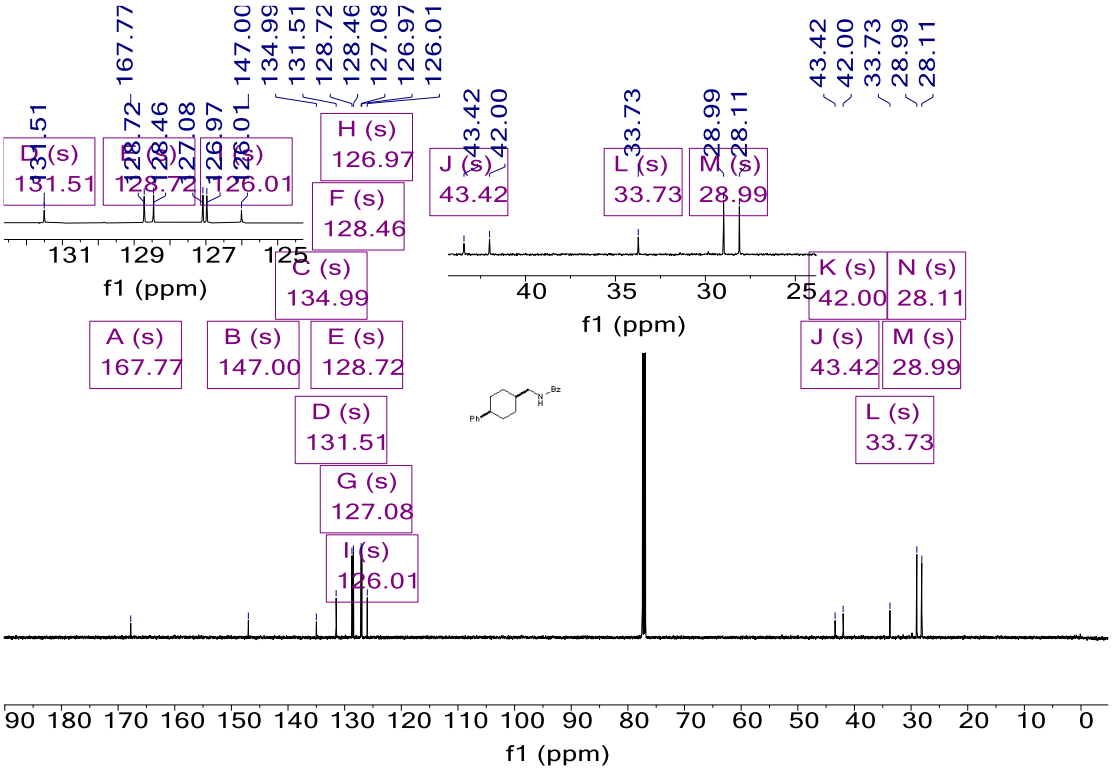

^{13}C-NMR of **7**

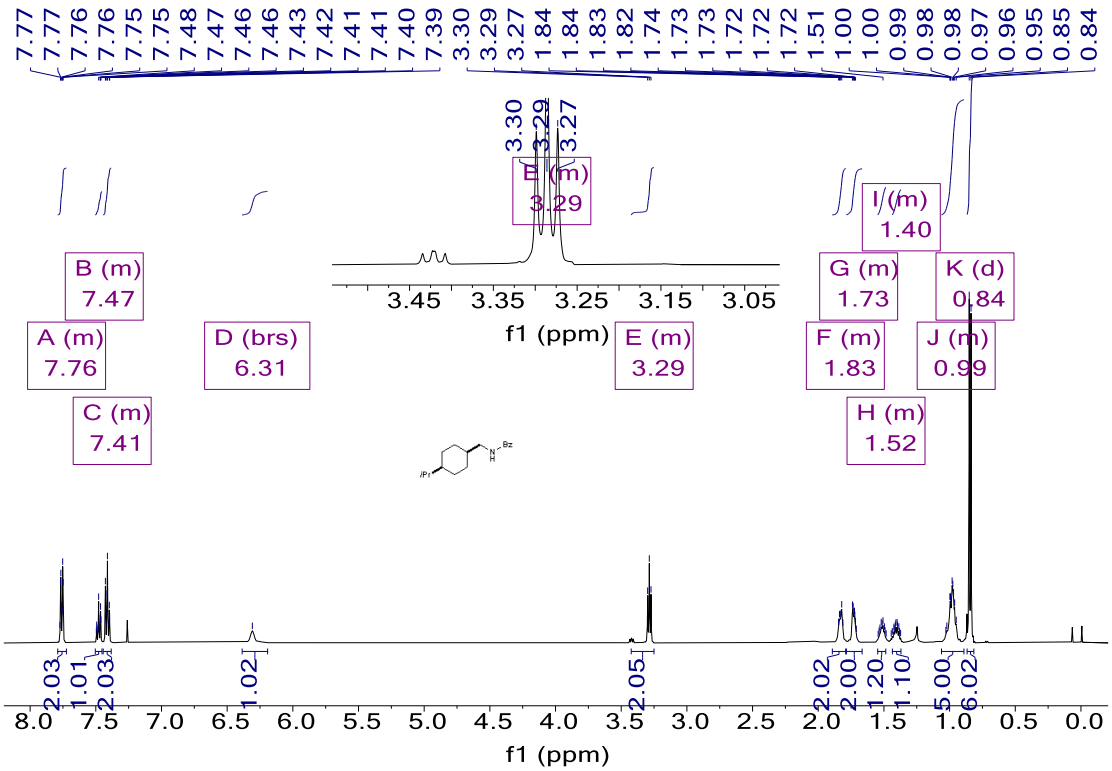

^{1}H-NMR of **8**

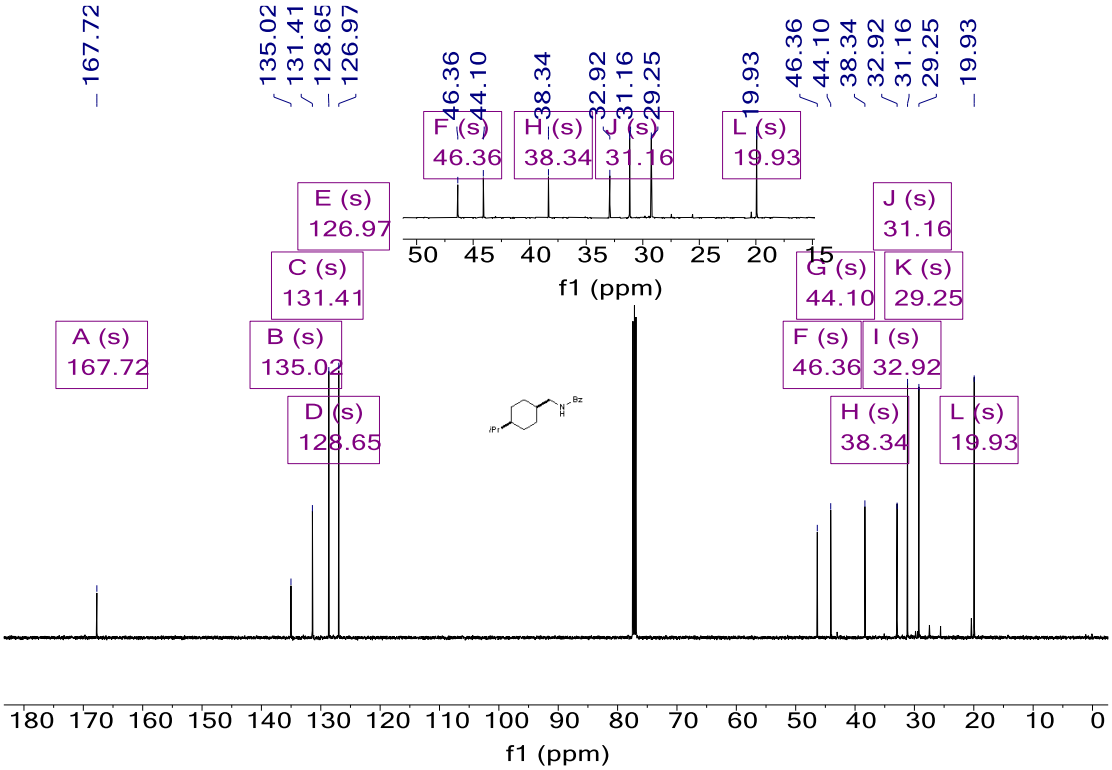

^{13}C-NMR of **8**

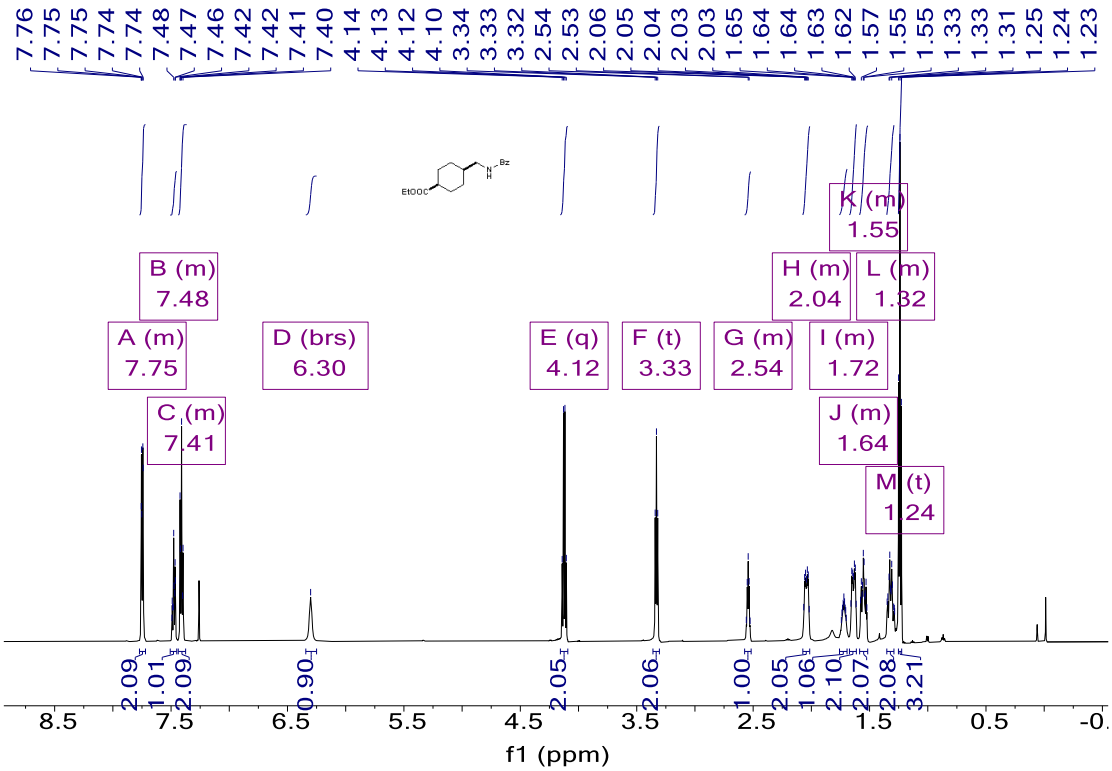

^{1}H-NMR of **9**

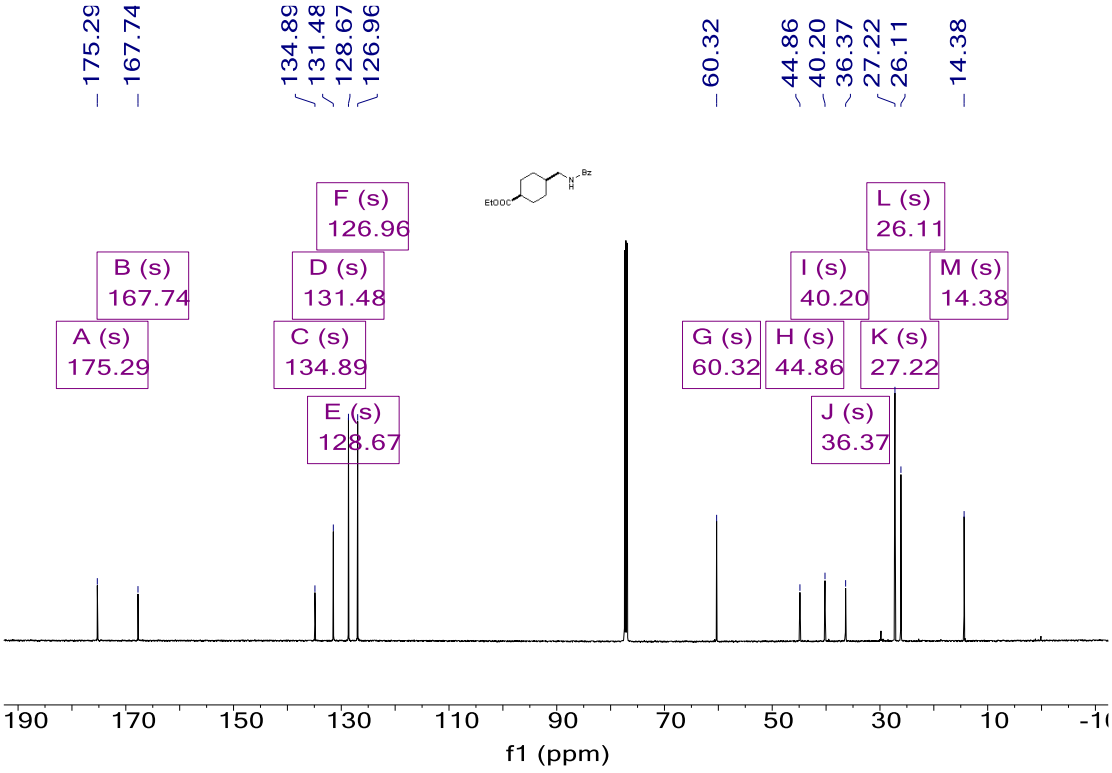

^{13}C-NMR of **9**

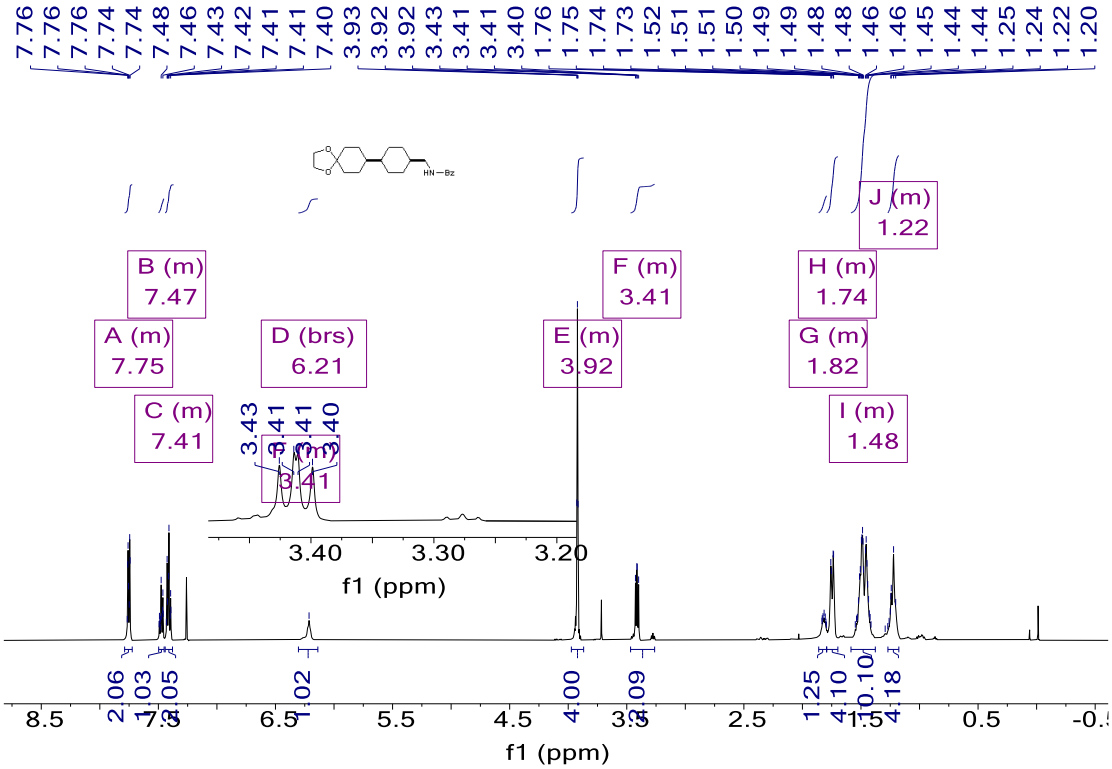

^{1}H-NMR of **10**

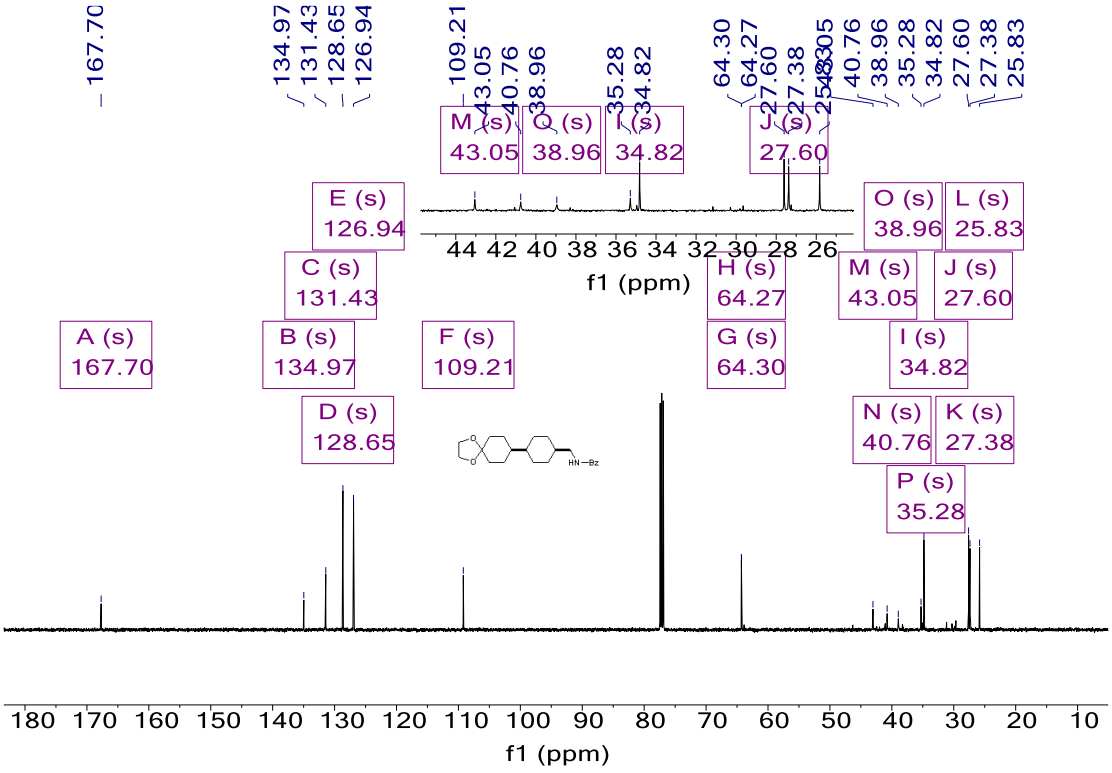

^{13}C-NMR of **10**

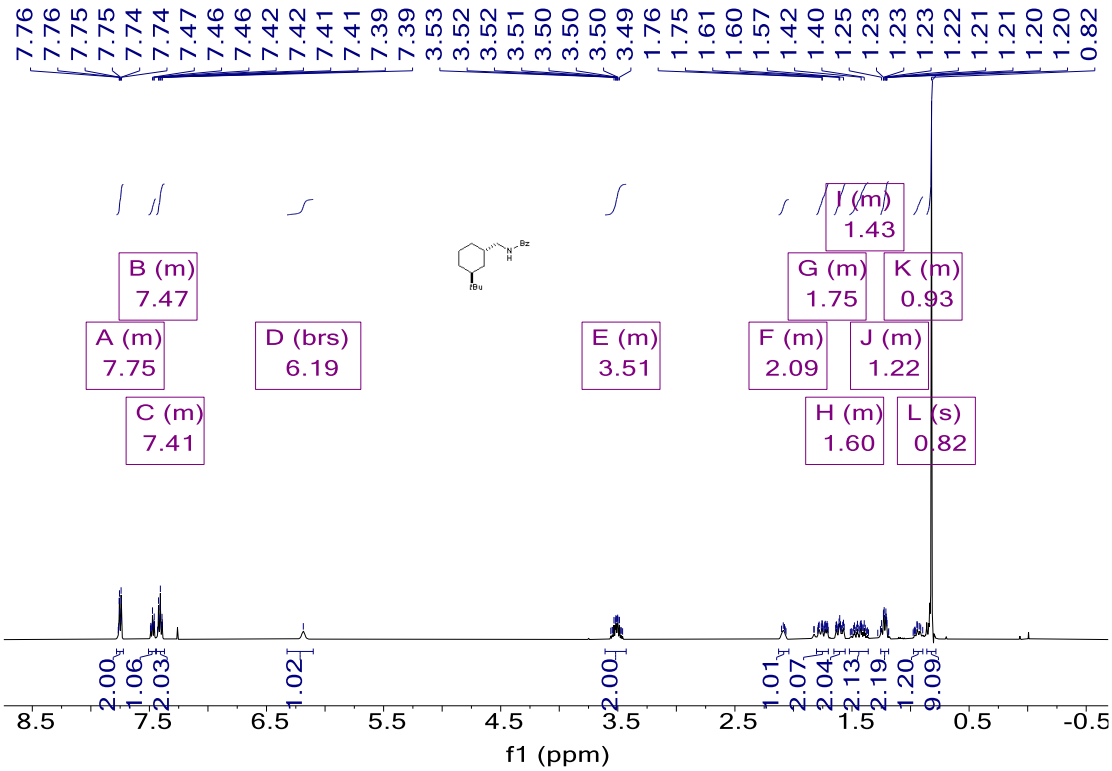

^{1}H-NMR of **11**

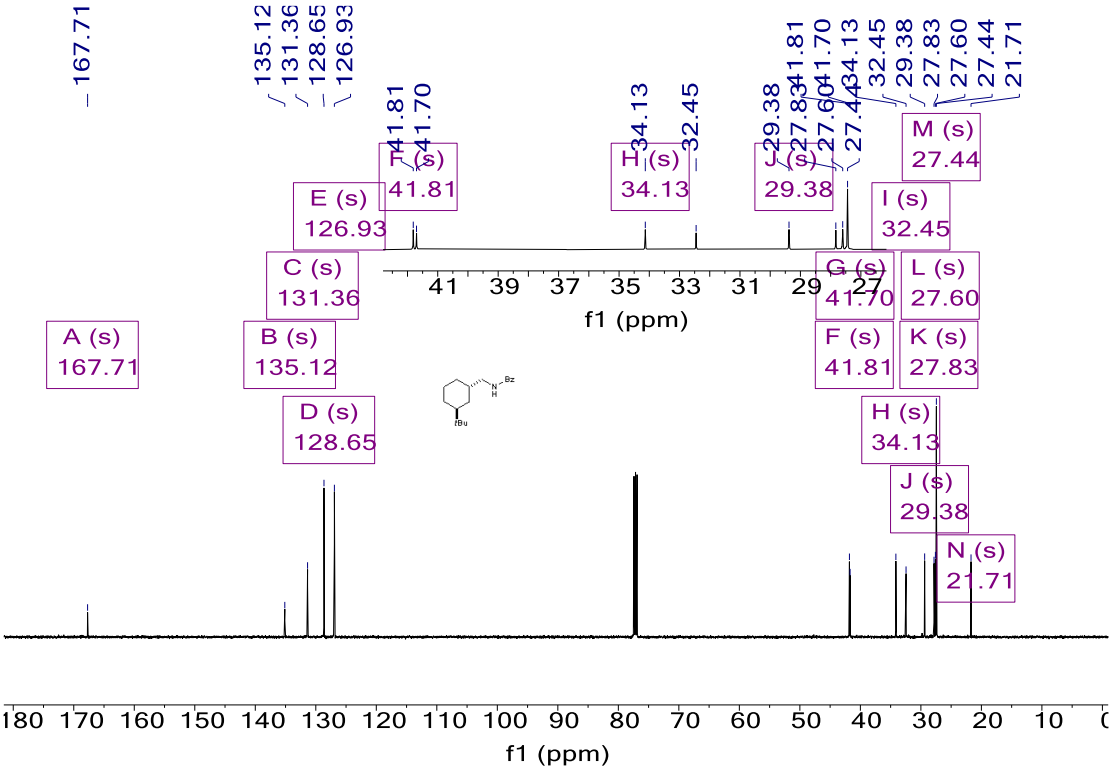

^{13}C-NMR of **11**

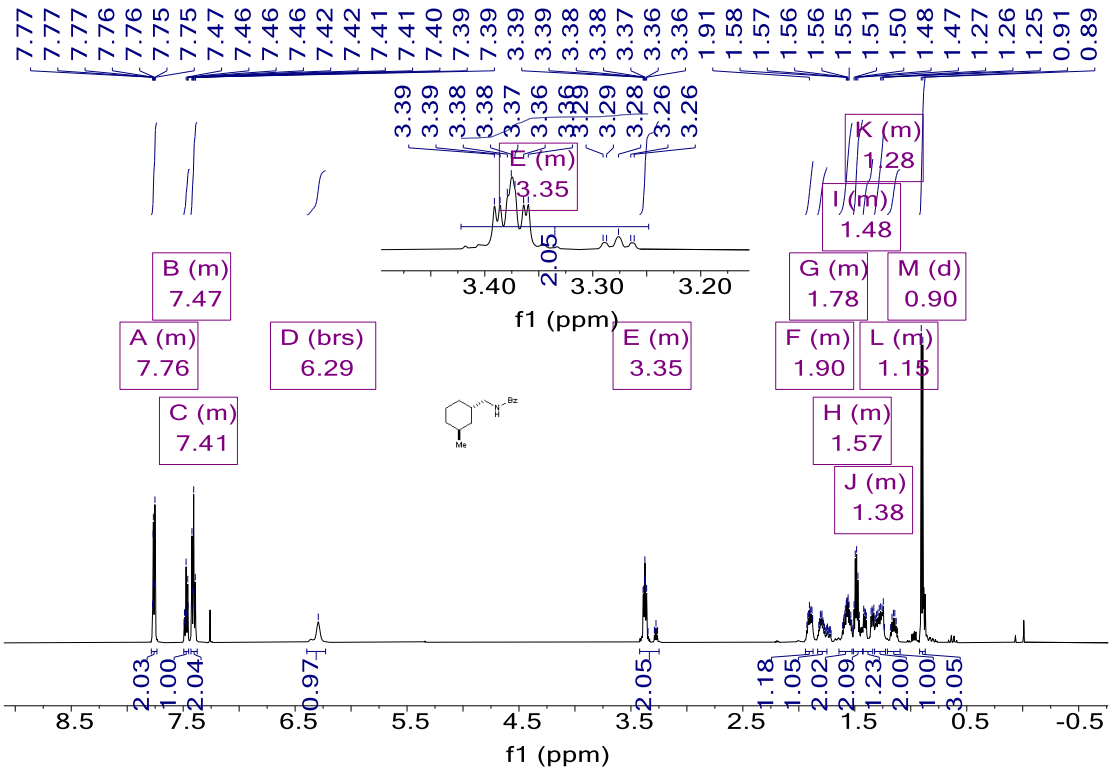

^{1}H-NMR of **12**

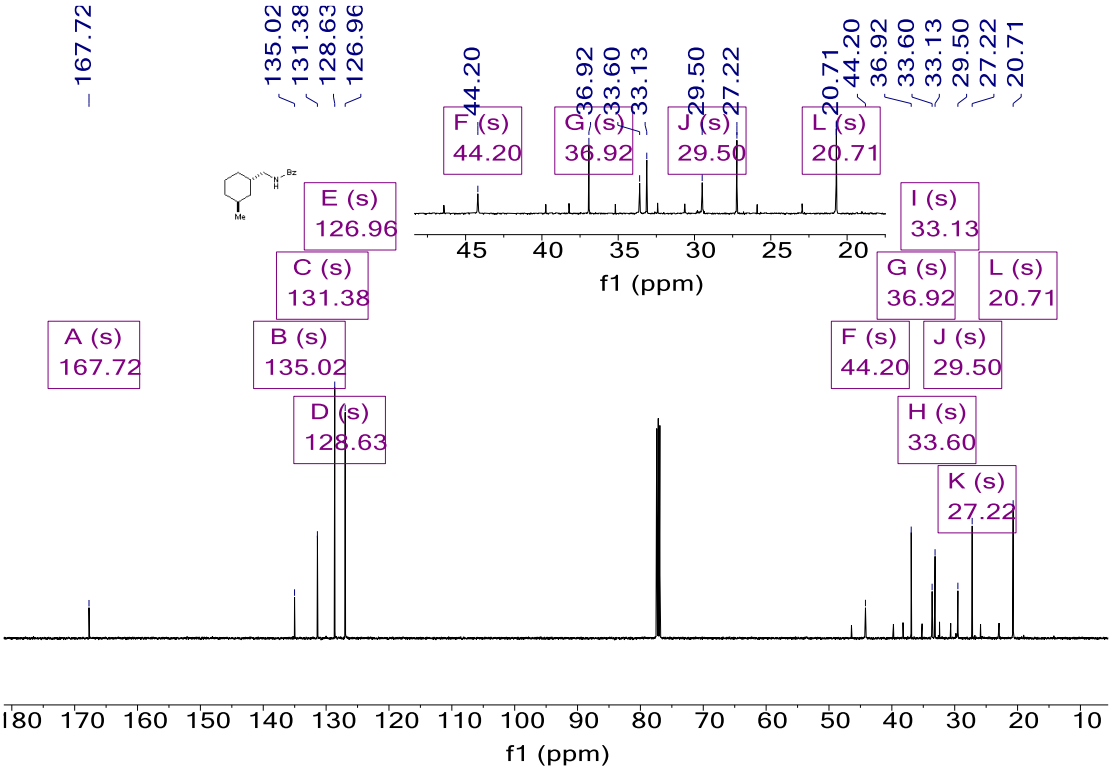

^{13}C-NMR of **12**

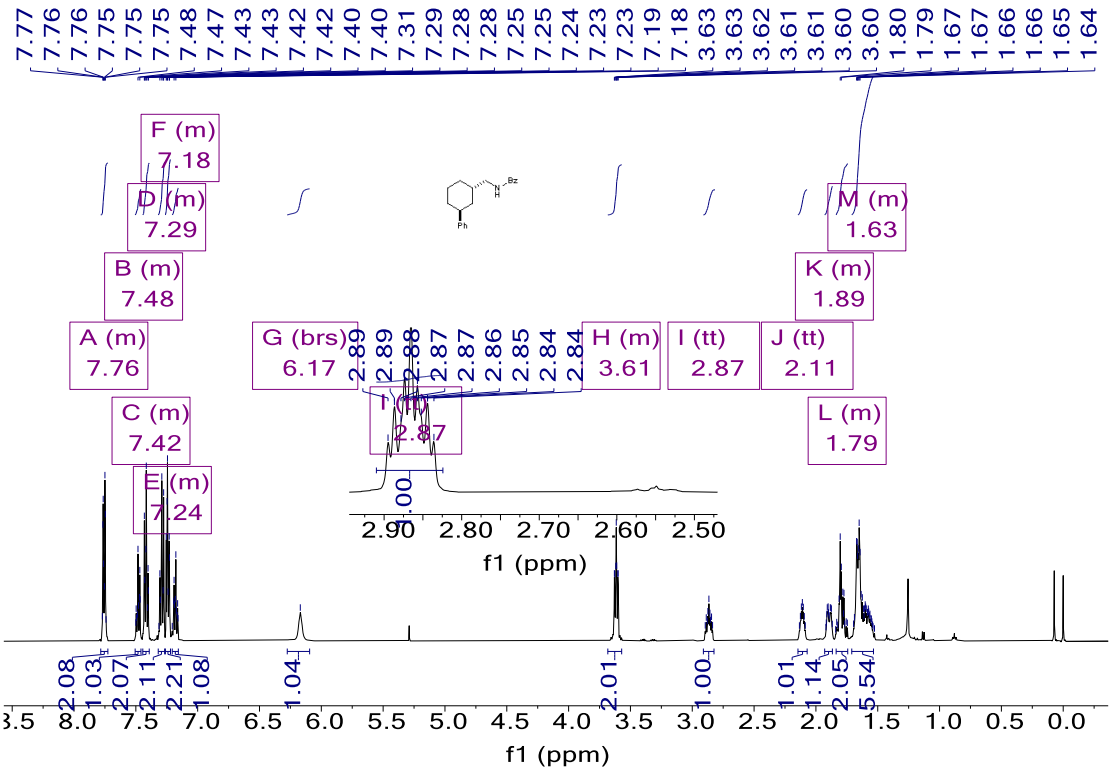

^{1}H-NMR of **13**

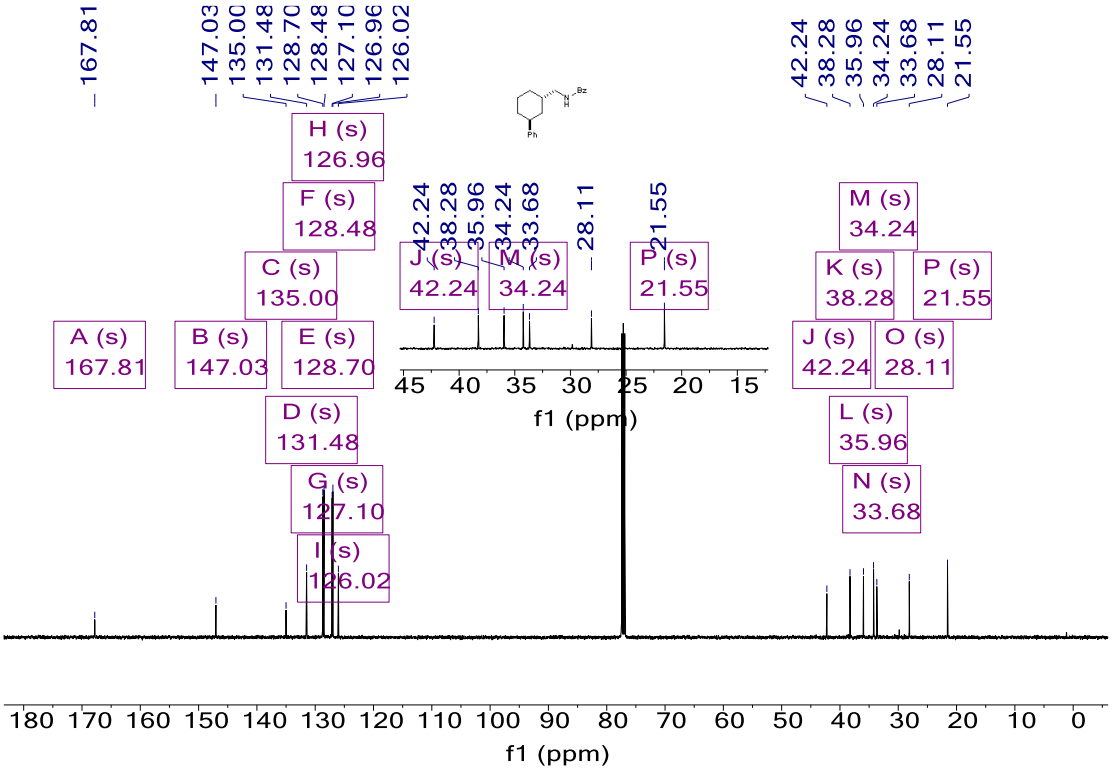

^{13}C-NMR of **13**

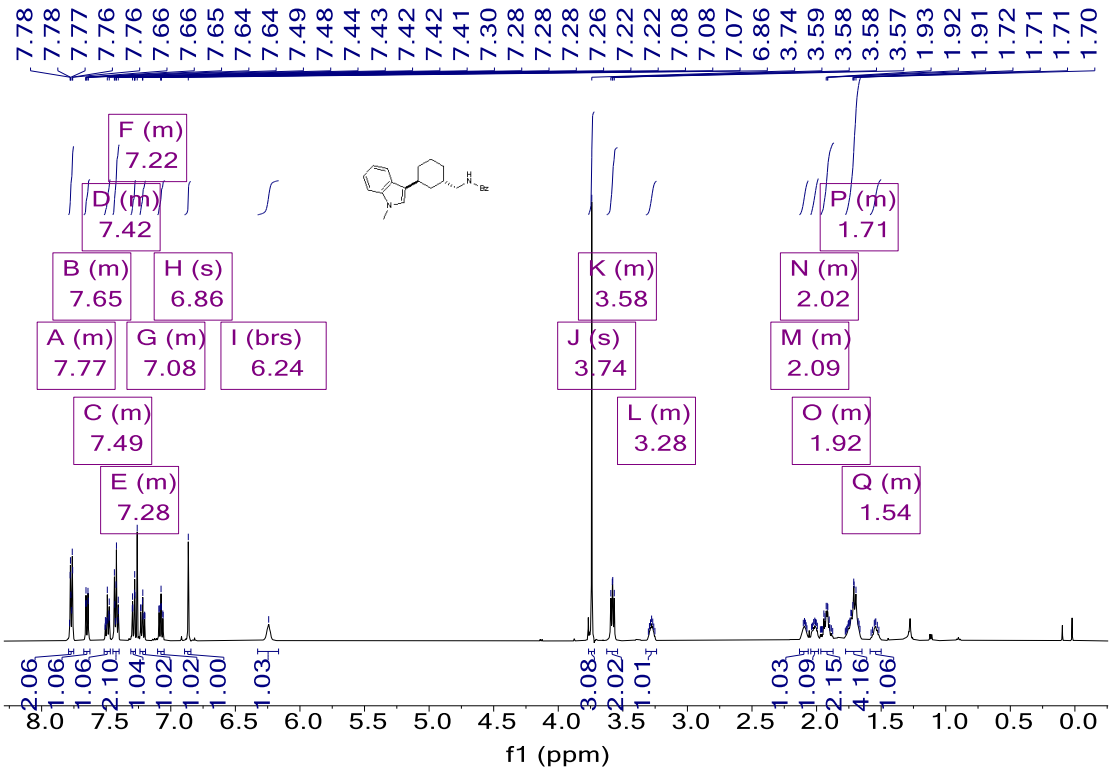

^{1}H-NMR of **14**

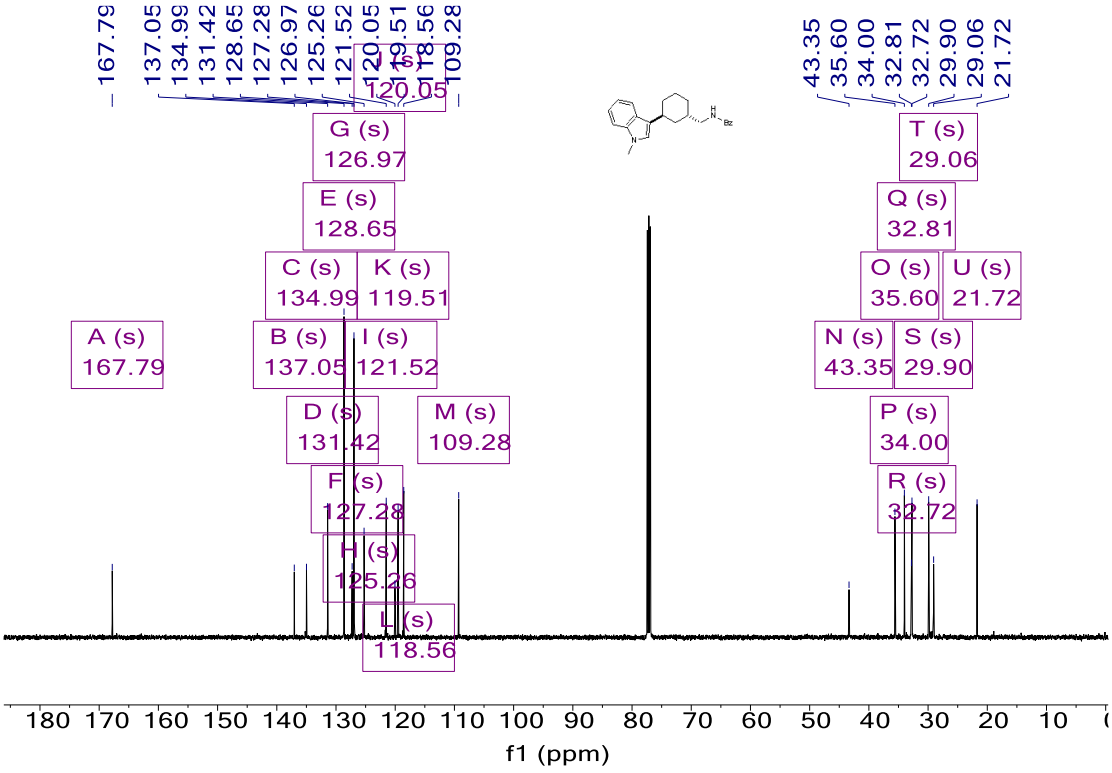

^{13}C-NMR of **14**

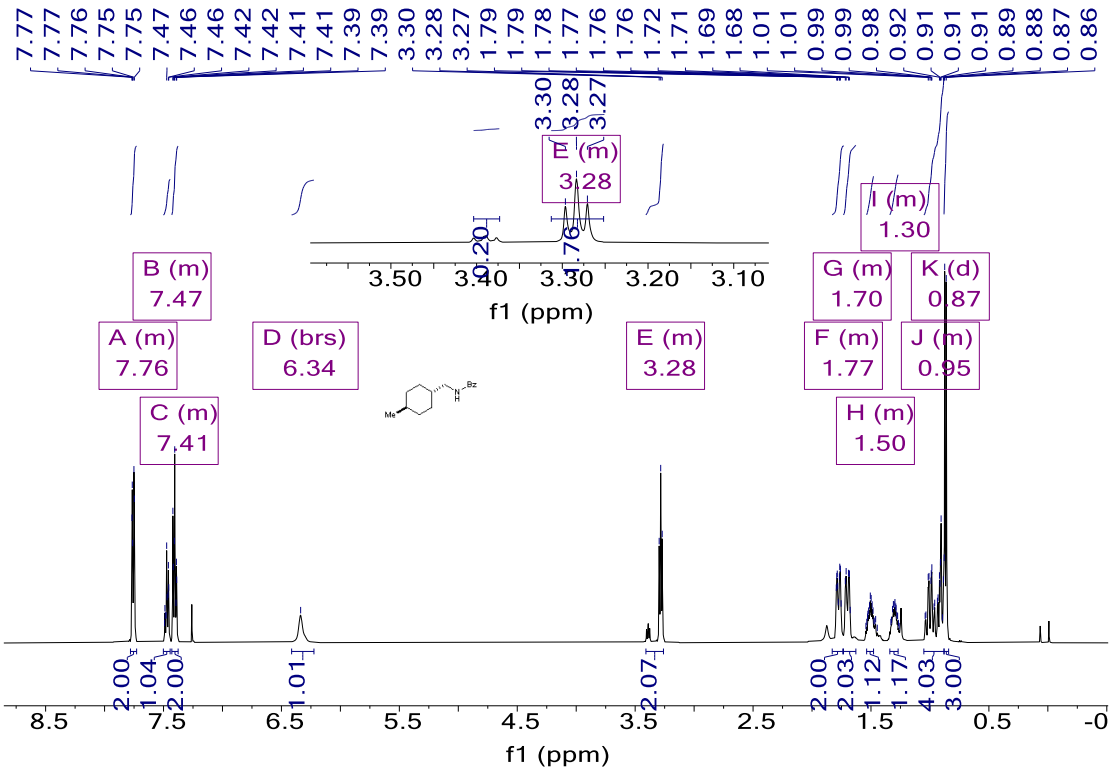

^{1}H-NMR of **15**

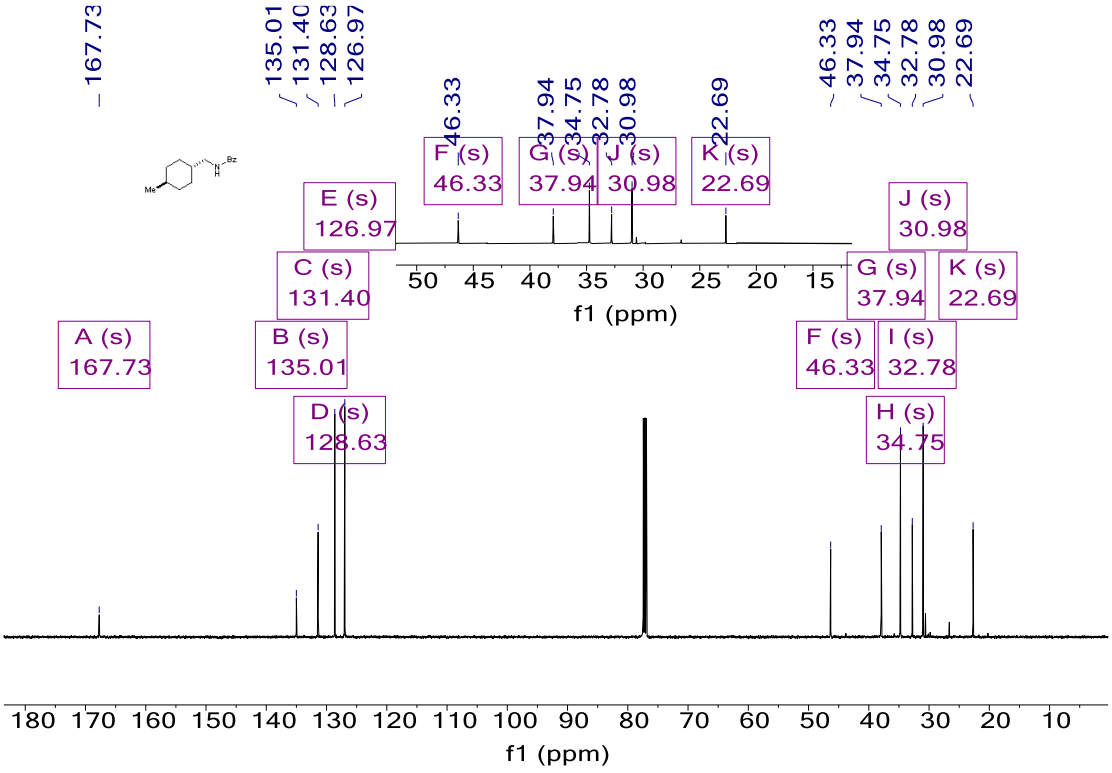

^{13}C-NMR of **15**

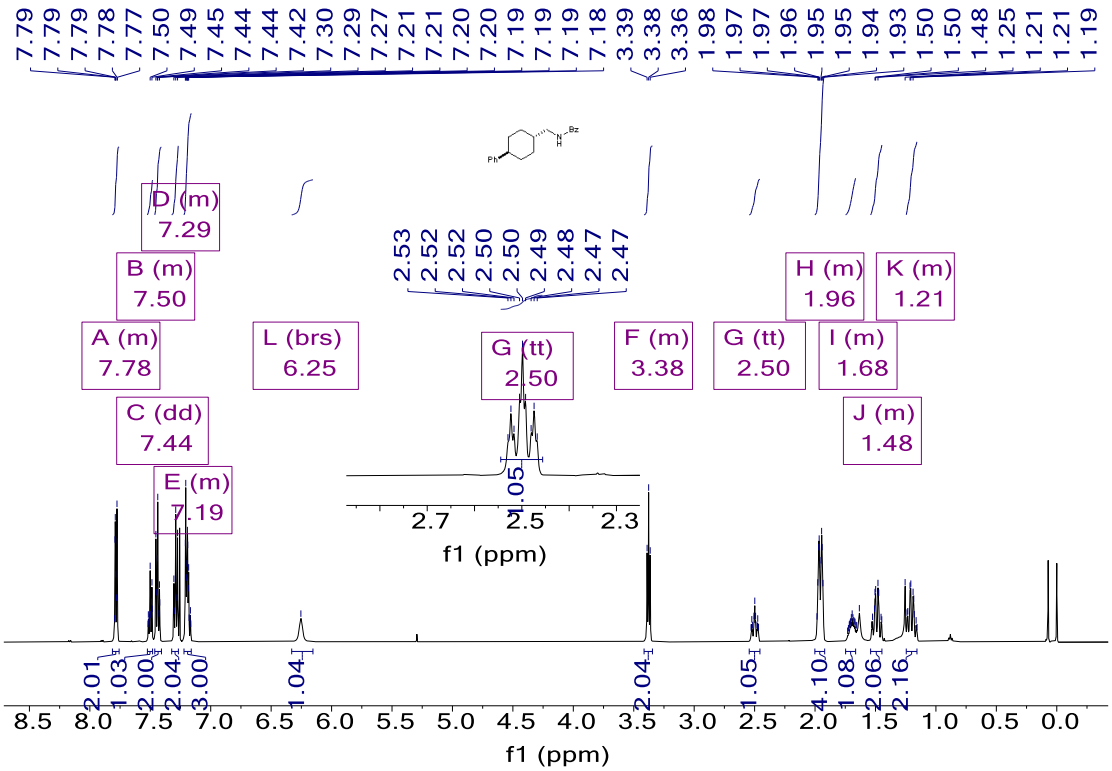

^{1}H-NMR of **16**

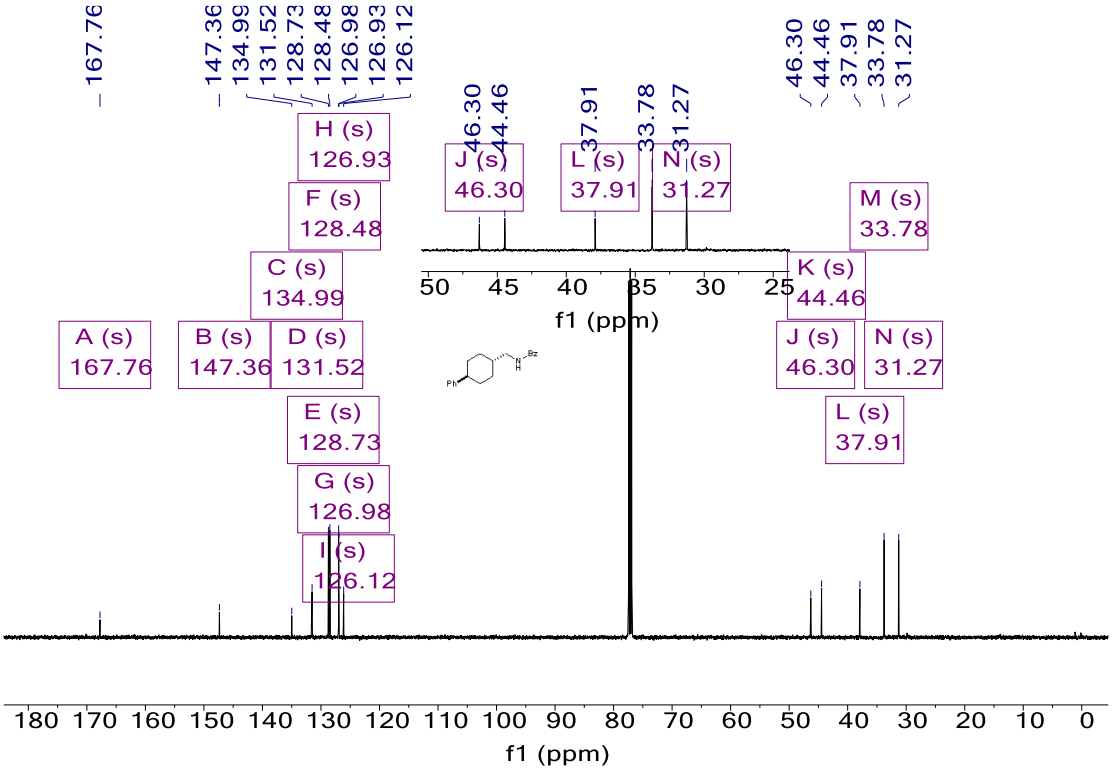

^{13}C-NMR of **16**

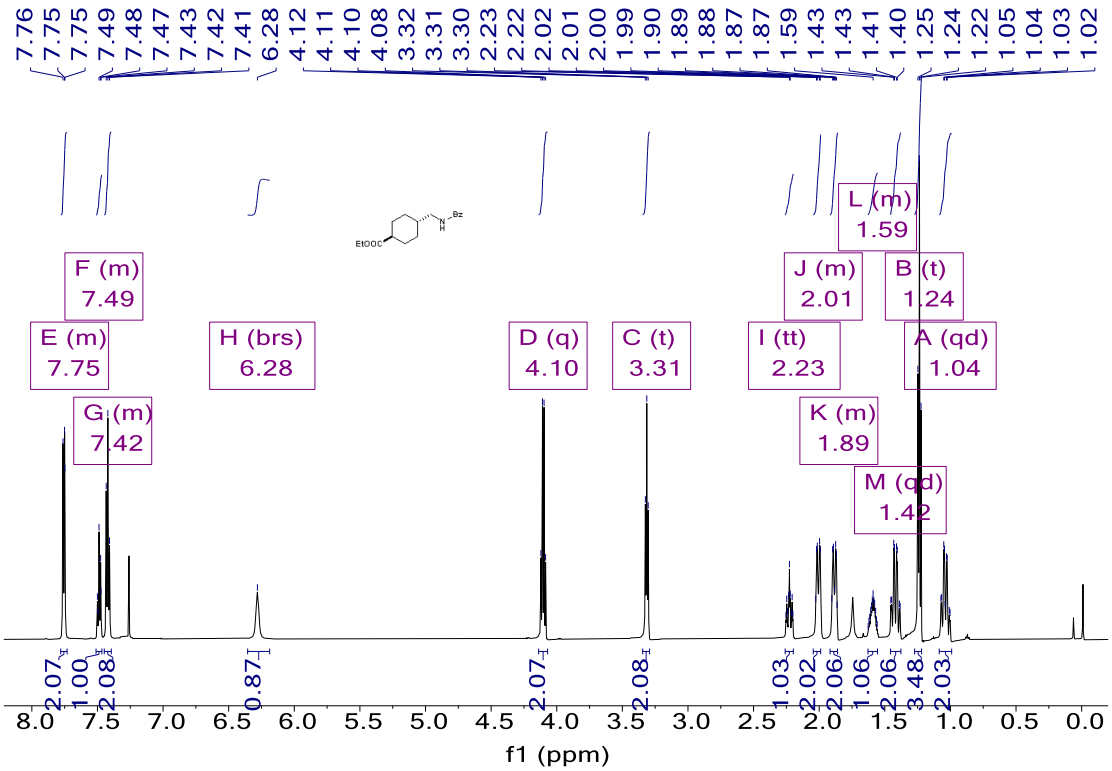

^{1}H-NMR of **17**

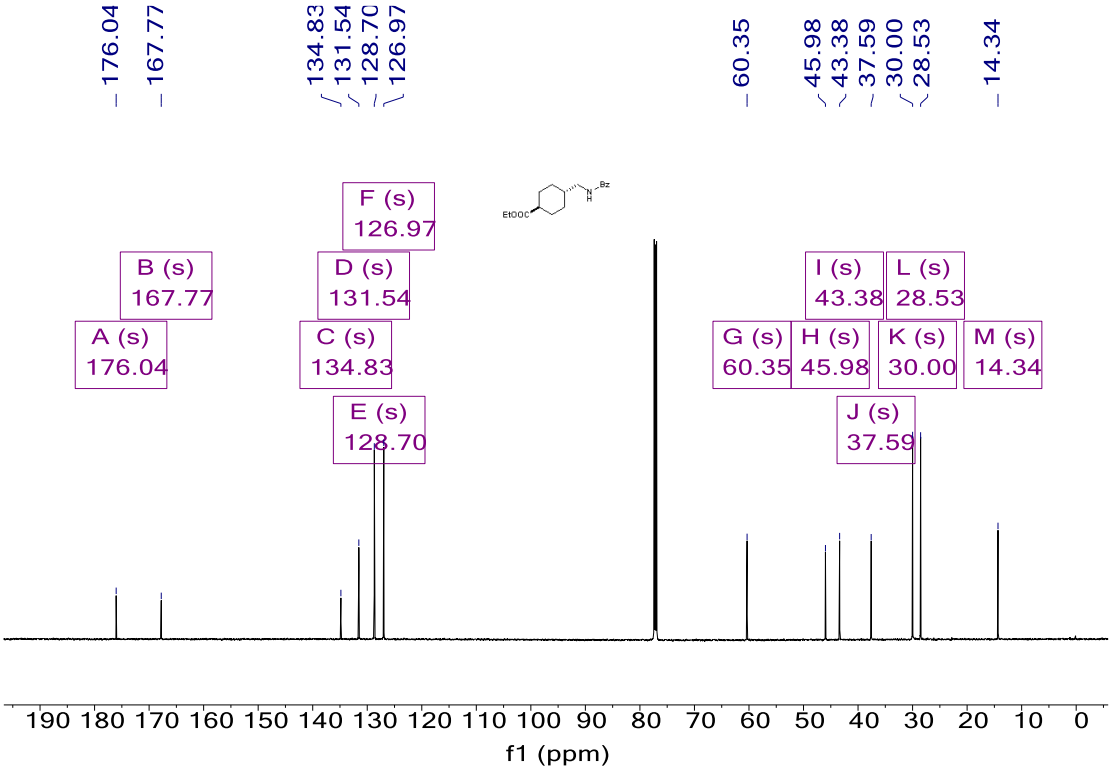

^{13}C-NMR of **17**

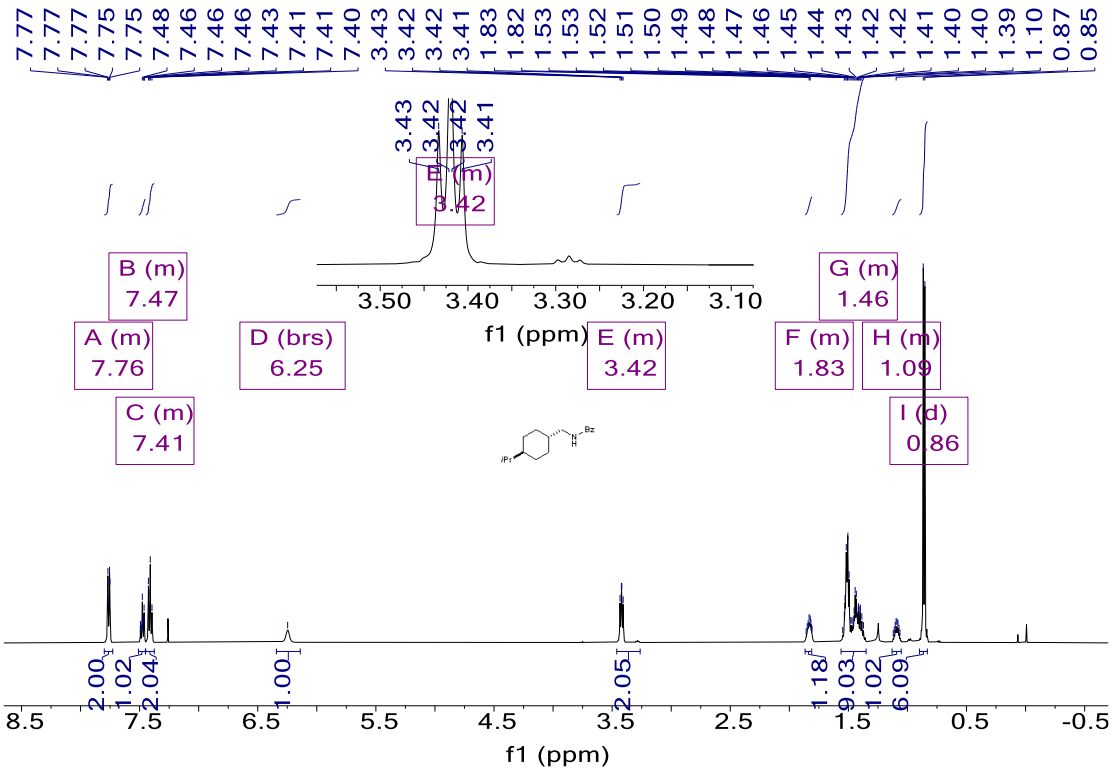

^{1}H-NMR of **18**

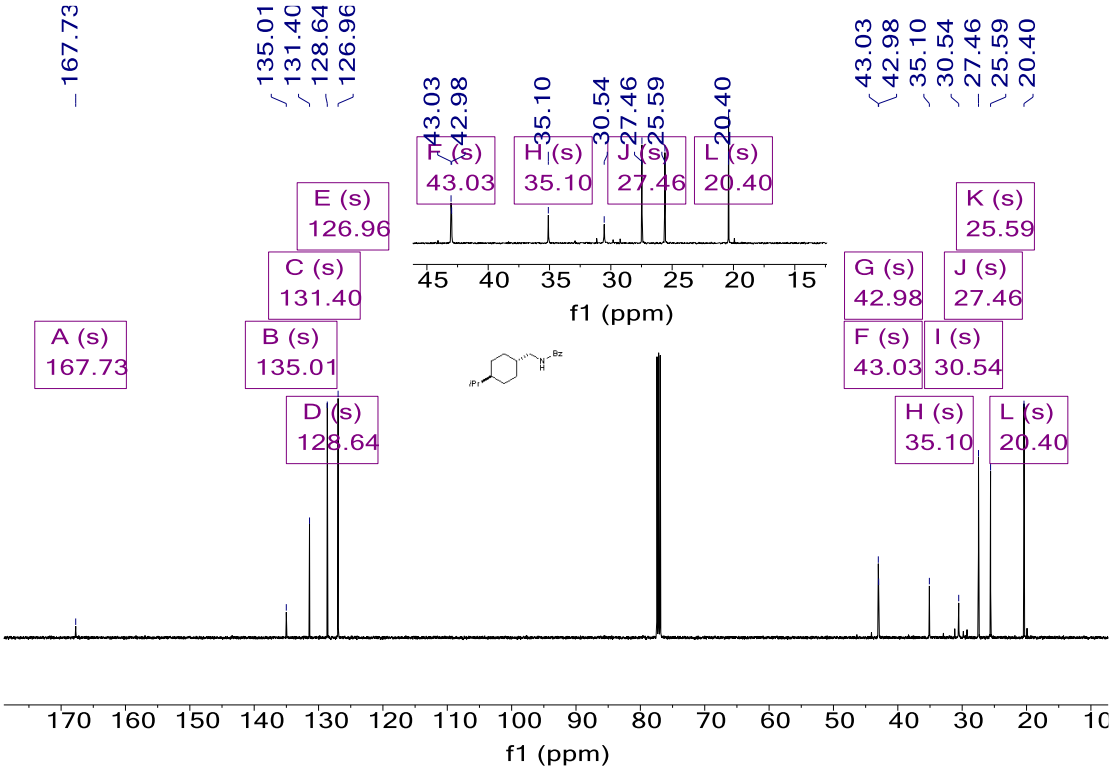

^{13}C-NMR of **18**

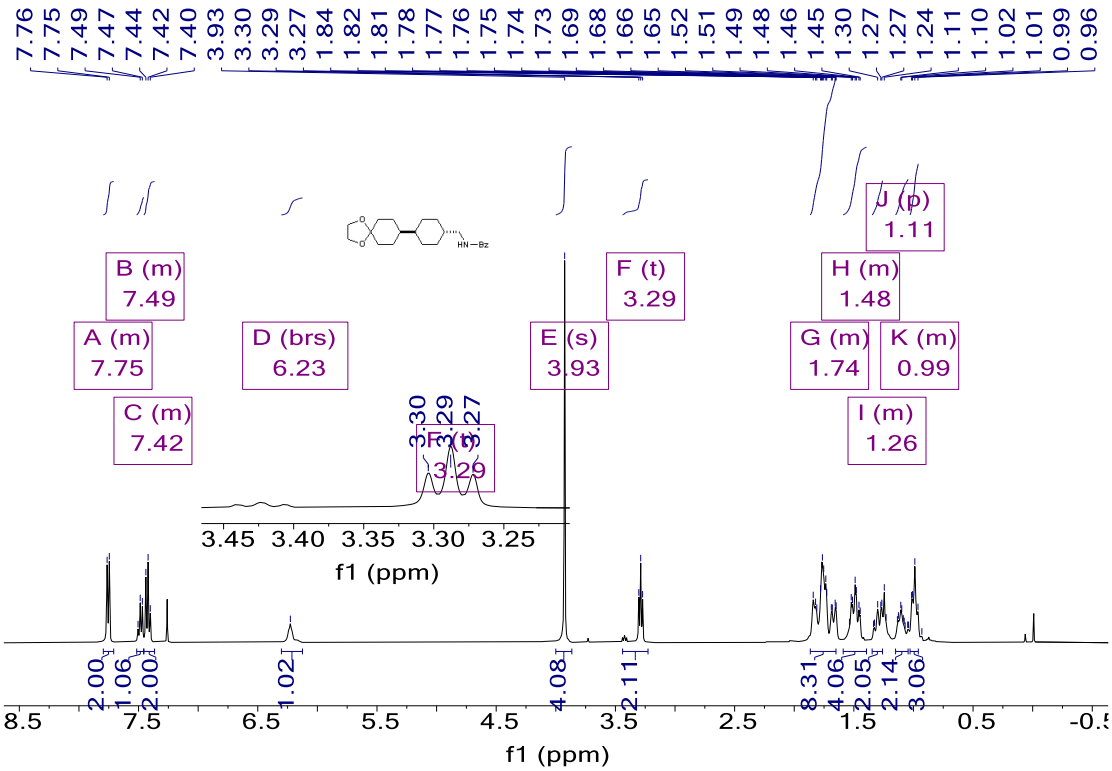

^{1}H-NMR of **19**

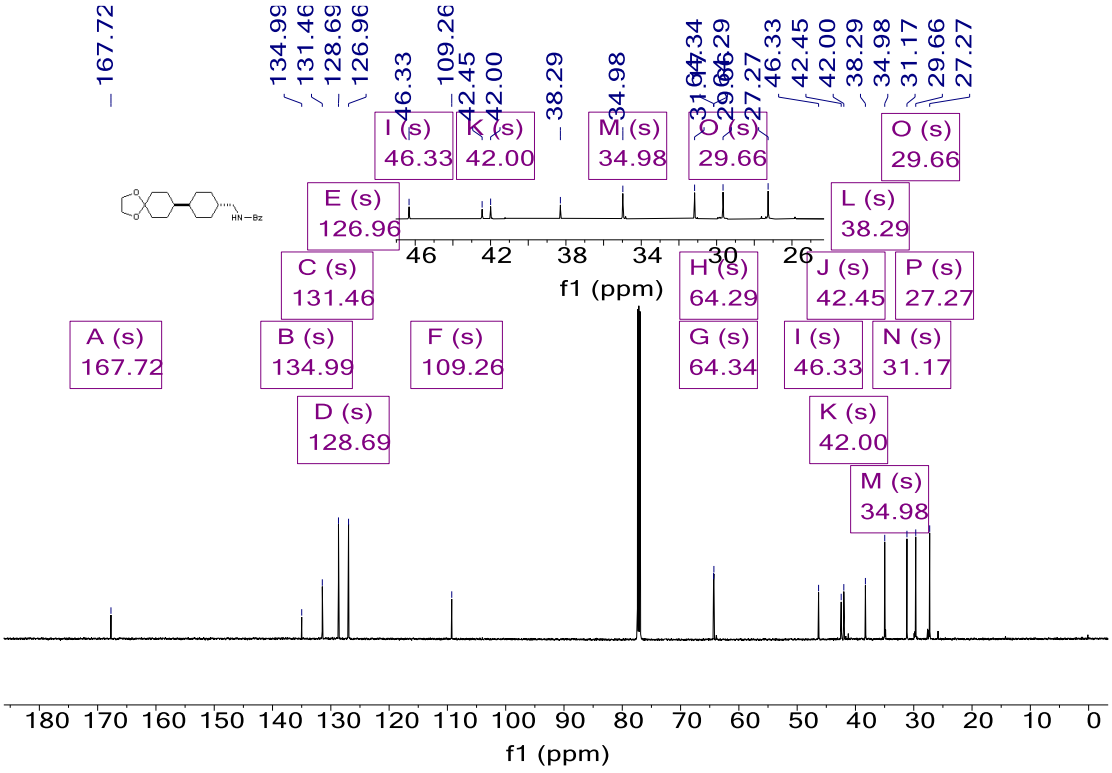

^{13}C-NMR of **19**

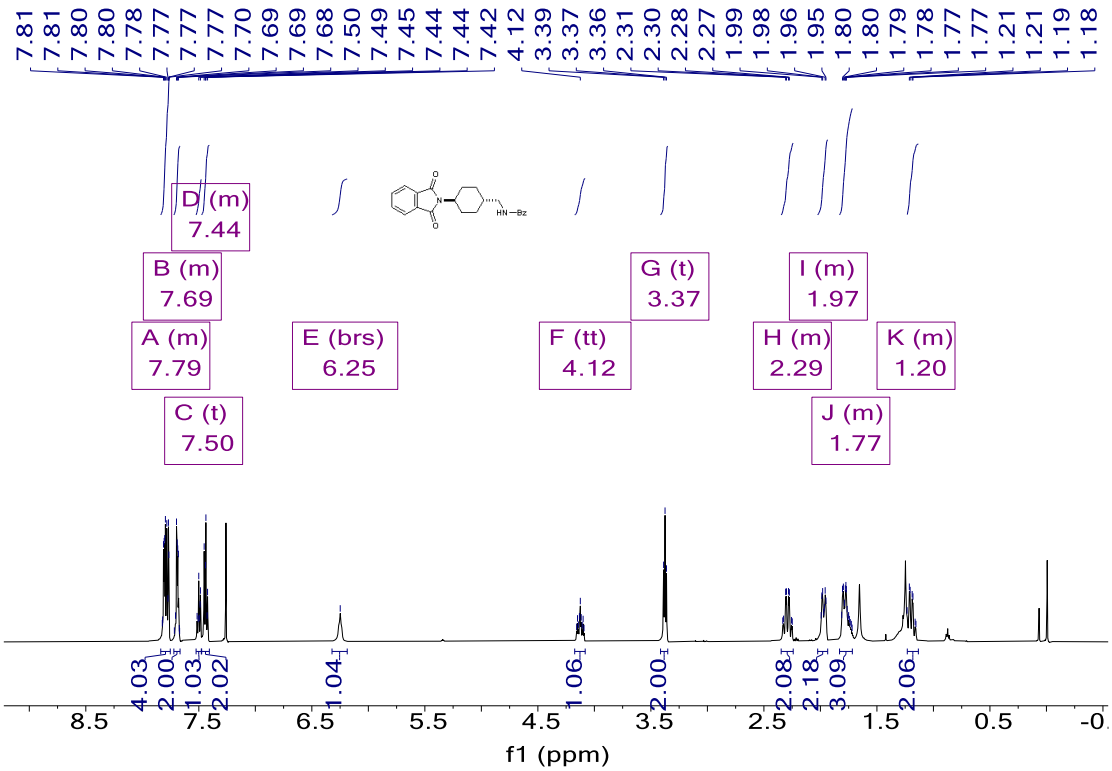

^{1}H-NMR of **20**

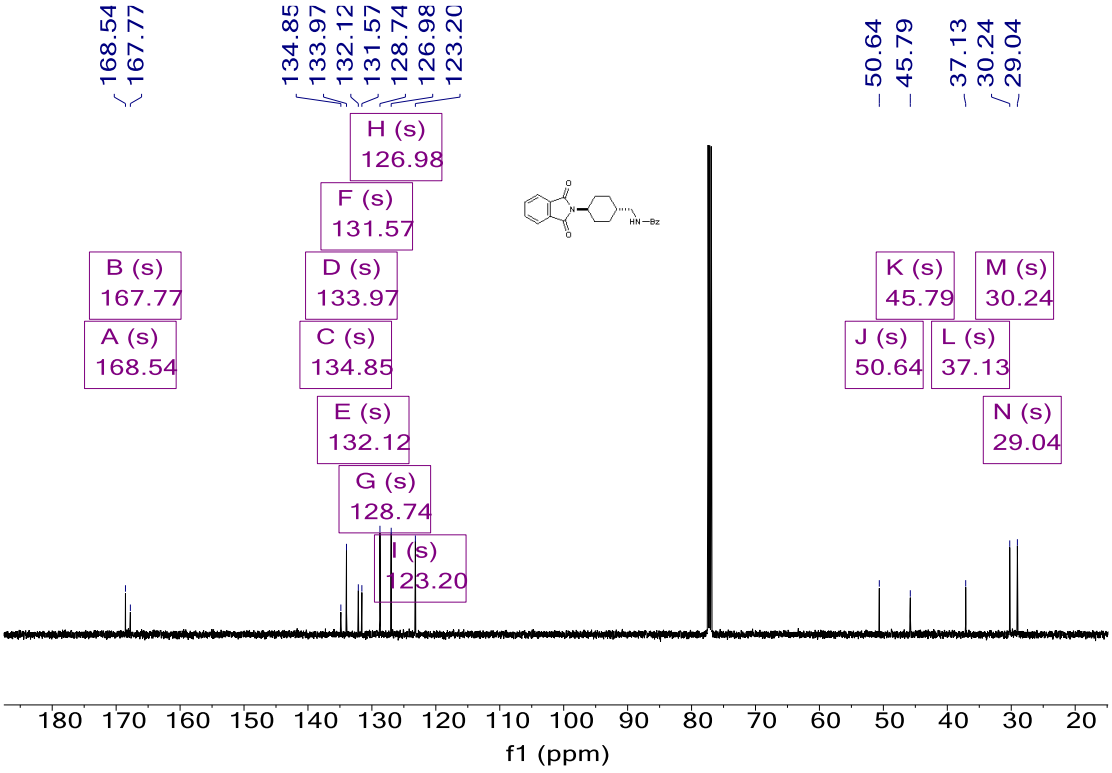

^{13}C-NMR of **20**

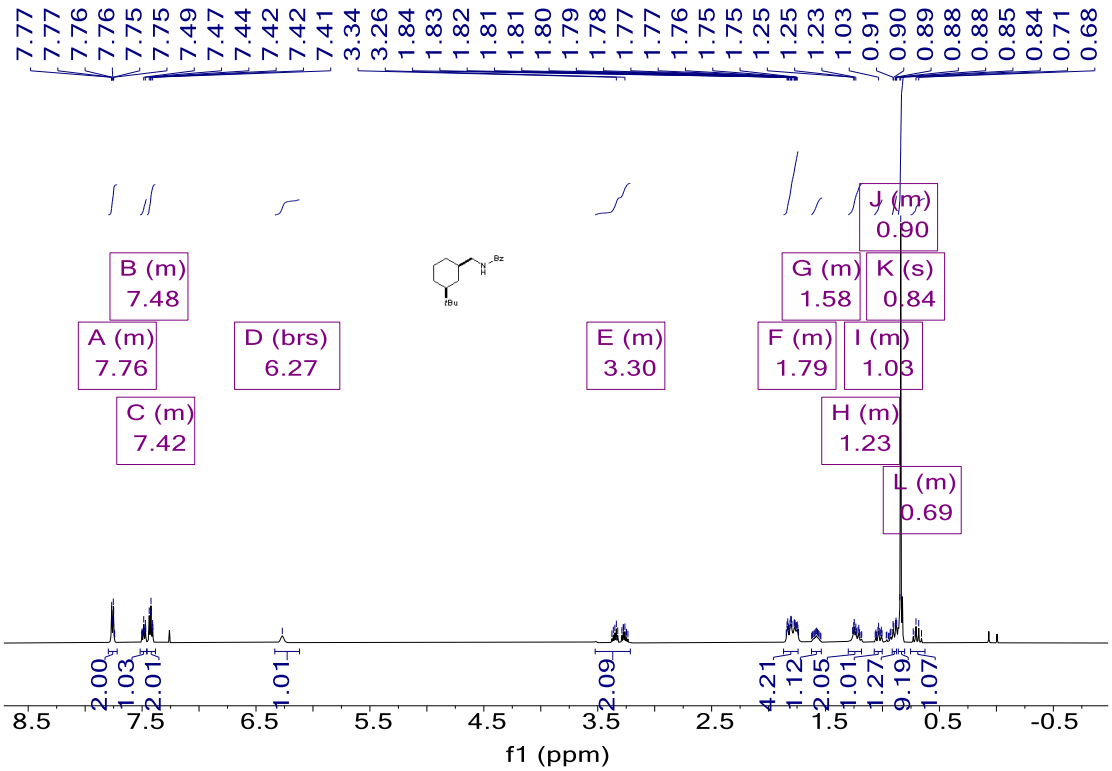

^{1}H-NMR of **21**

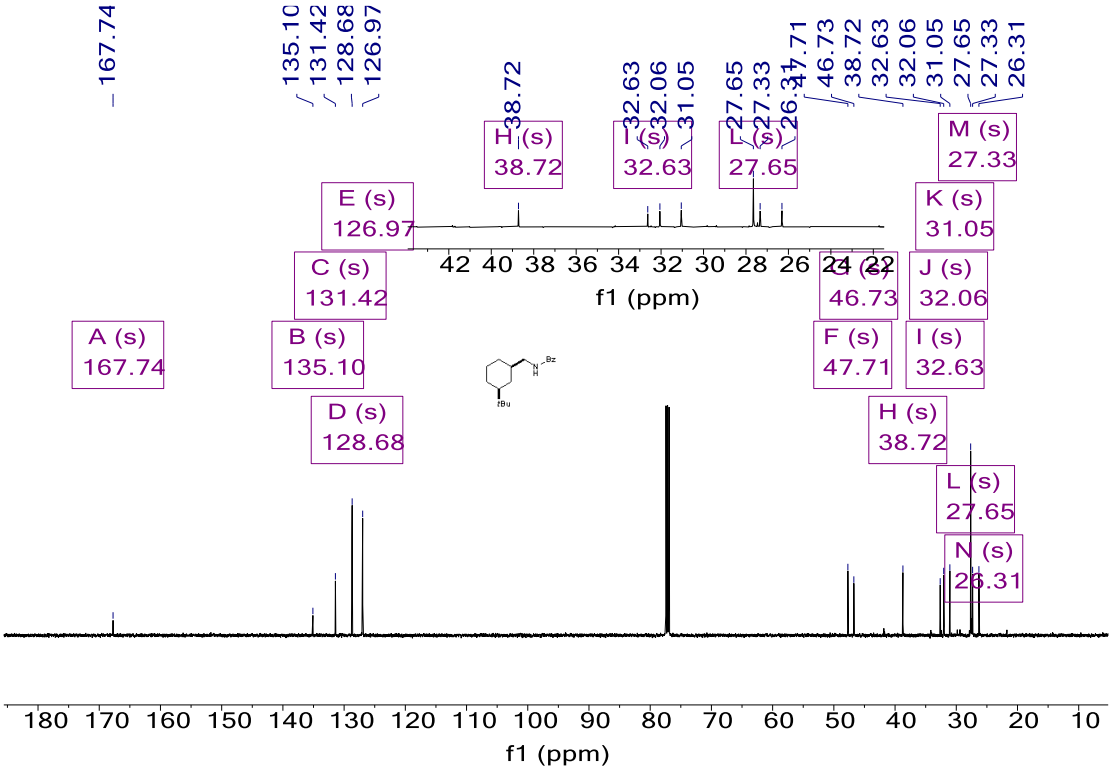

^{13}C-NMR of **21**

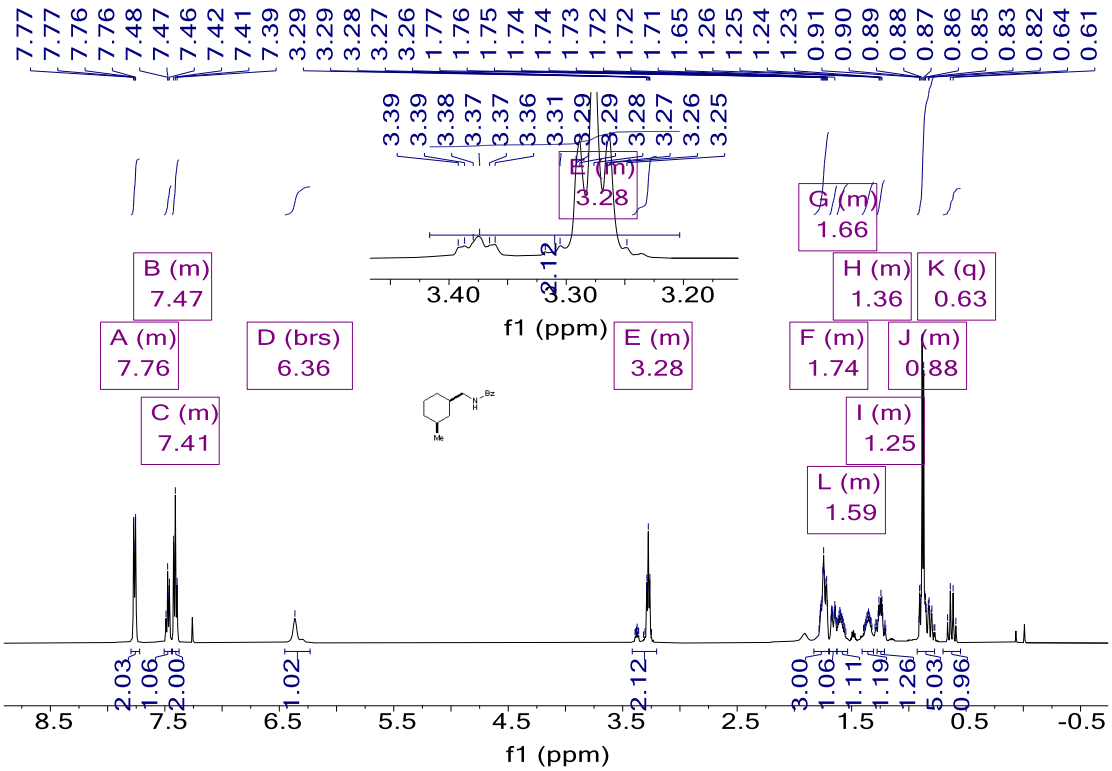

^{1}H-NMR of **22**

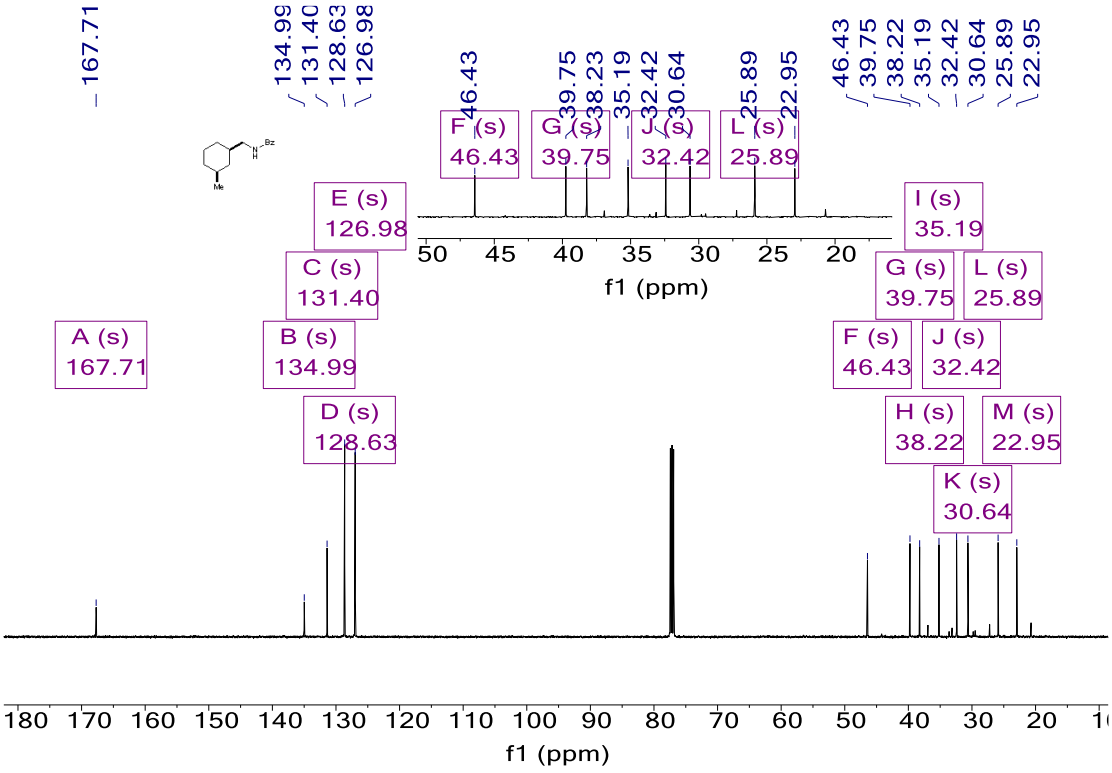

^{13}C-NMR of **22**

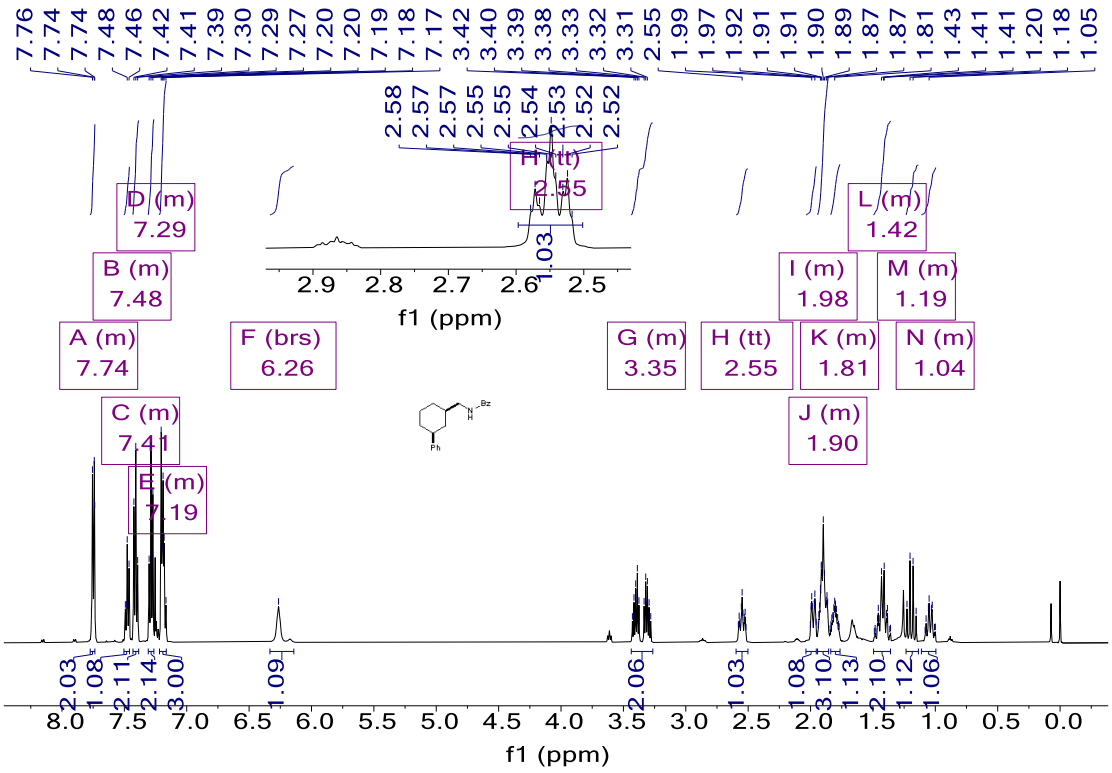

^{1}H-NMR of **23**

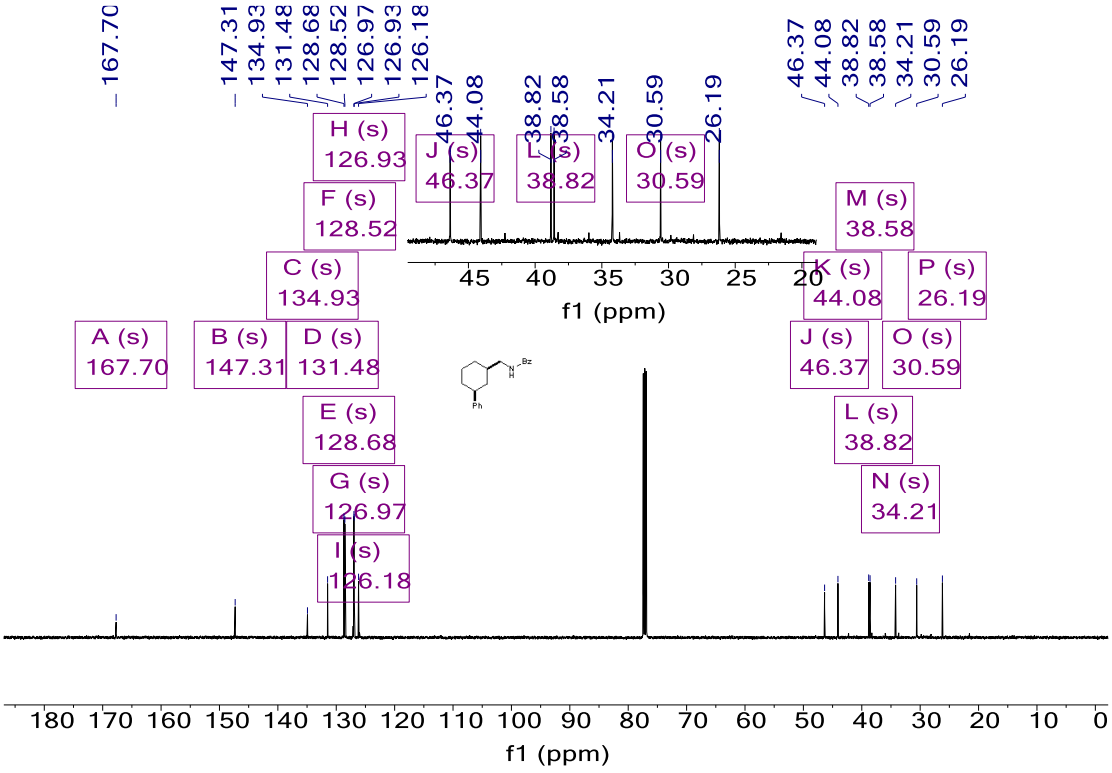

^{13}C-NMR of **23**

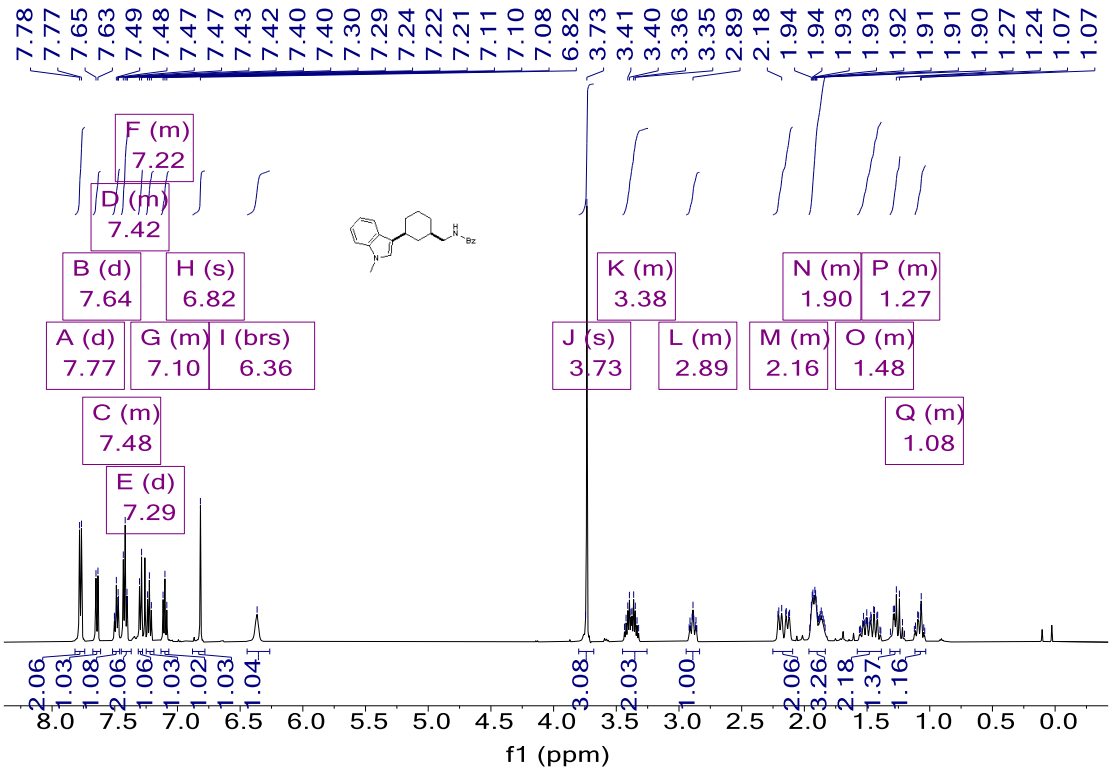

^{1}H-NMR of **24**

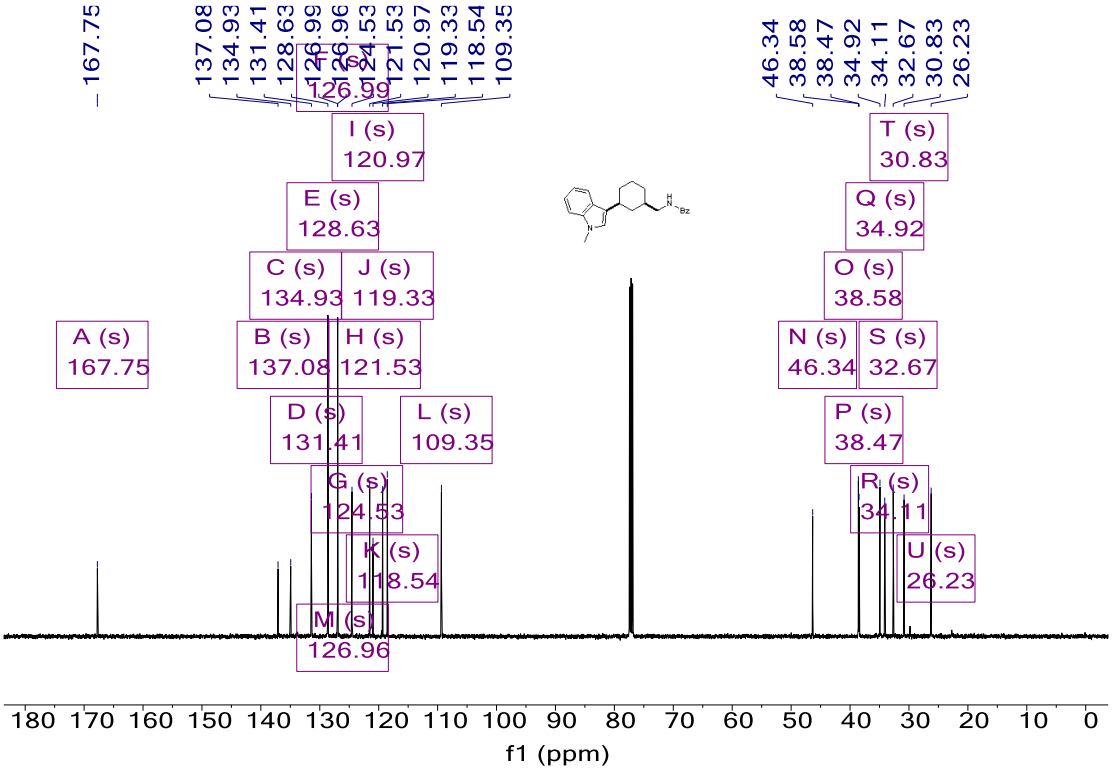

^{13}C-NMR of **24**

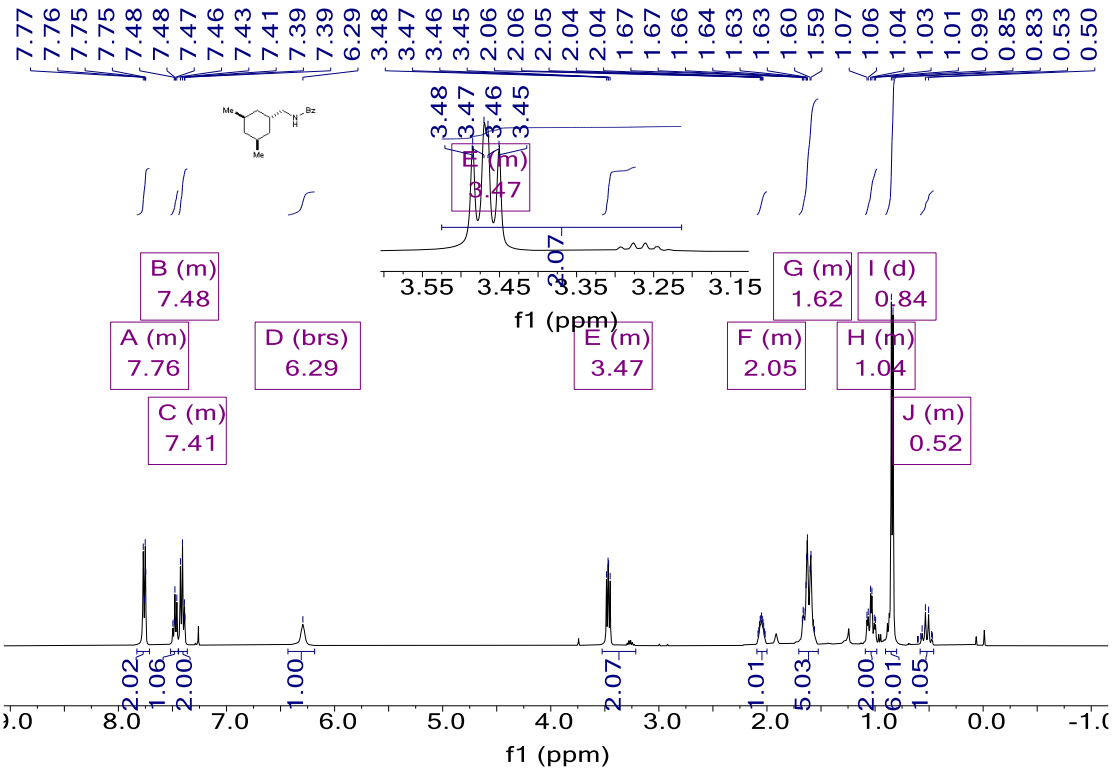

^{1}H-NMR of **25**

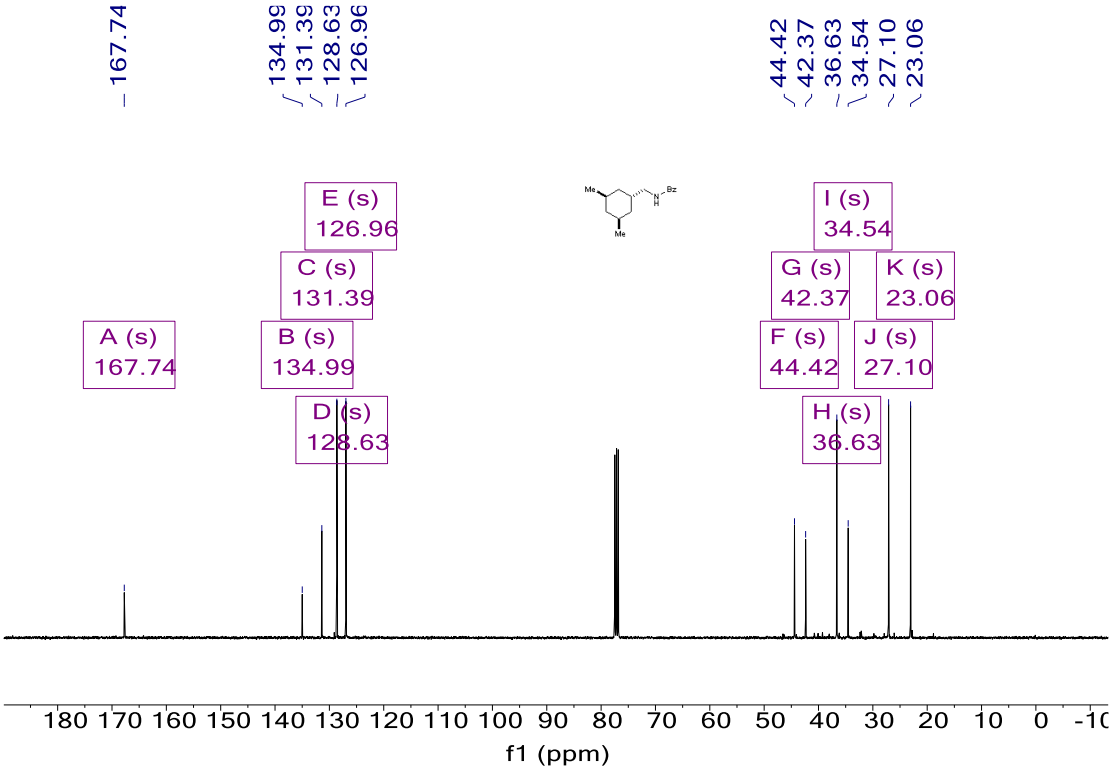

^{13}C-NMR of **25**

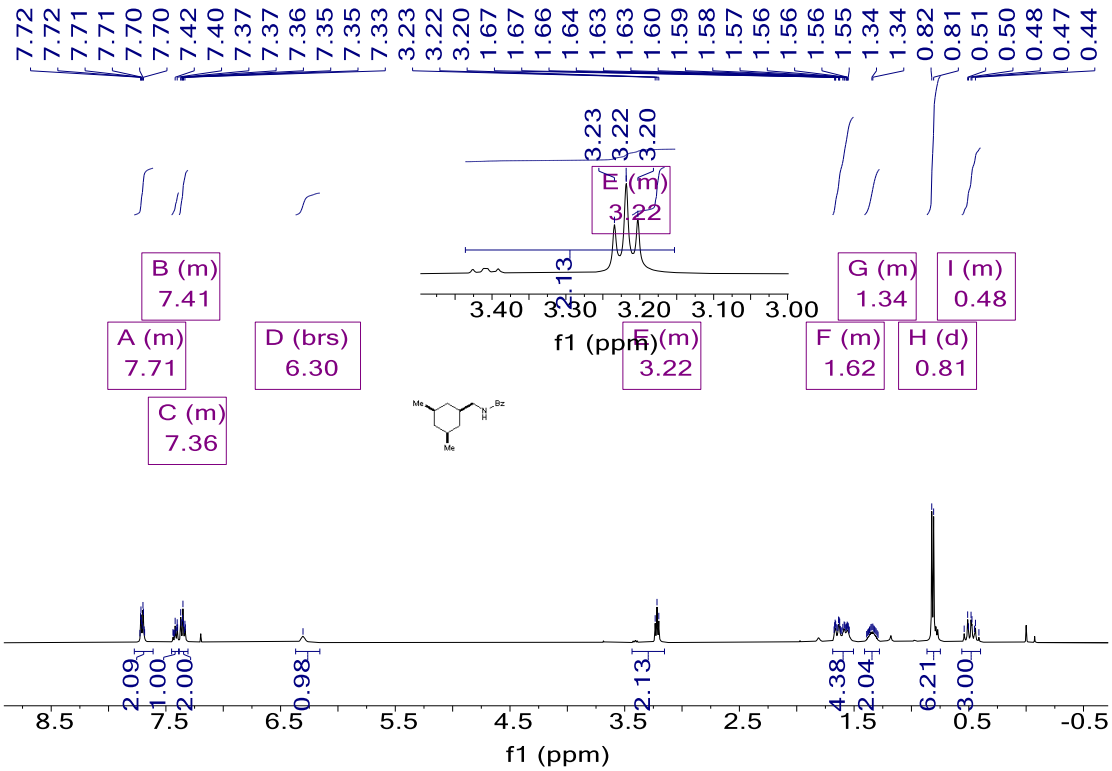

^{1}H-NMR of **26**

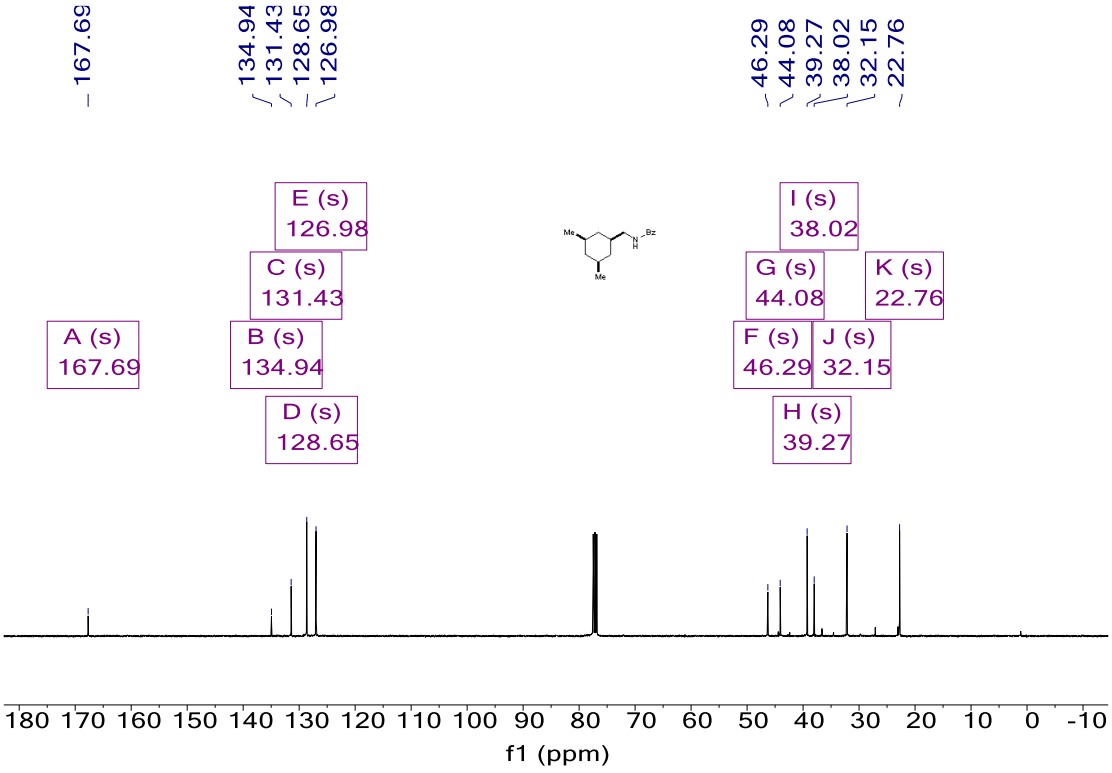

^{13}C-NMR of **26**

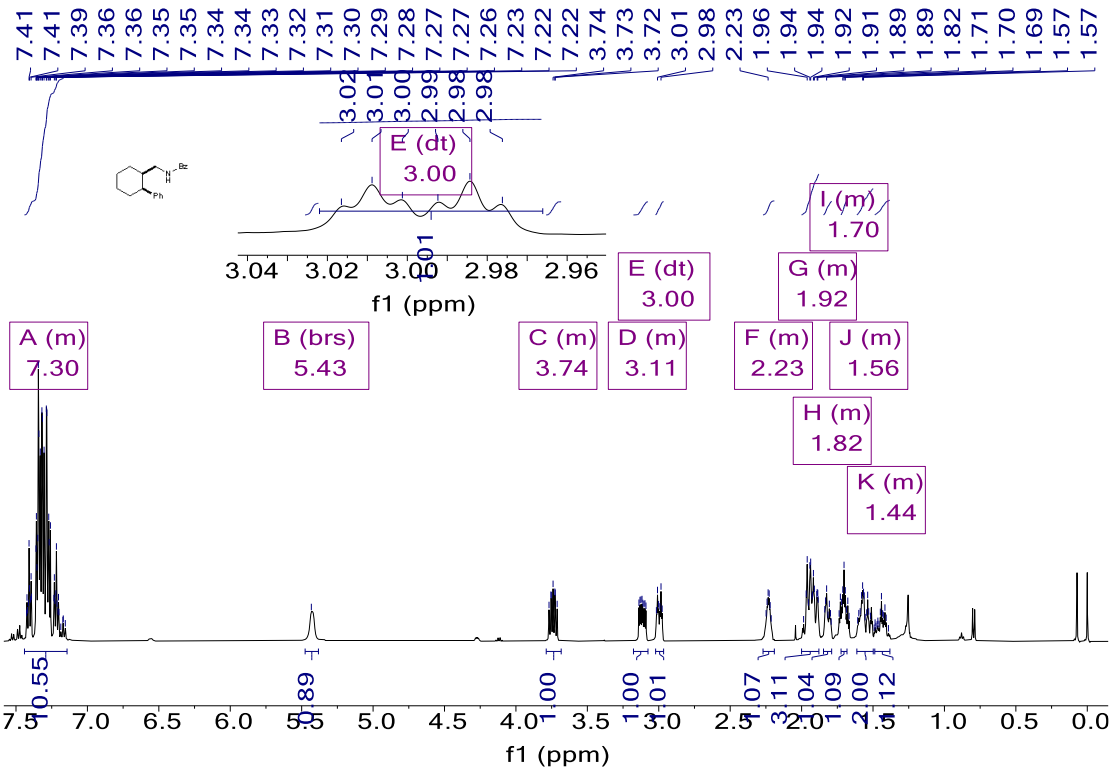

^{1}H-NMR of **27**

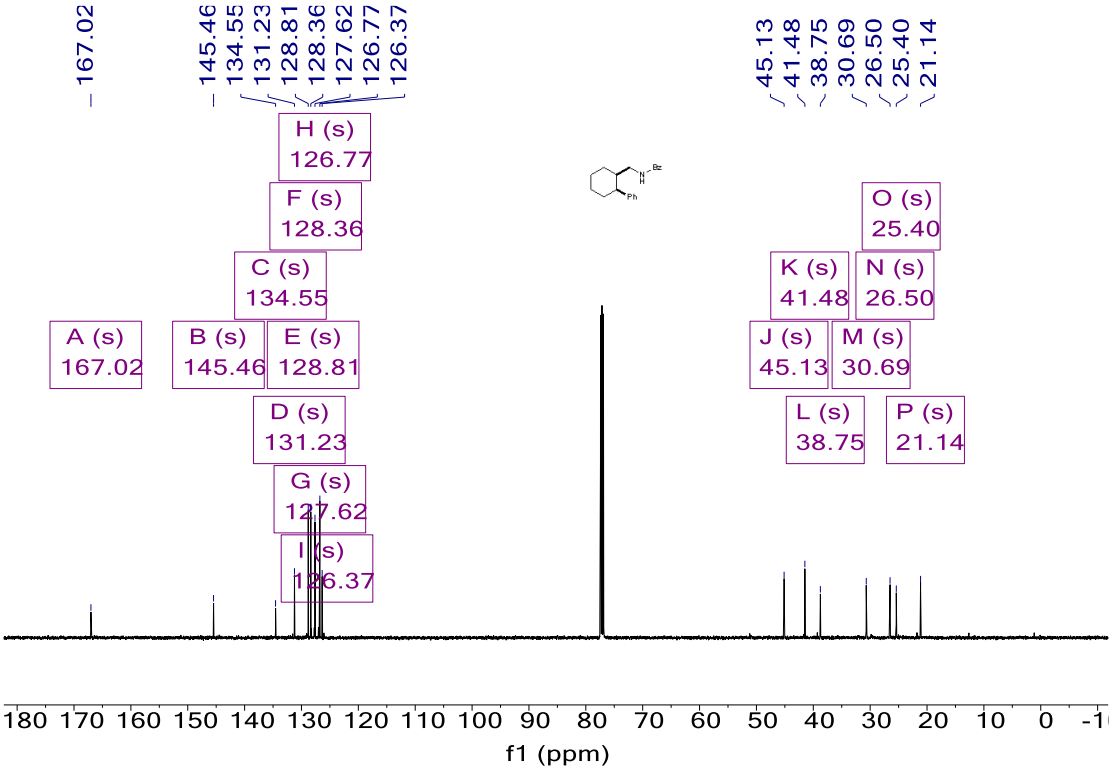

^{13}C-NMR of **27**

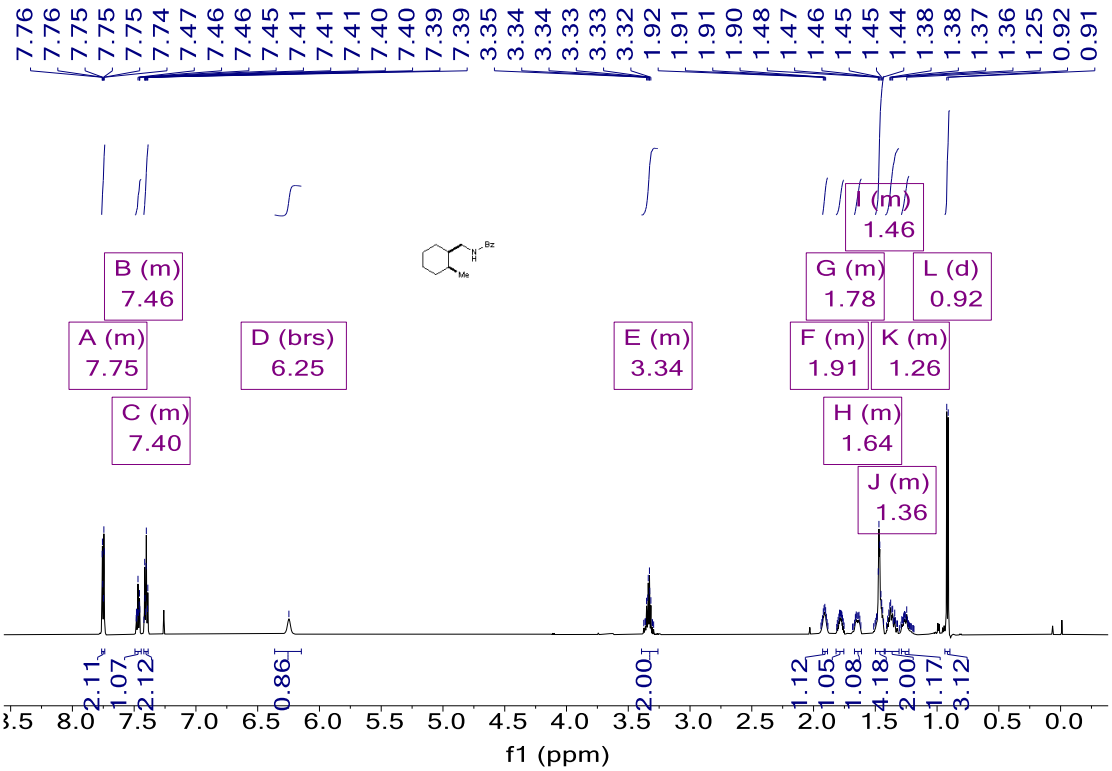

^{1}H-NMR of **28**

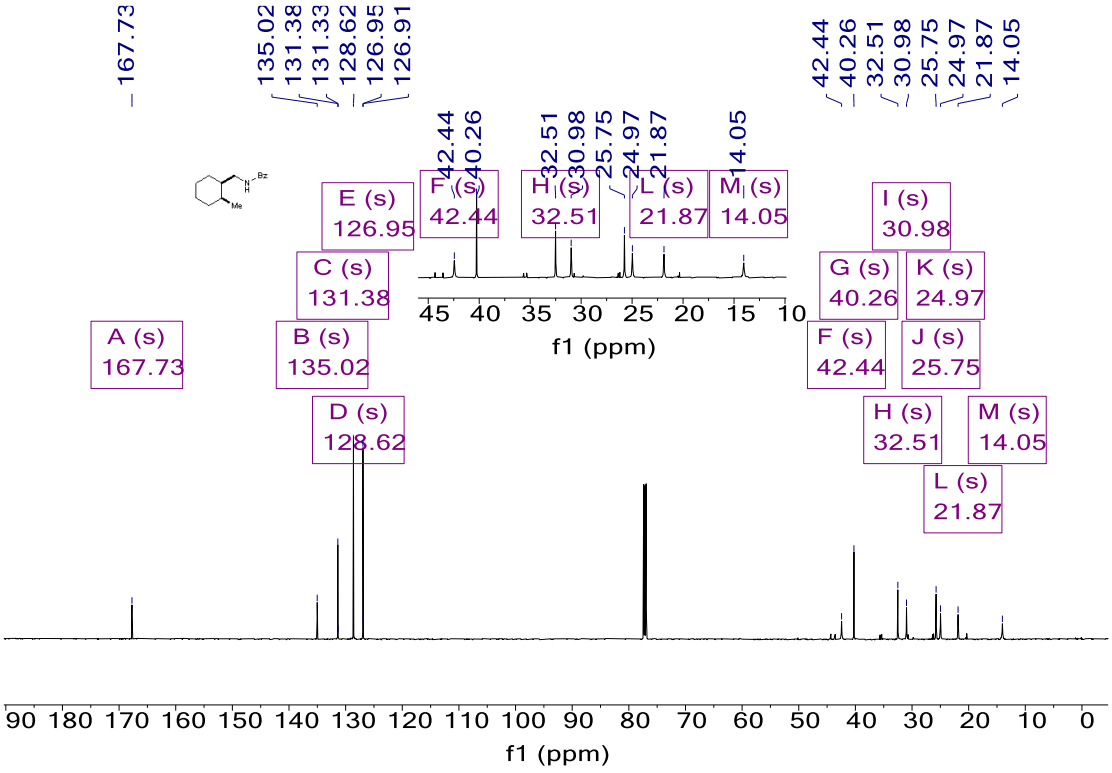

^{13}C-NMR of **28**

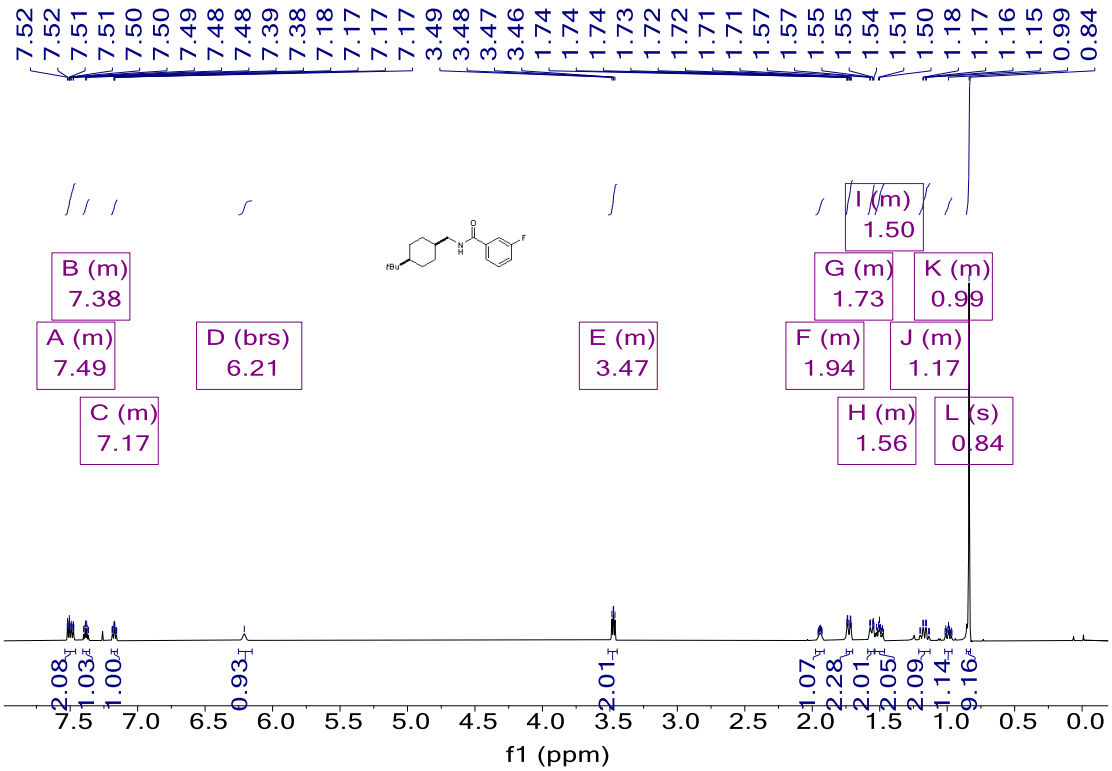

^{1}H-NMR of **29**

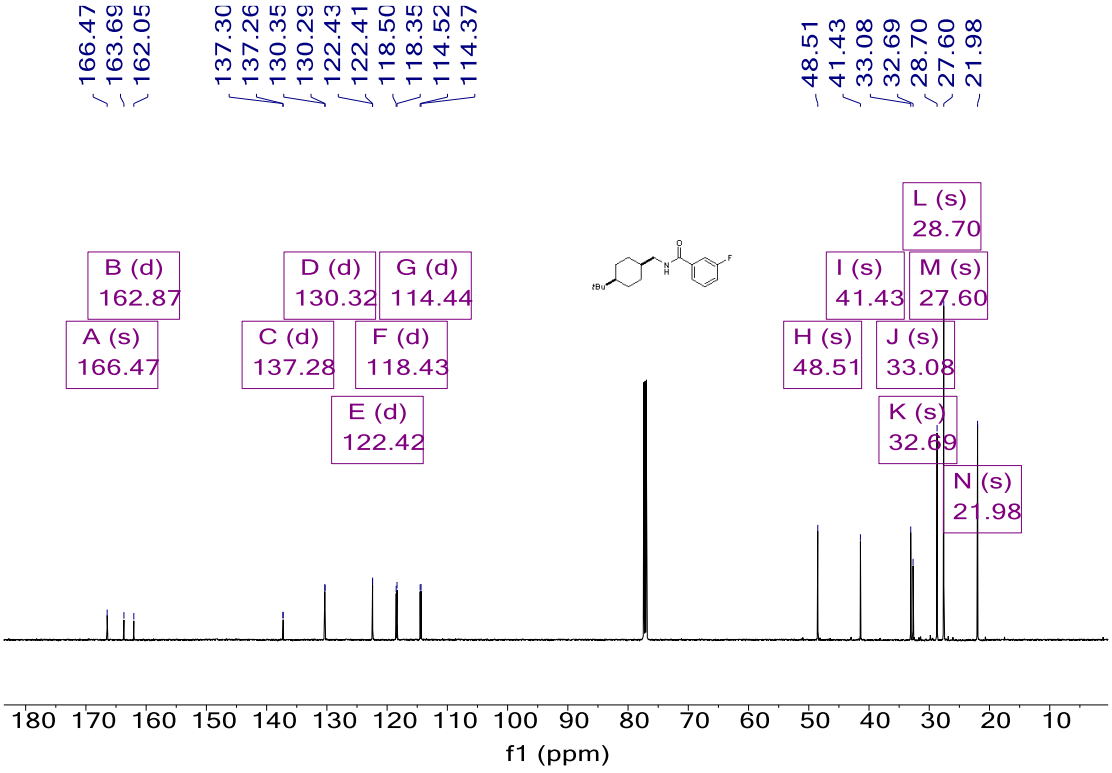

^{13}C-NMR of **29**

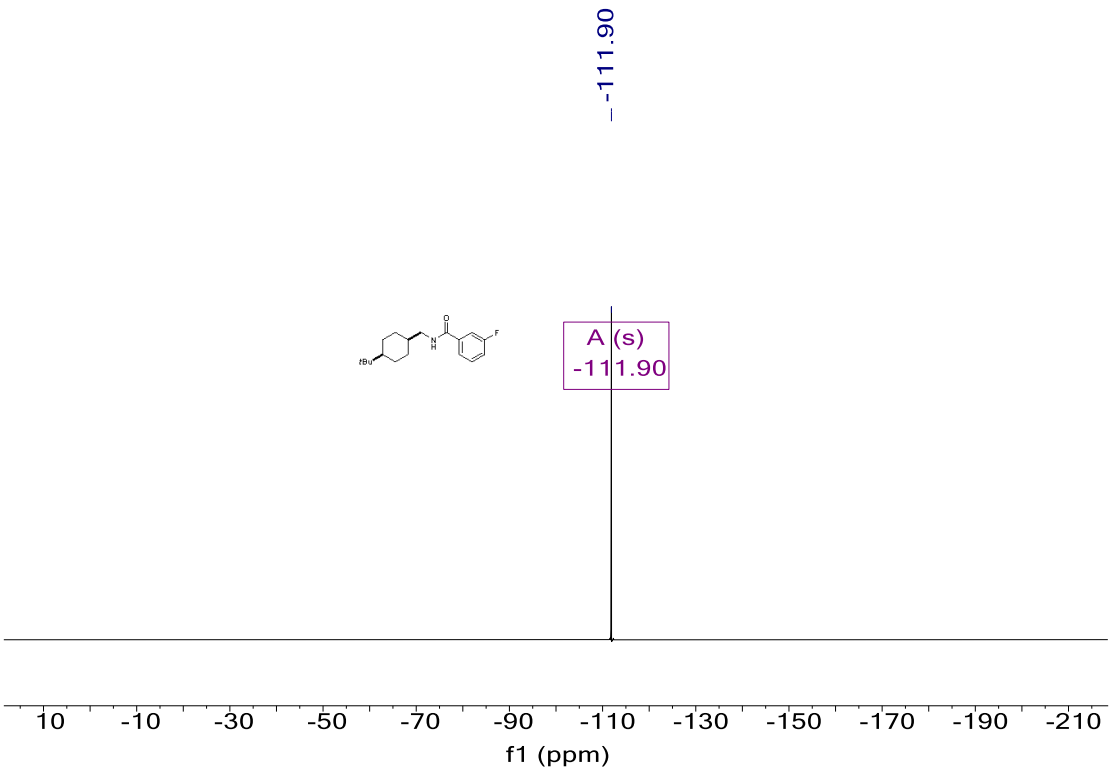

^{19}F-NMR of **29**

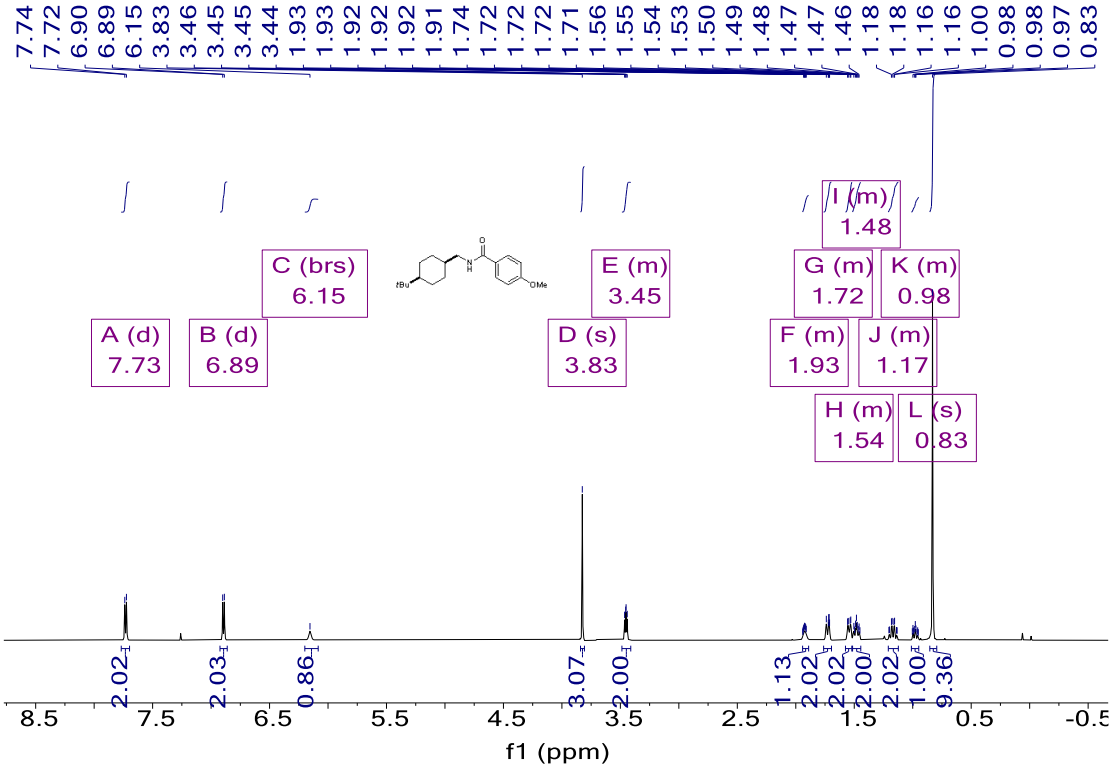

^{1}H-NMR of **30**

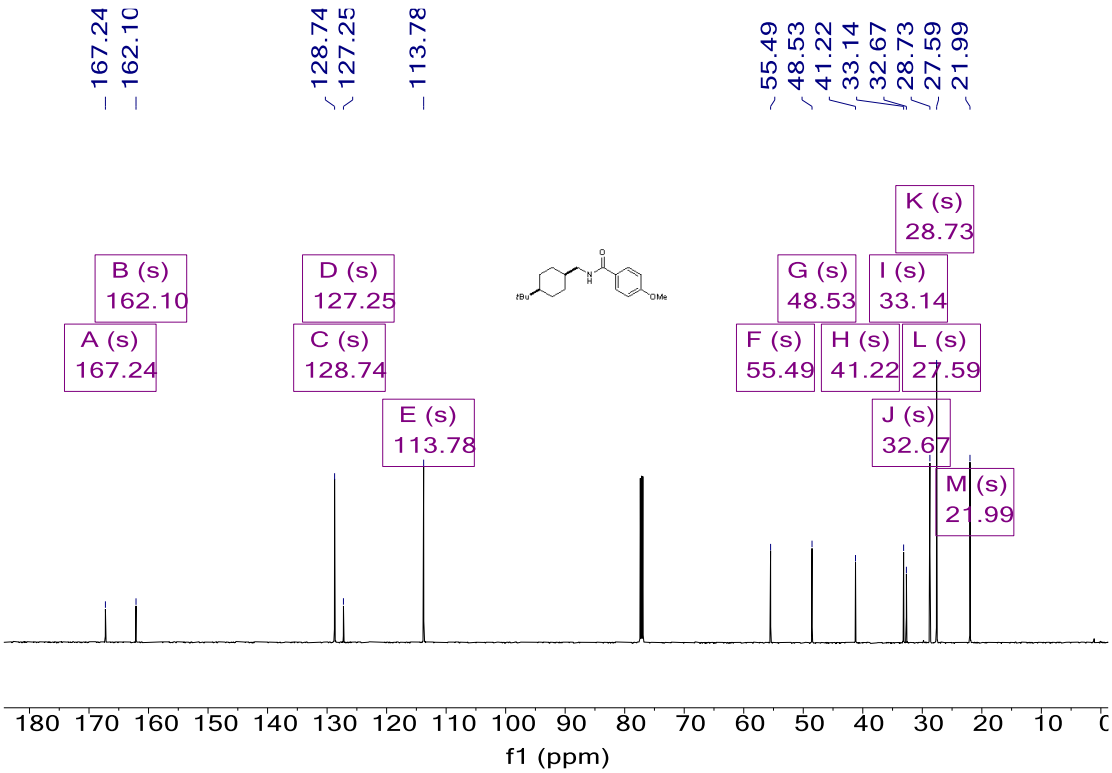

^{13}C-NMR of **30**

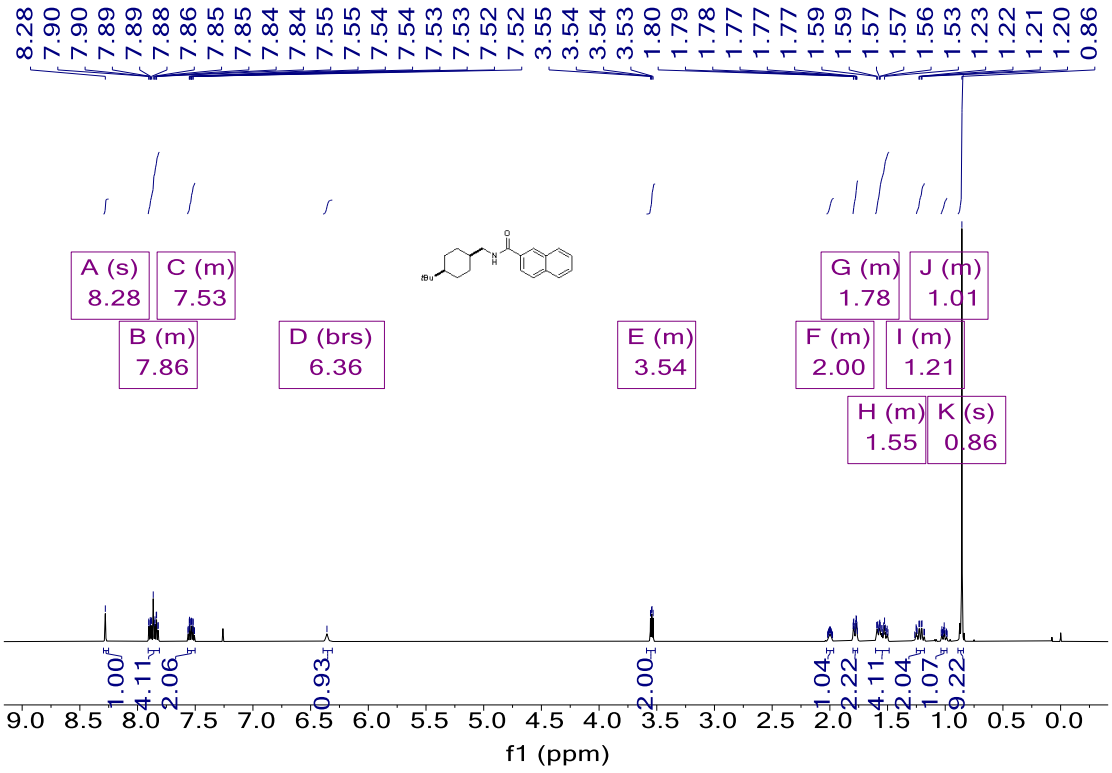

^{1}H-NMR of **31**

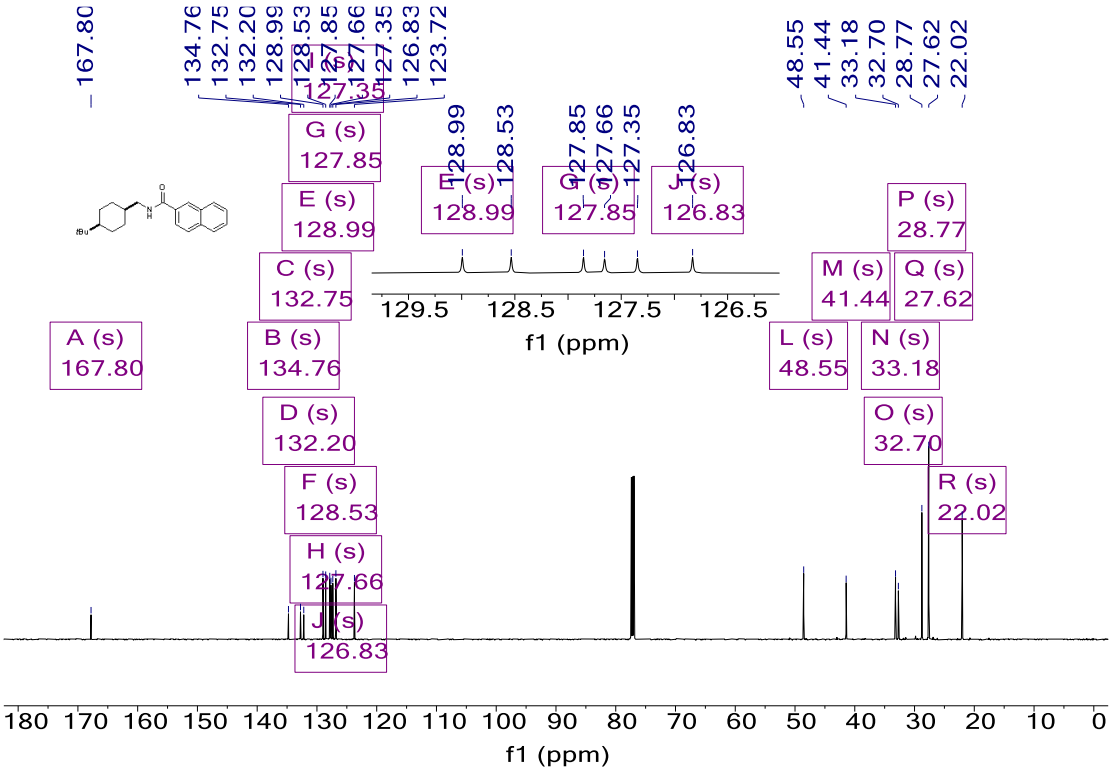

^{13}C-NMR of **31**

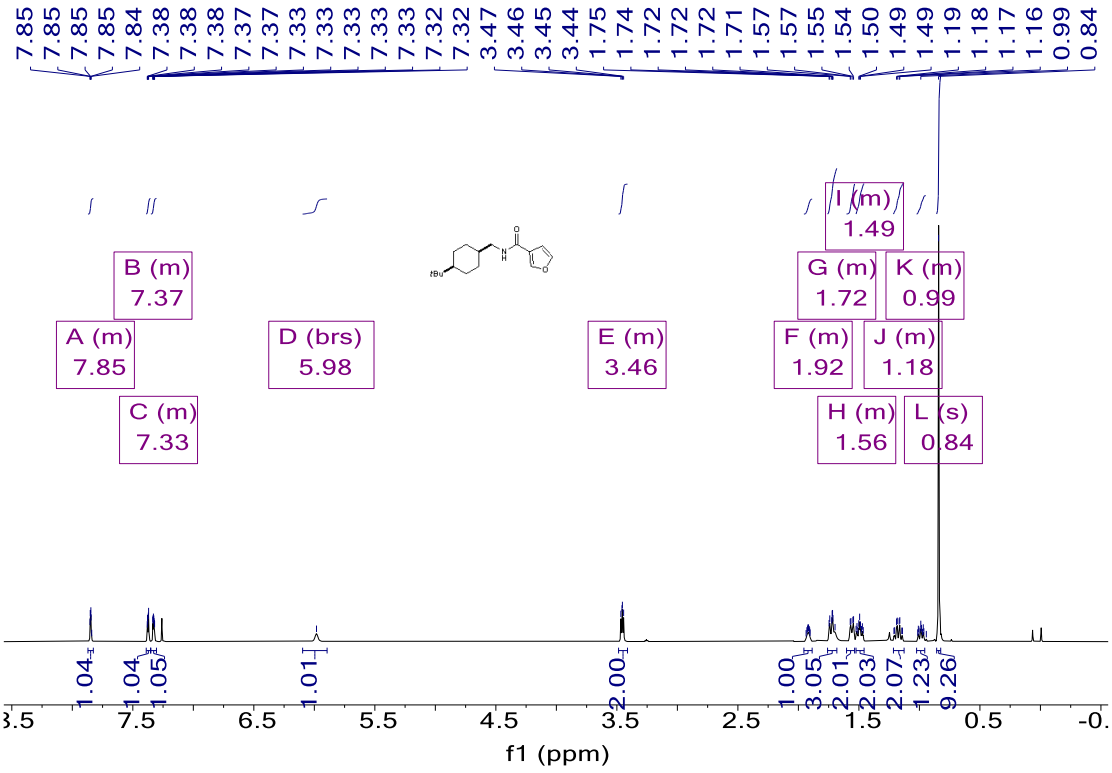

^{1}H-NMR of **32**

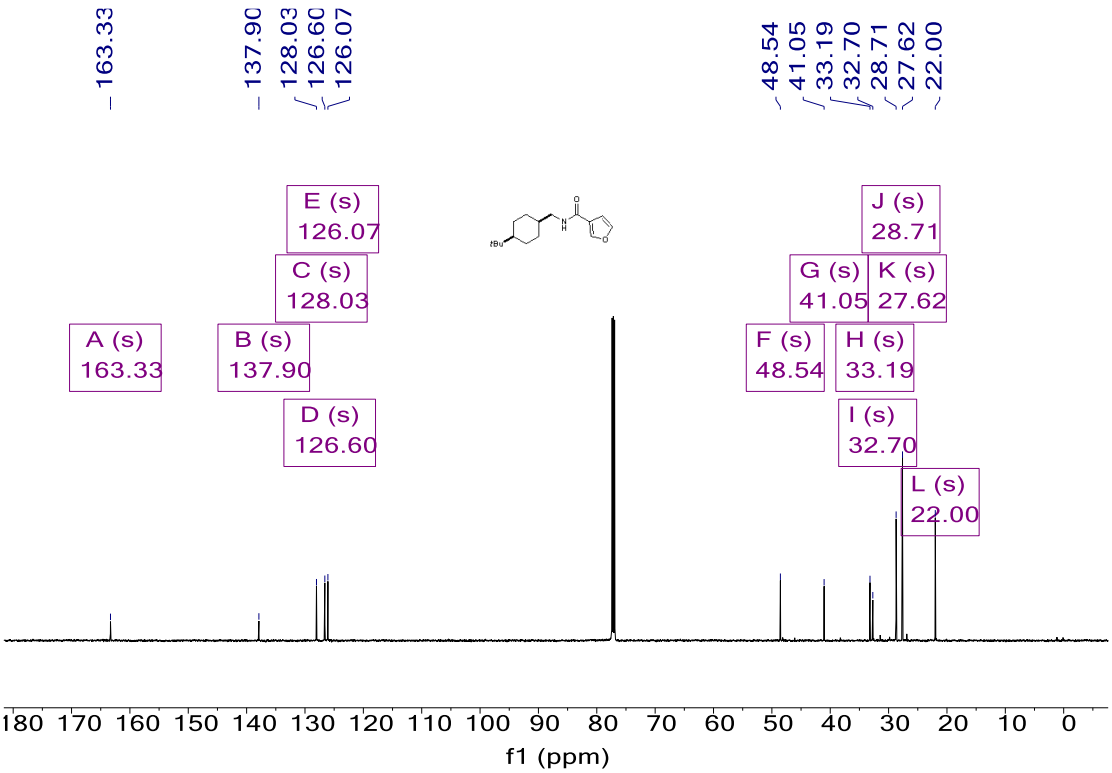

^{13}C-NMR of **32**

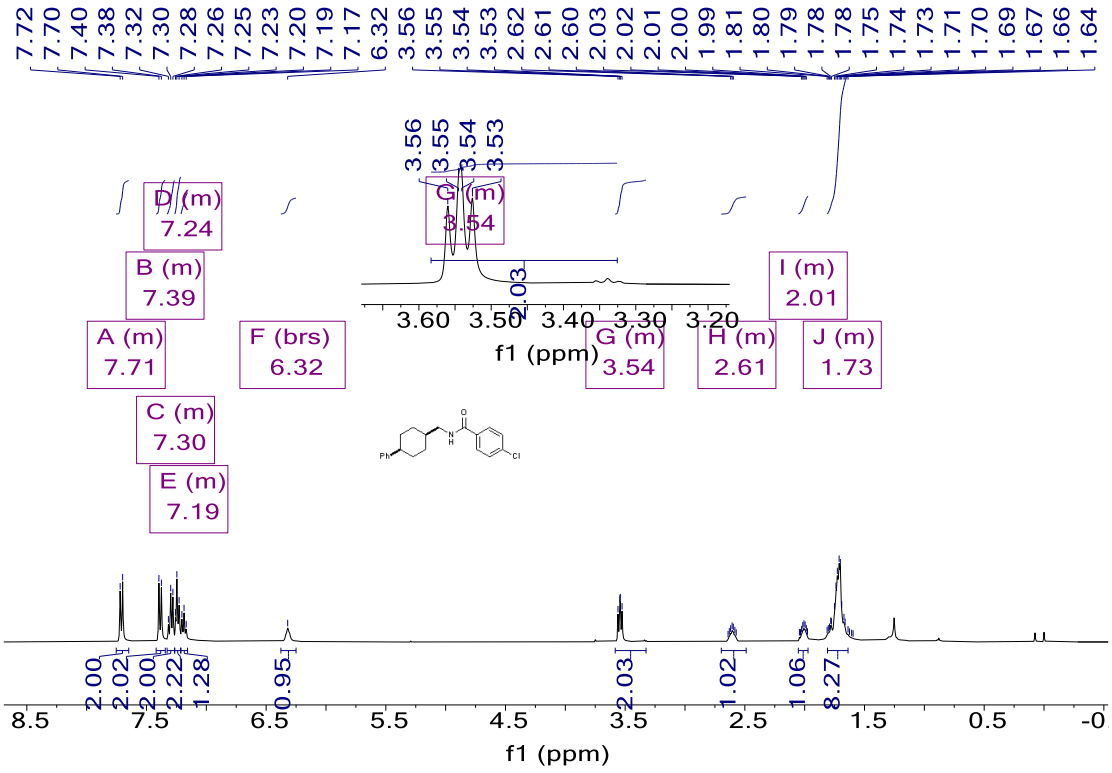

^{1}H-NMR of **33**

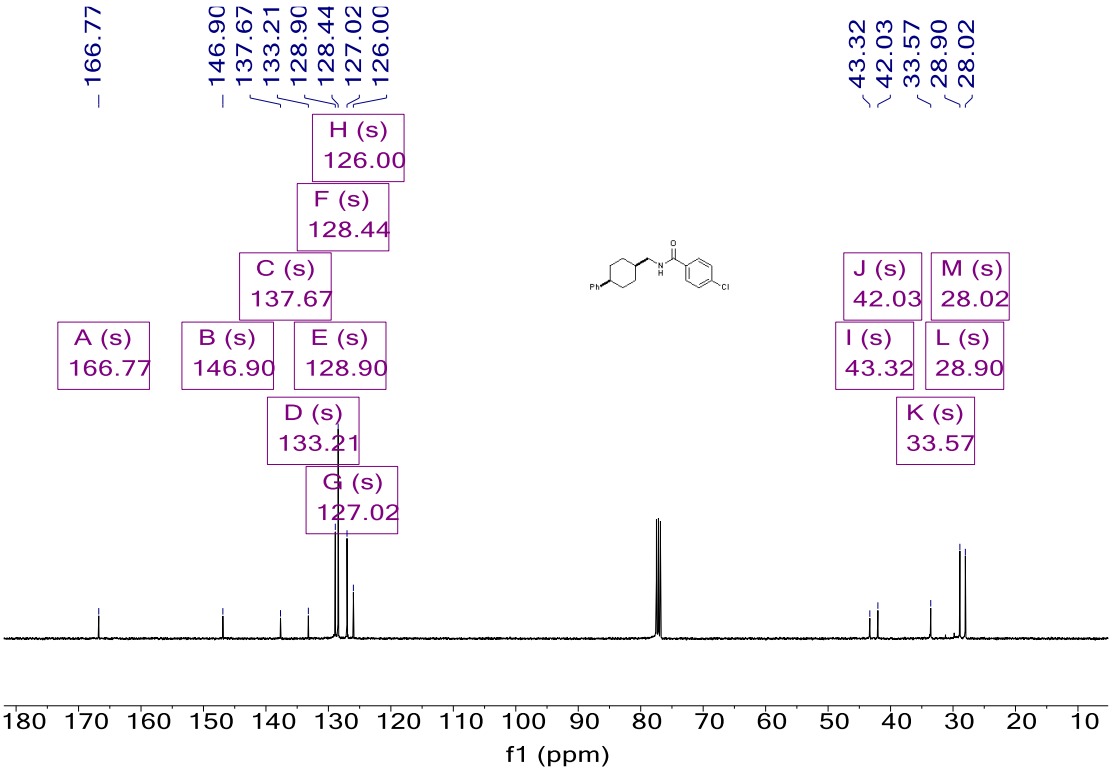

^{13}C-NMR of **33**

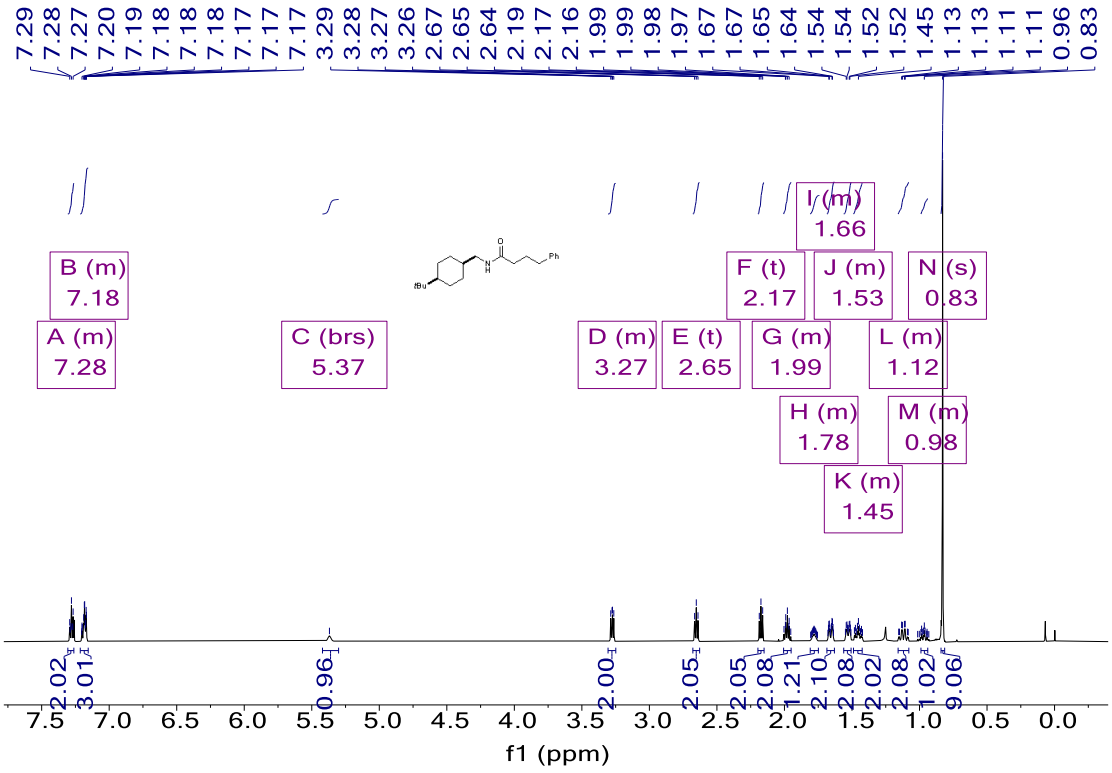

^{1}H-NMR of **34**

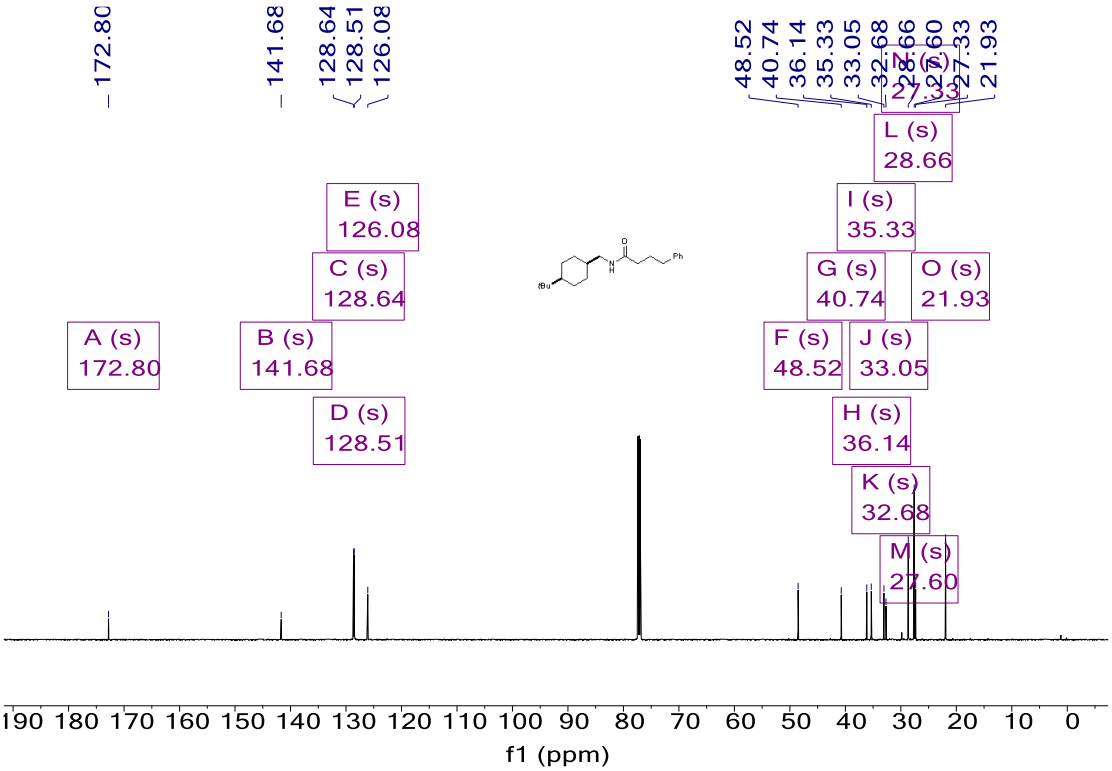

^{13}C-NMR of **34**

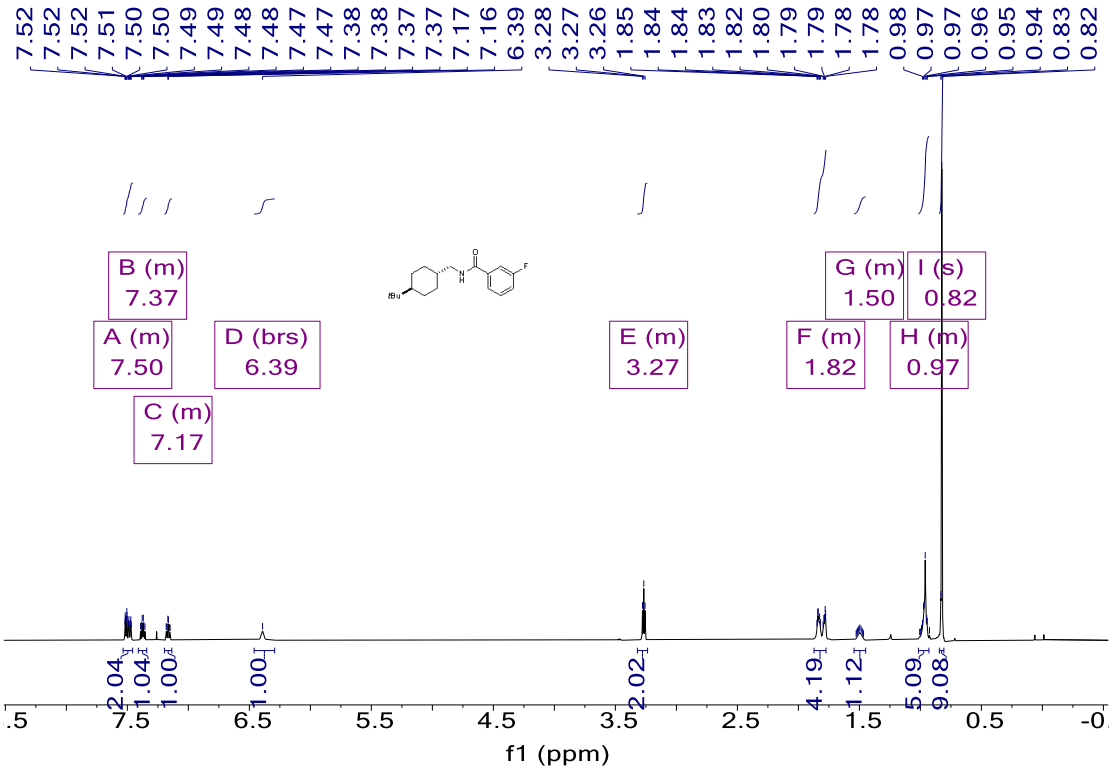

^{1}H-NMR of **35**

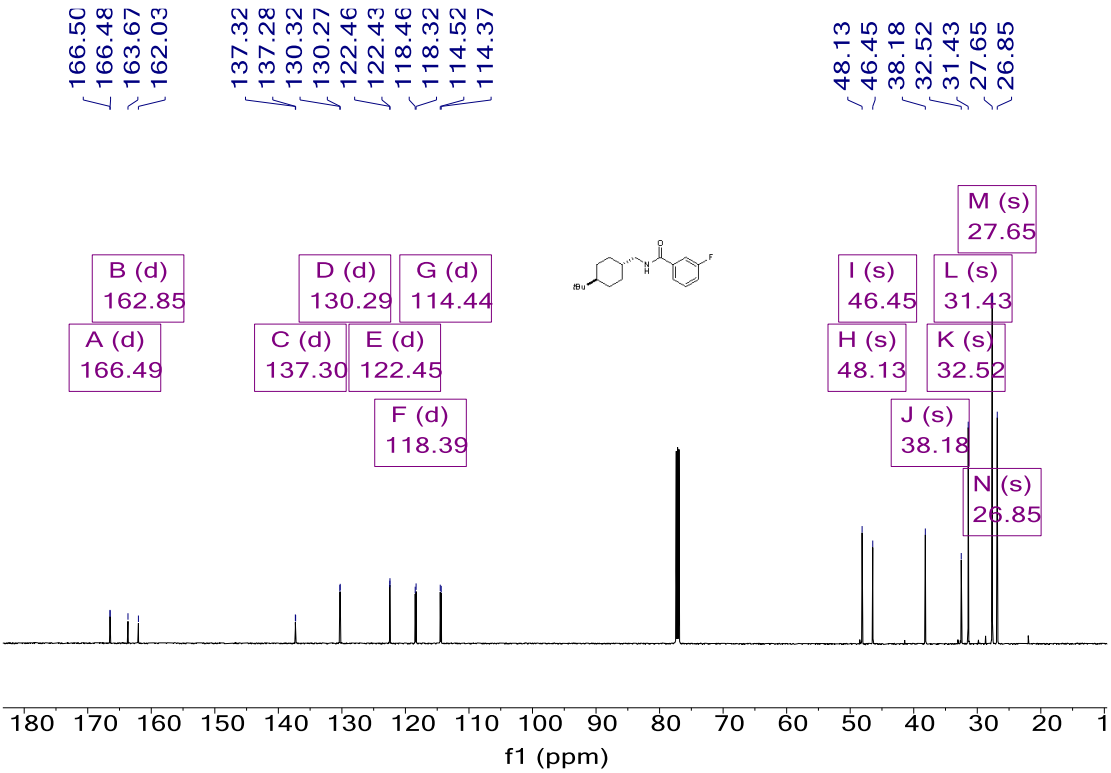

^{13}C-NMR of **35**

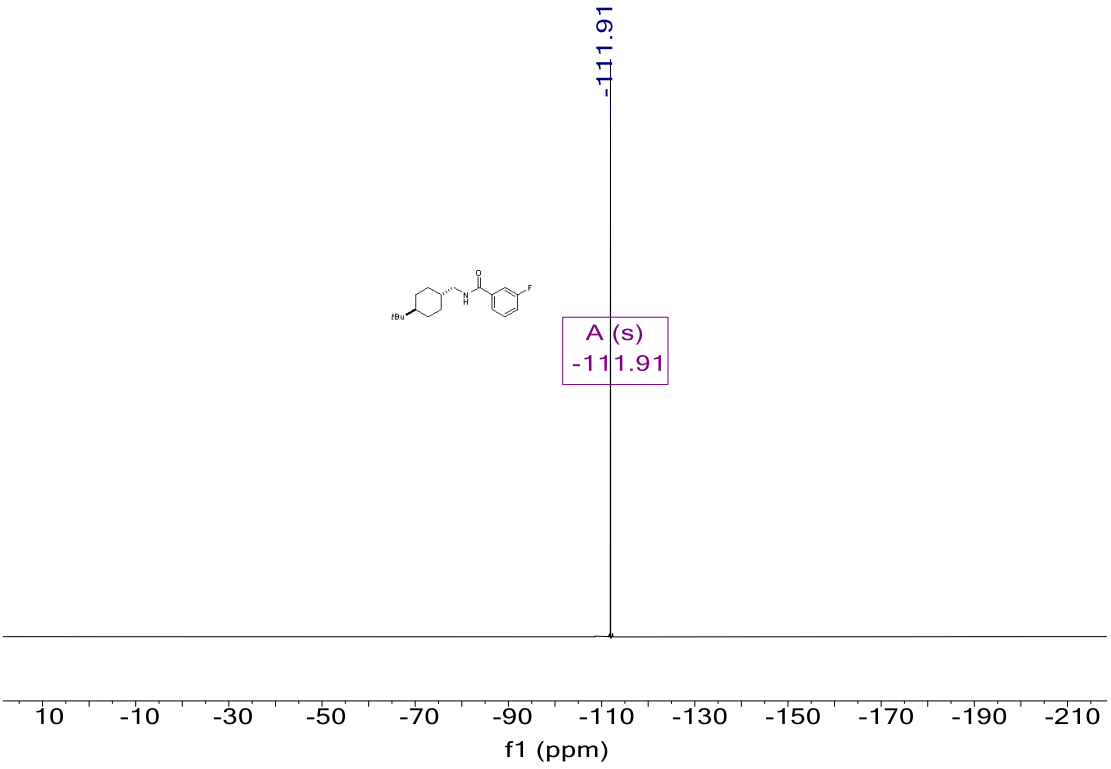

^{19}F-NMR of **35**

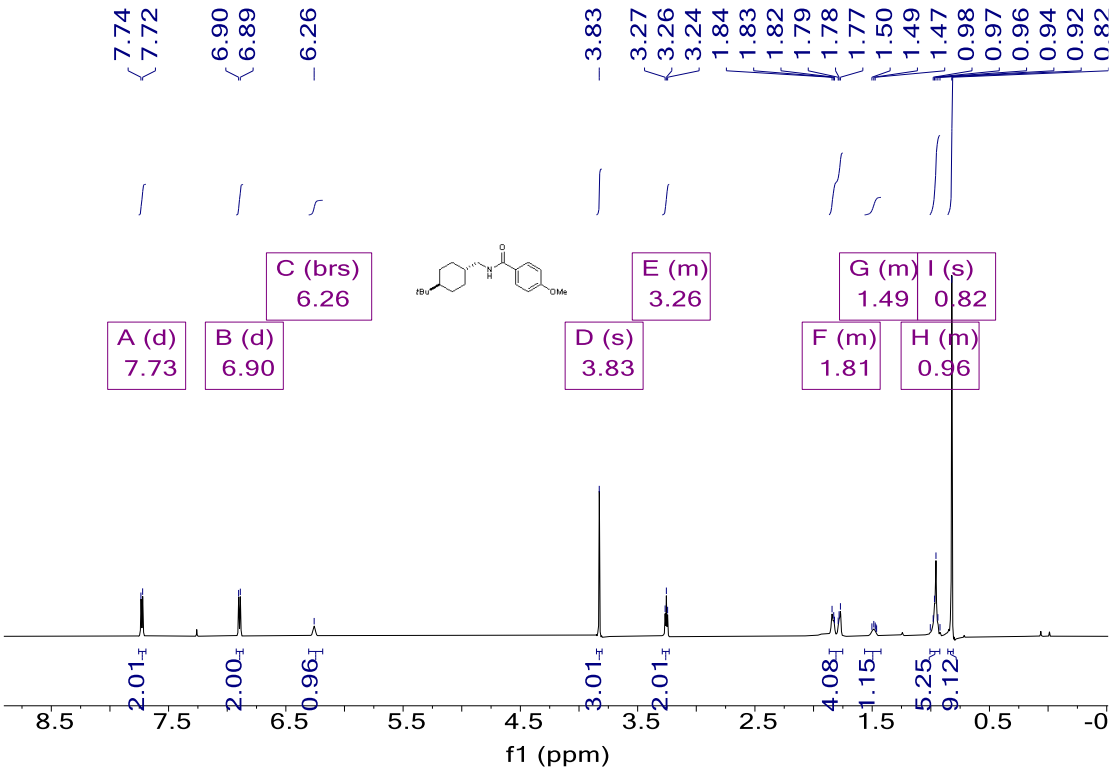

^{1}H-NMR of **36**

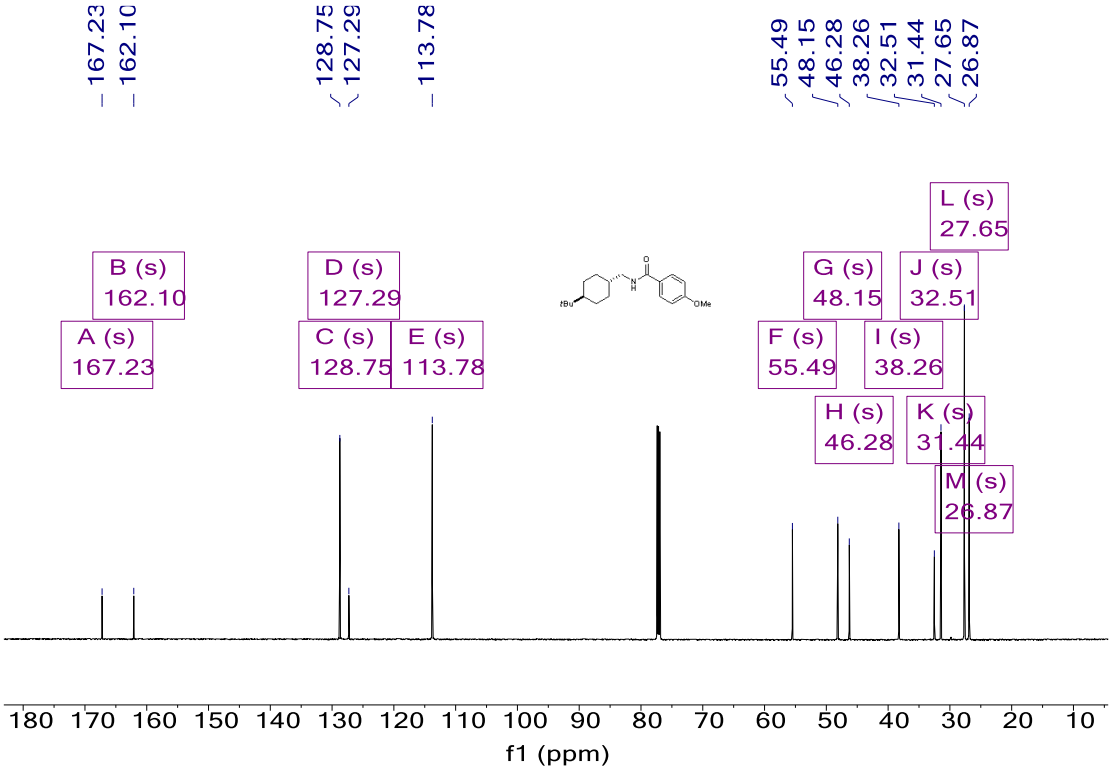

^{13}C-NMR of **36**

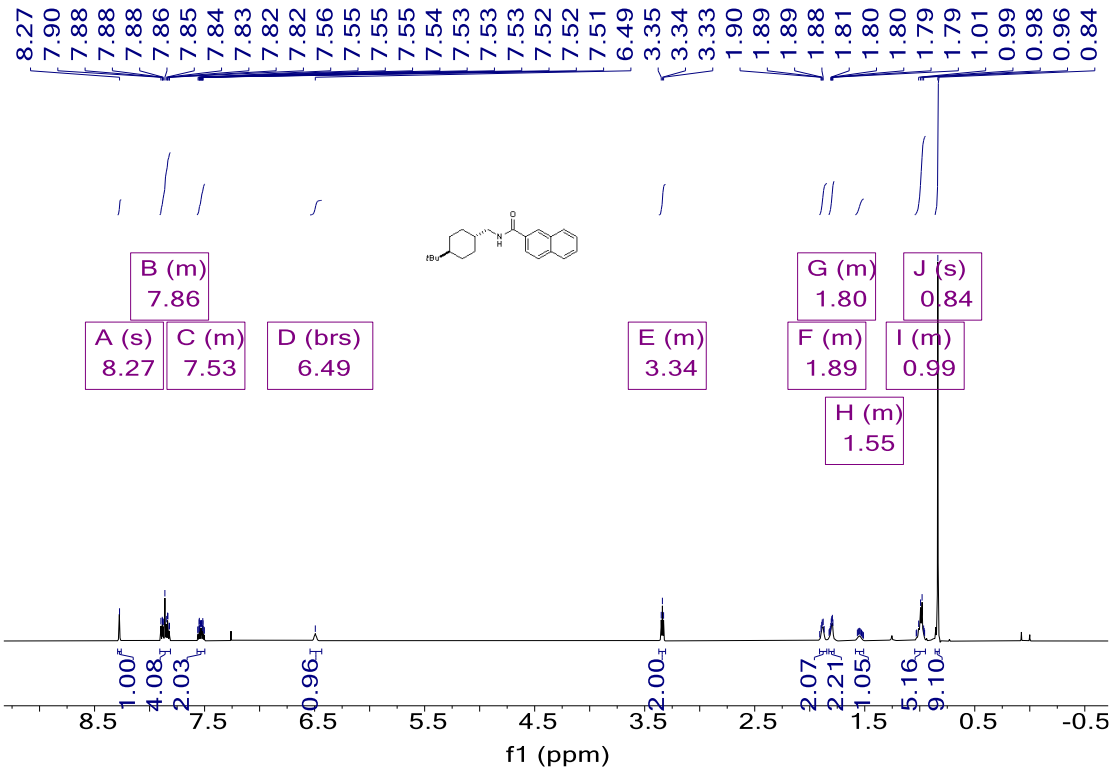

^{1}H-NMR of **37**

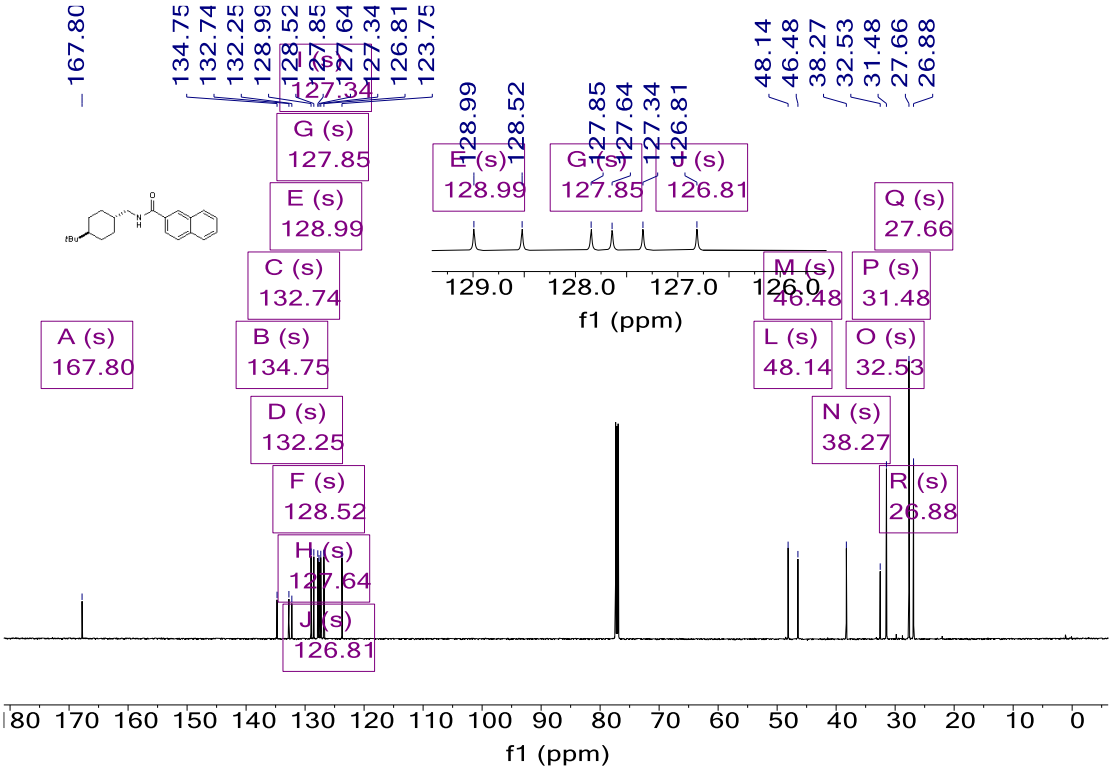

^{13}C-NMR of **37**

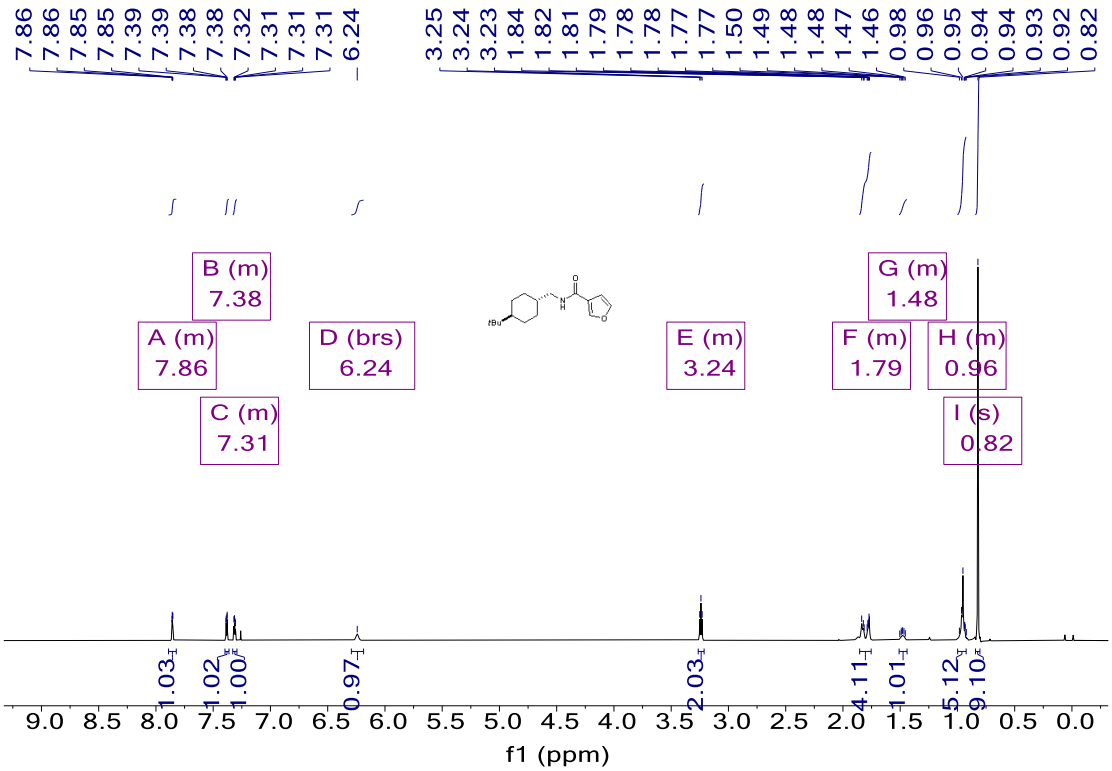

^{1}H-NMR of **38**

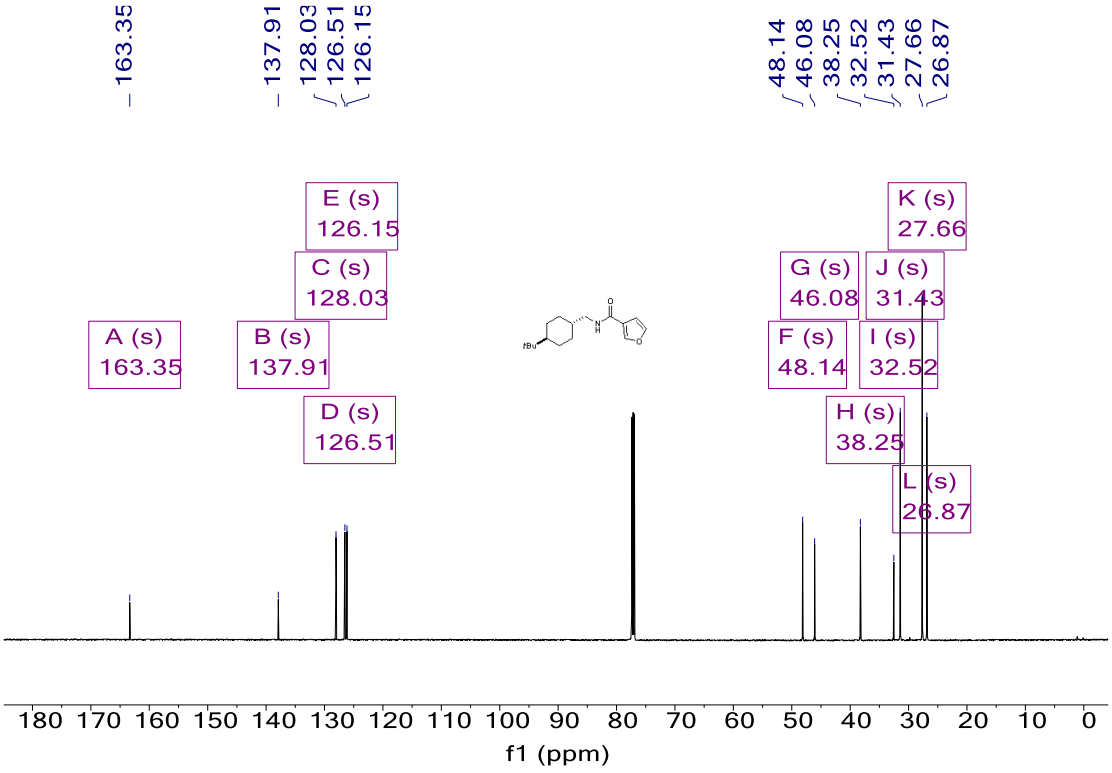

^{13}C-NMR of **38**

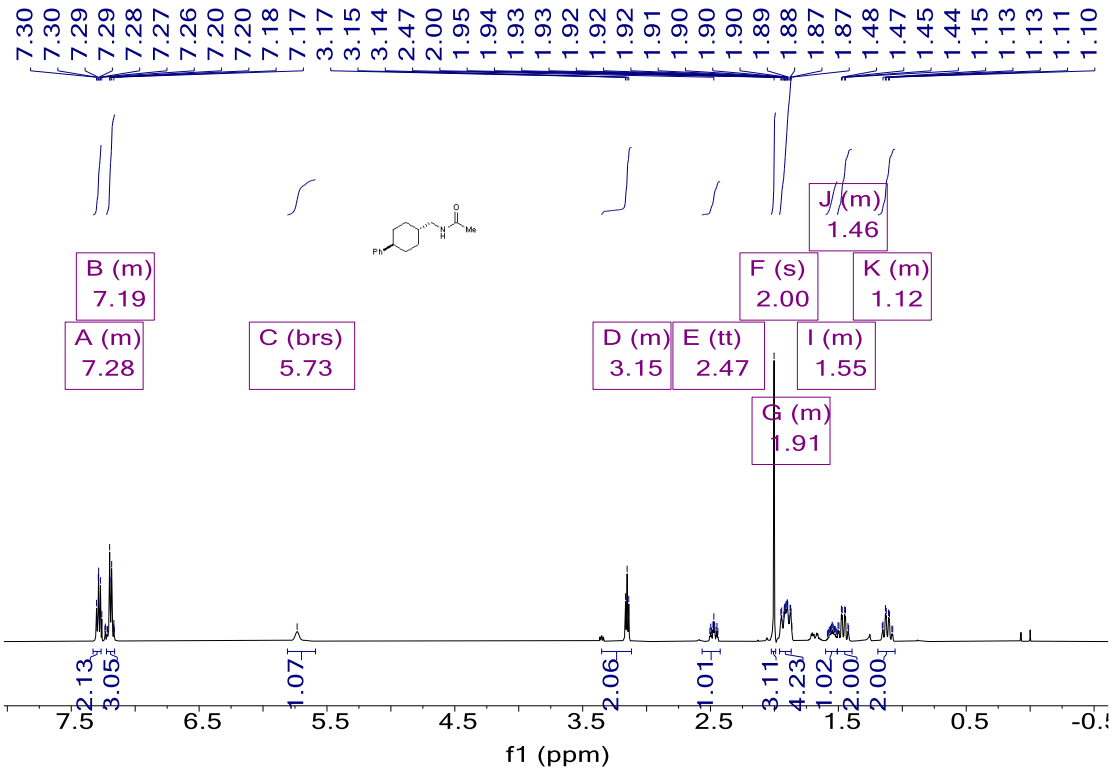

^{1}H-NMR of **39**

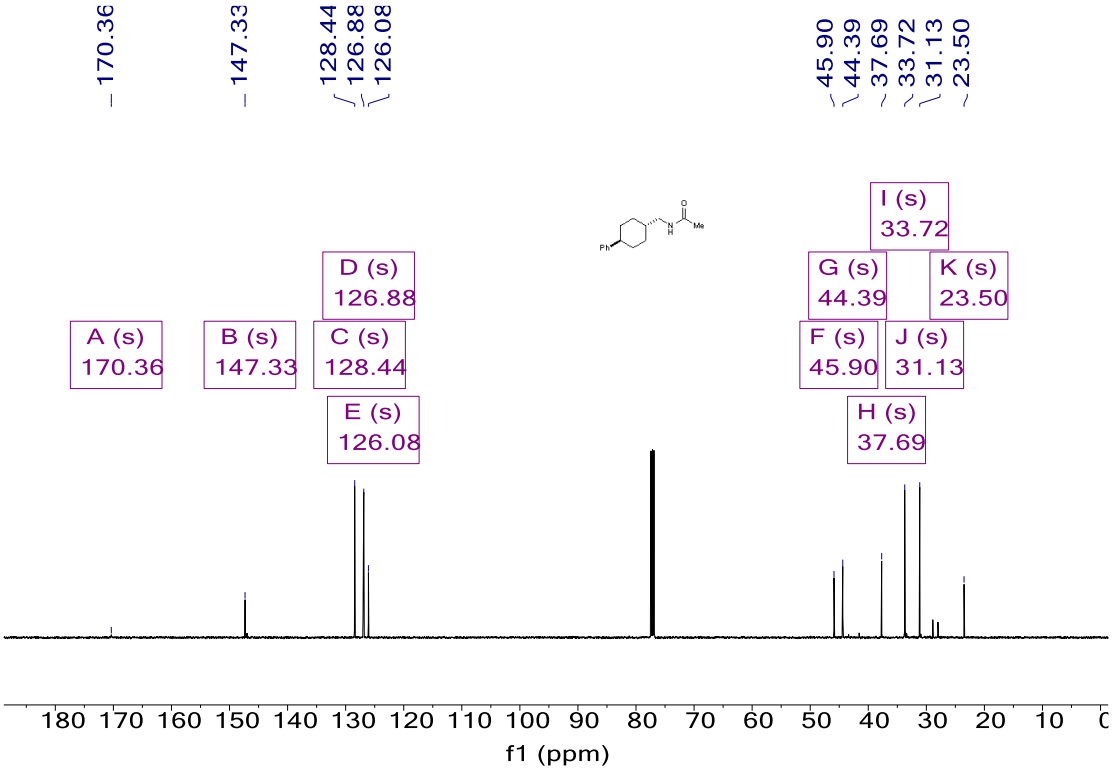

^{13}C-NMR of **39**

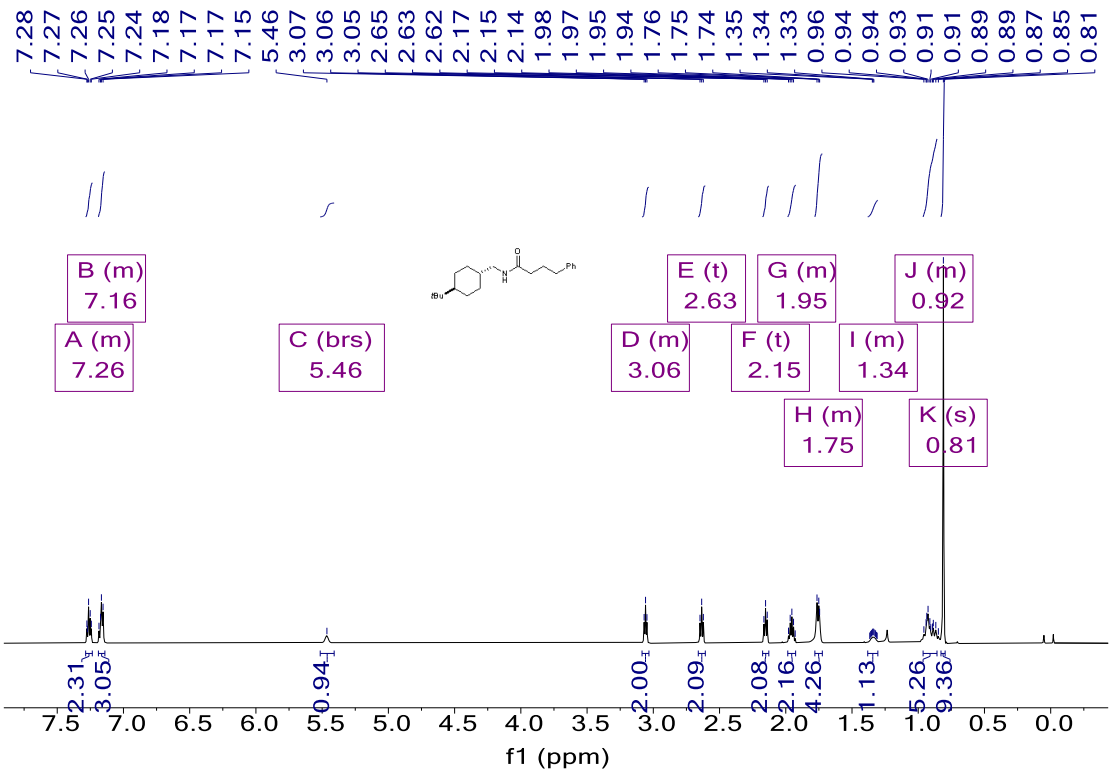

^{1}H-NMR of **40**

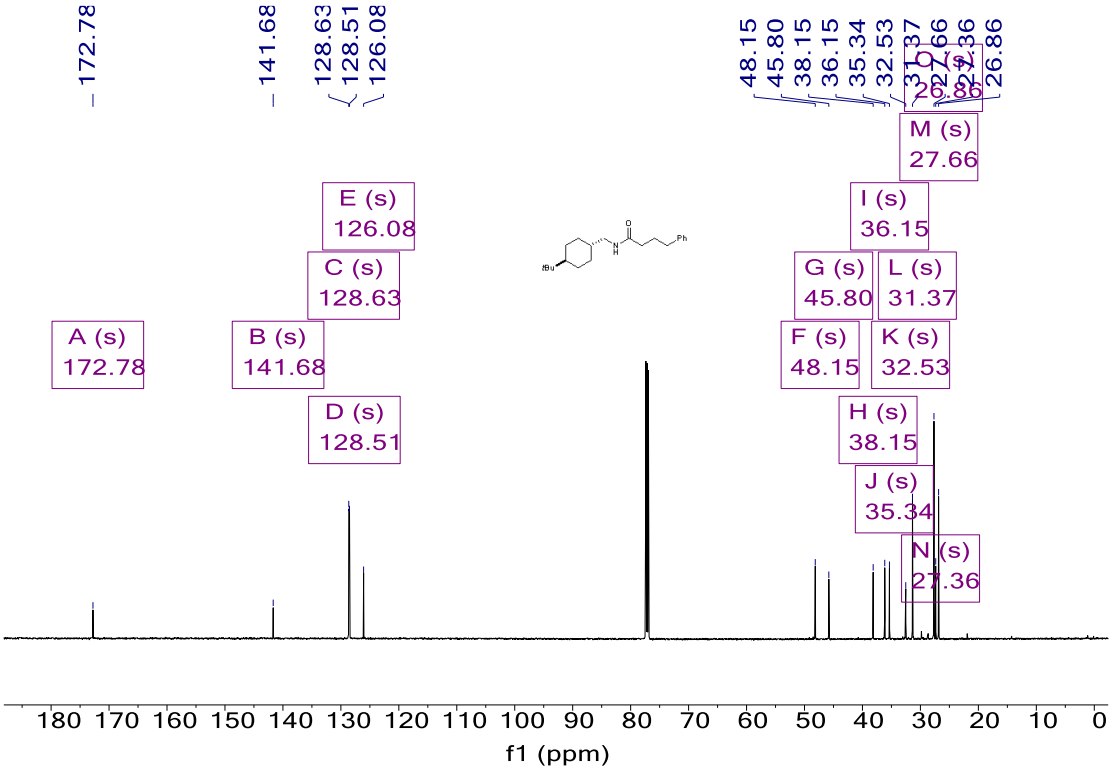

^{13}C-NMR of **40**

References

1 Zhu, S., Niljianskul, N. & Buchwald, S. L. Enantio- and Regioselective CuH-Catalyzed Hydroamination of Alkenes. *J. Am. Chem. Soc.* **135**, 15746-15749 (2013).

2 Lu, X. *et al.* Practical carbon-carbon bond formation from olefins through nickel-catalyzed reductive olefin hydrocarbonation. *Nat. Commun.* **7**, 11129 (2016).

3 Li, Y. *et al.* Cobalt-catalysed enantioselective C(sp^3)-C(sp^3) coupling. *Nat. Catal.* **4**, 901-911 (2021).

4 Tong, X., Yang, Z. P., Del Angel Aguilar, C. E. & Fu, G. C. Iron-Catalyzed Reductive Cross-Coupling of Alkyl Electrophiles with Olefins. *Angew. Chem. Int. Ed.* **62**, e202306663 (2023).

5 Zhou, Y., Engl, O. D., Bandar, J. S., Chant, E. D. & Buchwald, S. L. CuH-Catalyzed Asymmetric Hydroamidation of Vinylarenes. *Angew. Chem. Int. Ed.* **57**, 6672-6675 (2018).

6 Meng, L., Yang, J., Duan, M., Wang, Y. & Zhu, S. Facile Synthesis of Chiral Arylamines, Alkylamines and Amides by Enantioselective NiH-Catalyzed Hydroamination. *Angew. Chem. Int. Ed.* **60**, 23584-23589 (2021).

7 Zhang, Y., Qiao, D., Duan, M., Wang, Y. & Zhu, S. Enantioselective synthesis of α-aminoboronates by NiH-catalysed asymmetric hydroamidation of alkenyl boronates. *Nat. Commun.* **13**, 5630 (2022).

8 Lyu, X. *et al.* Intramolecular hydroamidation of alkenes enabling asymmetric synthesis of β-lactams via transposed NiH catalysis. *Nat. Catal.* **6**, 784-795 (2023).

9 Choi, H., Kim, D. & Chang, S. Regioselective Hydroamidation of α,β-Unsaturated Esters Enabled by Lewis Acid/Iron Relay Catalysis. *J. Am. Chem. Soc.* **147**, 33615-33624 (2025).

10 Liu, B. *et al.* Regiodivergent Hydroamidation of Alkenes via Cobalt-Hydride

Catalysis. *J. Am. Chem. Soc.* **147**, 13983-13992 (2025).

11 Li, Z. *et al.* Diastereodivergent synthesis of multi-substituted cycloalkanes. *Nat. Chem.* **17**, 1524-1533 (2025).

12 Li, W. & Zhang, J. Sadphos as Adaptive Ligands in Asymmetric Palladium Catalysis. *Acc. Chem. Res.* **57**, 489-513 (2024).

13 Pan, Q. *et al.* Ligand-Controlled, Nickel-Catalyzed Stereodivergent Construction of 1,3-Nonadjacent Stereocenters. *J. Am. Chem. Soc.* **146**, 15453-15463 (2024).

14 Xu, X.-Y., Liu, L.-G., Xu, L.-C., Zhang, S.-Q. & Hong, X. Transfer Learning-Enabled Ligand Prediction for Ni-Catalyzed Atroposelective Suzuki-Miyaura Cross-Coupling Based on Mechanistic Similarity: Leveraging Pd Knowledge for Ni Discovery. *J. Am. Chem. Soc.* **147**, 15318-15328 (2025).

15 Clemans, G. B. & Alemayehu, M. The Gamma Gauche Substituent Effect in ^{13}C NMR. *Tetrahedron Lett.* **34**, 1563-1566 (1993).

16 Karplus, M. Vicinal Proton Coupling in Nuclear Magnetic Resonance. *J. Am. Chem. Soc.* **85**, 2870-2871 (1963).

17 Zhong, R., Wei, Z., Zhang, W., Liu, S. & Liu, Q. A Practical and Stereoselective In Situ NHC-Cobalt Catalytic System for Hydrogenation of Ketones and Aldehydes. *Chem* **5**, 1552-1566 (2019).

18 Gaussian 16 Rev. C.01 (Wallingford, CT, 2016).

19 Lee, C., Yang, W. & Parr, R. G. Development of the Colle-Salvetti correlation-energy formula into a functional of the electron density. *Phys. Rev. B* **37**, 785-789 (1988).

20 Miehlich, B., Savin, A., Stoll, H. & Preuss, H. Results obtained with the correlation energy density functionals of becke and Lee, Yang and Parr. *Chem. Phys. Lett.* **157**, 200-206 (1989).

21 Becke, A. D. Density-functional thermochemistry. III. The role of exact exchange. *J. Chem. Phys.* **98**, 5648-5652 (1993).

22 Grimme, S., Antony, J., Ehrlich, S. & Krieg, H. A consistent and accurate ab

initio parametrization of density functional dispersion correction (DFT-D) for the 94 elements H-Pu. *J. Chem. Phys.* **132** (2010).

23 Grimme, S., Ehrlich, S. & Goerigk, L. Effect of the damping function in dispersion corrected density functional theory. *J. Comput. Chem.* **32**, 1456-1465 (2011).

24 von Szentpály, L., Fuentealba, P., Preuss, H. & Stoll, H. Pseudopotential calculations on Rb^{+2}, Cs^{+2}, RbH^{+}, CsH^{+} and the mixed alkali dimer ions. *Chem. Phys. Lett.* **93**, 555-559 (1982).

25 Dolg, M., Wedig, U., Stoll, H. & Preuss, H. Energy-adjusted ab initio pseudopotentials for the first row transition elements. *J. Chem. Phys.* **86**, 866-872 (1987).

26 Zhao, Y. & Truhlar, D. G. A new local density functional for main-group thermochemistry, transition metal bonding, thermochemical kinetics, and noncovalent interactions. *J. Chem. Phys.* **125** (2006).

27 Marenich, A. V., Cramer, C. J. & Truhlar, D. G. Universal Solvation Model Based on Solute Electron Density and on a Continuum Model of the Solvent Defined by the Bulk Dielectric Constant and Atomic Surface Tensions. *J. Phys. Chem. B* **113**, 6378-6396 (2009).

28 Lu, T. & Chen, Q. Independent gradient model based on Hirshfeld partition: A new method for visual study of interactions in chemical systems. *J. Comput. Chem.* **43**, 539-555 (2022).

29 Lu, T. & Chen, F. Multiwfn: A multifunctional wavefunction analyzer. *J. Comput. Chem.* **33**, 580-592 (2012).

30 Shen, Z. *et al.* A stereoselective reductive cross-coupling reaction with kinetic control. *Nat. Catal.*, DOI: 10.1038/s41929-41025-01440-41924 (2025).